NUREG/CR-2331
BNL-NUREG-51454
VOL. 4, NO. 1

SAFETY RESEARCH PROGRAMS SPONSORED BY OFFICE OF NUCLEAR REGULATORY RESEARCH

QUARTERLY PROGRESS REPORT
JANUARY 1 — MARCH 31, 1984

Date Published — August 1984

DEPARTMENT OF NUCLEAR ENERGY, BROOKHAVEN NATIONAL LABORATORY
UPTON, NEW YORK 11973

Prepared for the U.S. Nuclear Regulatory Commission
Office of Nuclear Regulatory Research
Contract No. DE-AC02-76CH00016

NUREG/CR-2331
BNL-NUREG-51454
VOL. 4, NO. 1
AN, R-1,4,5,7,8, RD

SAFETY RESEARCH PROGRAMS SPONSORED BY OFFICE OF NUCLEAR REGULATORY RESEARCH

QUARTERLY PROGRESS REPORT
JANUARY 1 — MARCH 31, 1984

Herbert J.C. Kouts, Department Chairman
Walter Y. Kato, Deputy Chairman

Principal Investigators:

R.A. Bari
R.J. Cerbone
C.J. Czajkowski
T. Ginsberg
G.A. Greene
J.G. Guppy
R.E. Hall
W.J. Luckas, Jr.
J.N. O'Brien
W.T. Pratt
M. Reich
P. Saha
C. Sastre
J.H. Taylor
J.R. Weeks
W. Wulff
D. van Rooyen

Compiled by: Allen J. Weiss
Manuscript Completed June 1984

DEPARTMENT OF NUCLEAR ENERGY
BROOKHAVEN NATIONAL LABORATORY, ASSOCIATED UNIVERSITIES, INC.
UPTON, NEW YORK 11973

Prepared for the
OFFICE OF NUCLEAR REGULATORY RESEARCH
U.S. NUCLEAR REGULATORY COMMISSION
CONTRACT NO. DE-AC02-76CH00016
FIN NOS. A-3011,-3014,-3015,-3016,-3024,-3041,-3208,-3215,-3219,-3225,
-3226,-3227,-3257,-3261,-3266,-3268,-3270,-3271

Available from
GPO Sales Program
Division of Technical Information and Document Control
U.S. Nuclear Regulatory Commission
Washington, D.C. 20555
and
National Technical Information Service
Springfield, Virginia 22161

FOREWORD

The Advanced and Water Reactor Safety Research Programs Quarterly Progress Reports have been combined and are included in this report entitled, "Safety Research Programs Sponsored by the Office of Nuclear Regulatory Research - Quarterly Progress Report." This progress report will describe current activities and techncial progress in the programs at Brookhaven National Laboratory sponsored by the Division of Accident Evaluation, Division of Engineering Technology, and Division of Facility Operations of the U. S. Nuclear Regulatory Commission, Office of Nuclear Regulatory Research.

The projects reported are the following: High Temperature Reactor Research, SSC Development, Validation and Application, CRBR Balance of Plant Modeling, Thermal-Hydraulic Reactor Safety Experiments, Development of Plant Analyzer, Code Assessment and Application (Transient and LOCA Analyses), Thermal Reactor Code Development (RAMONA-3B), Calculational Quality Assurance in Support of PTS; Stress Corrosion Cracking of PWR Steam Generator Tubing, Bolting Failure Analysis, Probability Based Load Combinations for Design of Category I Structures, Mechanical Piping Benchmark Problems, Identification of Age-Related Failure Modes; Analysis of Human Error Data for Nuclear Power Plant Safety-Related Events, Human Factors Aspects of Safety/Safeguards Interactions During Routine Reactor Operations and Off-Normal Conditions, Emergency Action Levels, and Protective Action Decision Making. The previous reports have covered the period October 1, 1976 through December 31, 1983.

TABLE OF CONTENTS

TABLE OF CONTENTS (Cont'd.)

TABLE OF CONTENTS (Cont'd.)

FIGURES

FIGURES (Cont'd.)

FIGURES (Cont'd.)

FIGURES (Cont'd.)

TABLES

I. DIVISION OF ACCIDENT EVALUATION

SUMMARY

High Temperature Reactor Research

After 6232 hours of accumulated oxidation time, the oxidation of four Stackpole 2020 medium sized samples (7.62 cm ϕ 15.24 cm long) was terminated. The weight losses ranged between 5.87% to 8.61%. The oxidation rate was increasing as a function of time. One of the samples will be profiled to study oxidation gradient. The elastic moduli of the rest of the samples will be measured by ultrasonic wave velocity measurement techniques. Compressive strength will be measured in a destructive way after that.

The effect of He coolant flow rate on the silver aerosol particle size was studied. The aerosol particle size is increasing as the flow rate increases.

For the integrated fission product transport study, the mechanism(s) for the cooling channel blockage were studied. Blank H-451 susceptors (without Mo_2C) heated at 2400°C and 2800°C did not show blockage. In the next run, it was observed that small globular clusters began to grow at 2850°C on the inner chimney wall, and after 1-1/2 hours at 3000°C, the cooling channel was ~98% (in cross section) blocked. Electron dispersive x-ray analysis results showed that Si played an important role in the blockage of the cooling channel.

The approximate amount of SiC per fuel block is calculated to be ~2.3% by weight. Thus, two experimental runs were conducted with 3.7% and 1.39% of SiC by weight, respectively, filling the fuel channels. In the run with 3.7% SiC, the chimney began to show initiation of a blockage at 2400°C, and after about 15 minutes it was almost completely blocked. In the run with 1.39% SiC, it took 2 hours to block more than half of the cross section of the chimney.

An initial assessment of heat transfer conditions in the Containment Building (CB) atmosphere during Unrestricted Core Heat-up Accident (UCHA) scenarios shows that reliable analyses of the temperature evolution can be obtained from simplified models. Corresponding programming is currently in progress with results expected during the third quarter.

The analysis of vapor migration in PCRV concrete during UCHA scenarios has progressed to the point where first results have been obtained. These indicate that due to the gradul PCRV heat-up, initially with the liner in place, a dry region next to the core cavity is being formed, and that at time of liner failure the actual water ingress into the core cavity appears to be significantly lower than previously assumed. Final revision of the code to obtain reasonable computing efficiency is currently in progress.

SSC Development, Validation and Application

The Super System Code (SSC) Development, Validation and Application Program encompasses a series of three computer codes; (1) SSC-L for system transients in loop-type liquid metal-cooled reactors (LMRs); (2) SSC-P for system transients in pool-type LMRs, and (3) SSC-S for long term shutdown transients. In addition to these code development and application efforts, validation of these codes is an ongoing task.

Under SSC-L activities, two additional models were completed for the SSC representation of the SNR-300 system. These were: 1) the power limiter control, which is designed to ensure that the reactor power remains below 107% for a long period as well as limiting the decay heat and avoiding scram during slow transients, and 2) the temperature limiting control, which is designed to ensure that the hot leg sodium temperatures in the primary and secondary loops cannot remain at higher than design level for long periods. Work was done on the development of appropriate numerical schemes for including inter-assembly heat transfer effects into SSC. Several finite-difference based schemes and nodal schemes have been developed and are being evaluated.

Efforts on the SSC-P code were directed at improving the input deck for the EBR-II simulations. Additionally, code modifications were implemented to better simulate the EBR-II primary system hydraulics. In related areas, the pool version is being modified to take advantage of recent improvements made to the base program library under the loop version development, but which are nevertheless applicable to SSC-P as well.

Work on the SSC-S code remains concentrated on improving the upper plenum representation by providing an optional two-dimensional model. A representation of the FFTF upper plenum was carried out to 300 seconds of transient simulation time for a coastdown to natural circulation event.

Validation areas pursued during this reporting period included: development of a fourth, standard test problem, designed to detect unintentional asymmetries which might be introduced by code modifications; testing of the newest entire update set with the standard problems; and evaluating the fuel-clad gap conductivity model for possible revision.

CRBR Balance of Plant Modeling

The Balance of Plant (BOP) Modeling Program deals with the development of safety analysis tools for system simulation of nuclear power plants. It provides for the development and validation of models to represent and link together BOP components (e.g., steam generator components, feedwater heaters, turbine/generator, condensers) that are generic to all types of nuclear power plants. This system transient analysis package is designated MINET to reflect the generality of the models and methods, which are based on a momentum integral network method. The code is to be fast-running and capable of operating as a self-standing code or to be easily interfaced to other system codes.

Models for Version 1 of the MINET code have been completed and tested. A major activity recently has been to complete the initial report containing the code documentation and user's manual. A 1,000 node test case has been successfully completed, although it required usage of Large Core Memory on the BNL 7600 machine. A new utility routine has been added to MINET, which performs data management and interpolation for tabular boundary condition and internal driving functions. Also, other system time constants have now been included when the check is made for the smallest time constant, which helps in determining the next timestep size.

Control system models for the SNR-300 steam generator system were incorporated into Version 0 of MINET, which operates concurrently with the SSC code. These models include; 1) main feedwater valve control, 2) emergency feedwater valve control, 3) feedwater pump speed control, 4) steam drum drain valve flow control, 5) feedwater temperature control, and 6) steam pressure control. A null transient and a normal plant trip transient were performed to ensure that all these models were functioning properly.

Further parametric tests were performed using the helical coil steam generator representation and comparing to experimental data. The EBR-II representation was used to simulate the full 44 minutes of an actual test, run previously at that facility. MINET representations were developed for a specific once-through steam generator design as well as for a particular U-tube steam generator design. In both cases, comparisons were drawn to available experimental data.

Work is progressing on implementing the interface between the RAMONA-3B code (for BWR transient analysis) and the MINET code. The code locations and key variables have been identified and a means for performing the interface has been developed. Test input decks for the combined RAMONA/MINET code have been accomplished.

Thermal-Hydraulic Reactor Safety Experiments

A description is presented of core melt-water mixing simulation experiments. The experiments are designed to evaluate one- and two-dimensional models of core melt-water mixing in a drop-mode contact configuration. Experiments are performed with spherical steel particles, preheated to desired temperature, and dropped into a pool of saturated water. Initial experiments are conducted with 3-mm particles and pools of saturated water up to depths of one meter. Both the diameter of the column of shot and the pool diameter are constrained to 100 mm. Results for the steam generation rate transient are presented, along with observations taken from motion pictures. Results indicate that the initial particulate to enter the water transfers energy to the water and produces steam fluxes large enough to fluidize and disperse (upwards) the particles which did not yet encounter the water.

A comparison is presented of theoretical results based upon a simplified model for debris bed quench under bottom reflood conditions and experimental results for the vapor flux at the top of the bed from one of the experiments. Experiments were conducted under conditions of constant liquid flux. The results, which show reasonable agreement between the predicted and measured vapor flux, demonstrate the effectiveness of the model and suggest the importance of accurate modeling of the particle-water heat transfer coefficients.

The liquid-liquid film boiling apparatus was rebuilt after it was accidentally destroyed during a test. During the reconstruction period, additional improvements were made to the hardware and software. During the quarter, 21 R11/liquid metal film boiling experiments with non-condensable gas flux through boiling interface were performed. The range of gas superficial velocity in these tests was from 0.6 cm/s to 5.0 cm/s. The liquid metal pool was observed to cool isothermally and freeze as a porous slurry. No vapor explosions occurred during these tests. The data for the case with J_G = 0 cm/s (Run 131) were found to behave similarly to the Berenson film boiling model but were greater in magnitude by a factor of two. When the gas superficial velocity was increased to 0.77 cm/s (Run 212) and 5.0 cm/s (Run 219), the measured boiling heat flux was enhanced over the zero gas flux case by a factor of 1.25 and 2.3, respectively, approaching as an upper limit the critical heat flux.

Development of Plant Analyzer

The LWR* Plant Analyzer Program is being conducted to develop an engineering plant analyzer capable of performing accurate, real-time and faster than real-time simulations of plant transients and Small-Break Loss of Coolant Accidents (SBLOCAs) in LWR power plants. The first program phase was carried out earlier to establish the feasibility of achieving faster than real-time simulations and faster than mainframe, general-purpose computer (CDC-7600) simulations through the use of modern, interactive, high-speed, special-purpose minicomputers, which are specifically designed for interactive time-critical systems simulations. It has been successfully demonstrated that special-purpose minicomputers can compete with, and outperform, mainframe computers in reactor simulations. The current program phase is being carried out to provide a complete BWR simulating capability, including on-line, multicolor graphics display of safety-related parameters.

The plant analyzer program is directed primarily toward reactor safety analyses, but its results are also useful for on-line plant monitoring and accident diagnosis, for accident mitigation, further for developing operator training programs and for assessing and improving existing and future training simulators. Major assets of the simulator under development are its extremely low cost, unsurpassed convenience of operation and high speed of simulation. Major achievements of the program are summarized below.

Existing simulator capabilities and limitations regarding their representation of the Nuclear Steam Supply System have been assessed previously. Simulators reviewed at the time have been found to be limited to steady-state simulations and to restricted quasi-steady transients within the range of normal operating conditions.

A special-purpose, high-speed peripheral processor had been selected earlier, which is specifically designed for efficient systems simulations at real-time or faster computing speeds. The processor is the AD10 from Applied Dynamics International (ADI) of Ann Arbor, Michigan. A PDP-11/34 Minicomputer serves as the host computer to program and control the AD10 peripheral processor. Both the host computer and the peripheral processor have been operating at BNL since March 15, 1982.

An existing model for nonequilibrium, nonhomogeneous two-phase flow in a specific BWR hydraulics system had been implemented on the AD10 processor for the purpose of comparing the computing speed and accuracy of the AD10, as it executed the code called HIPA-PB2 for High-Speed Interactive Plant Analysis of the Peach Bottom-2 BWR power plant. The implementation of HIPA-PB2 had been carried out in the high-level language MPS-10 of the AD10.

It had been demonstrated during the last quarter of 1982 that the AD10 special-purpose peripheral processor can produce accurate simulations of BWR design base transients at computing speeds ten times faster than real-time and 110 times faster than the CDC-7600 mainframe computer carring out the same simulation.

After the successful completion of the feasibility demonstration, work has continued to expand the hydraulics simulation used for that demonstration to produce the capability of simulating the entire nuclear steam supply system as well as the flow of the working medium through turbines, condensers and feedwater trains.

Models have been developed and implemented for point neutron kinetics with six feedback mechanisms and seven automatic scram trip initiations, for thermal conduction in fuel elements, for steam line dynamics capable of simulating acoustical effects from sudden valve actions, for turbines, condensers, feedwater preheaters and feedwater pumps and for emergency coolant injection systems.

The software systems of both the PDP-11/34 host computer and the AD10 special-purpose peripheral processor have been upgraded to achieve greater computing speed and a larger number of analog input/output channels. Two AD10s are coupled via a direct bus-to-bus interface to compute in parallel.

Models had been developed, scaled and implemented for the feedwater controller, the pressure regulator and the recirculation flow controller. Twenty-eight parameters for initiating control systems and valve failures and for selecting set points can now be changed on-line from a 32-channel control panel. Sixteen dedicated analog output lines are provided for the simultane-

ous display of 15 selected parameters versus time. All input-output channels are addressed approximately 200 times per second.

During the previous reporting period, all program modules have been combined into the HIPA-BWR/4 code. The entire BWR power plant simulation, including the nuclear steam supply system, the steam lines with all valves, the turbines, condensers, feedwater preheater and pumps and the control systems, has been executed. Fifteen selected parameters can be stored simultaneously in the IBM Personal Computer and then displayed as functions of time in labelled diagrams. A silent movie has been produced to show how the plant analyzer is operated and how it responds to on-line analog signals.

During the last reporting period, we compared plant analyzer results with published results from GE for 10 different ATWS events. Selected comparisons are presented in this report. The plant analyzer code has been generalized to simulate any BWR-4 power plant in response to input data changes from the keyboard. The code is called HIPA-BWR/4. A draft report has been completed to document the plant analyzer.

The interest in the Plant Analyzer Development Program continues to be high, both in domestic and foreign institutions. Four presentations with demonstrations were given at BNL to foreign visitors, and two invited papers have been presented and submitted for publication during the current reporting period. Five presentations were given during March and April 1984 in laboratories and institutions abroad.

Code Assessment and Application (Transient and LOCA Analyses)

Two major code application tasks, namely, the RESAR-3S large break LOCA study and the typical BWR/4 MSIV closure ATWS analysis, have been completed, and are being documented in two separate topical reports.

The first task showed that there is an overall safety margin of ~1200°F for a large break LOCA in Westinghouse 4-loop RESAR-3S type plants. Approximately 500°F of this total margin is due to the conservative initial and boundary conditions prescribed in Appendix K of 10 CFR 50, and the remaining 700°F is due to the conservative physical models recommended in the same Appendix K. It is suggested that this study be further continued to determine conservatism due to each individual assumption in order to make objective recommendations for Appendix K revision.

The second task showed that both RAMONA-3B and TRAC-BD1 are capable of calculating the overall behavior of a typical BWR/4 during an MSIV closure ATWS. However, TRAC-BD1 with a point kinetics model is unable to predict the significant spatial power variations that occur during such transients, and predicted by the RAMONA-3B code with three-dimensional neutron kinetics. The computer running time for RAMONA-3B with significantly more computational cells was also lower (by a factor of ~4) than that for the TRAC-BD1 code.

Therefore, it is recommended that the RAMONA-3B code be extensively used for further analysis of ATWS type events in a BWR.

Progress has been made in implementation of TRAC-BD1/MOD1 on the BNL CDC-7600 computer. Work has also begun in preparing an input deck for the FIST faciity for TRAC-BD1/MOD1 assessment.

Thermal Reactor Code Development (RAMONA-3B)

Extended support has been provided to three RAMONA-3B application projects, namely, BWR/4 MSIV closure ATWS analysis for the Code Assessment and Application program, eccentric control rod drop analysis for NRC/NRR, and the Browns Ferry ATWS study under the NRC Severe Accident Sequence Analysis (SASA) program. Several improvements and corrections have been made as a part of this user support activity.

Corrections for the reactivity edits have been received from Scandpower. A RAMONA-3B User's Manual has been prepared, and the code (RAMONA-3B/MODO/ Cycle 7) has been distributed to five U. S. organizations for analysis of U. S. reactors.

Calculational Quality Assurance in Support of PTS

The detailed, in-depth review of six selected Calvert Cliffs PTS transients has been completed. The TRAC results of primary side temperature and pressure have been verified using a simple method developed at BNL. In general, the TRAC results have been found to be quite reasonable, and the review work has been documented in a BNL topical report.

The RELAP5 input decks for the H. B. Robinson-2 PTS calculations have been reviewed. In general, the input decks have been found to be acceptable. Work has begun in reviewing the RELAP5 transient calculations.

1. High Temperature Reactor Research

1.1 Graphite and Ceramics (B. S. Lee, J. H. Heiser, III, and D. R. Wales)

1.1.1 Long Term Oxidation Experiments

After 6232 hours (260 days) of accumulated oxidation time, four Stackpole 2020 medium sized specimens (7.62 cm ϕ x 15.24 cm long) were removed from the furnace and weighed, and the results are shown in Table 1.1.1 and Figure 1.1.1. These samples have been oxidized at 850°C in an environment of which the H_2O and H_2 levels were maintained at ~500 vppm and ~5000 vppm, respectively. The level of oxidation products (CO_2 + CO + CH_4) was maintained below 250 vppm, and the balance was He (total pressure = ~1 atm).

As shown in Table 1.1.1, the weight losses are between 5.87% to 8.61% after 6232 hours, which are much higher than expected. Thus, it was decided to stop the oxidation of these Stackpole 2020 medium sized samples.

The samples did not show any significant dimensional changes or pit formations. However, the surface was very friable, and the skin easily spalled off as shown in Figure 1.1.2.

Table 1.1.1 Weight Losses for the Stackpole 2020 Samples

Sample	Wt. Loss (%)		
	After 2424 hrs.	After 3020 hrs	After 6232 hrs
No. 1 (Closest to the gas inlet)	0.71	1.06	5.87
No. 2		1.58	8.61
No. 3		2.08	7.80
No. 4		1.72	6.12

Figure 1.1.3(a) is a SEM micrograph of the inside of the spalled skin. Electron dispersive x-ray analysis (EDAX) showed that the major impurities in this area are Fe and Ca, and an x-ray map for the Fe of the same area is shown in Figure 1.1.3(b). Ca is more dispersed than Fe for the same region.

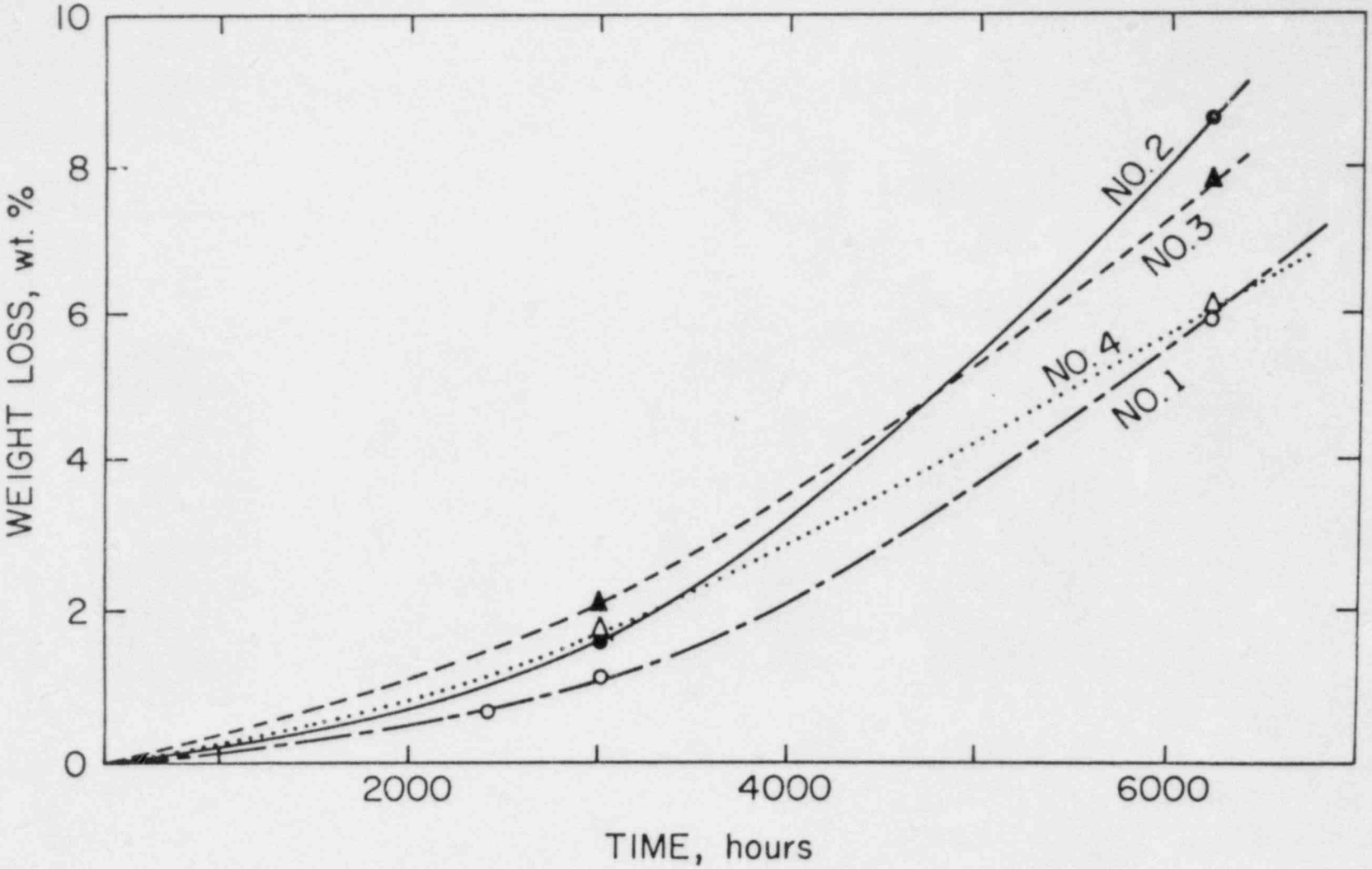

Figure 1.1.1 Weight Losses as a Function of Time for Stackpole 2020 Mid-Sized Samples.

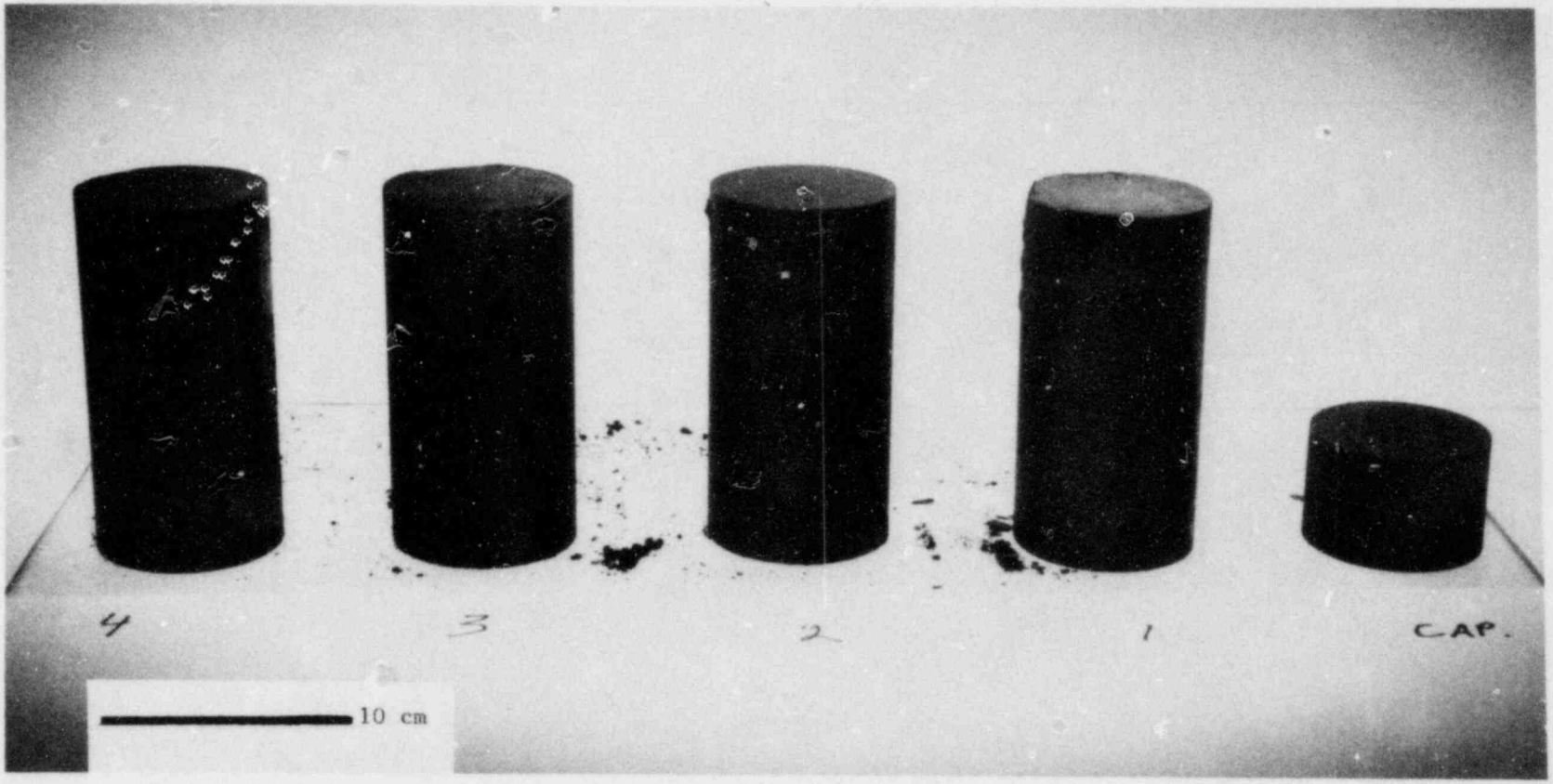

Figure 1.1.2 Stackpole 2020 Samples Oxidized for 6232 Hours (~260 Days) at 850^{0}C.

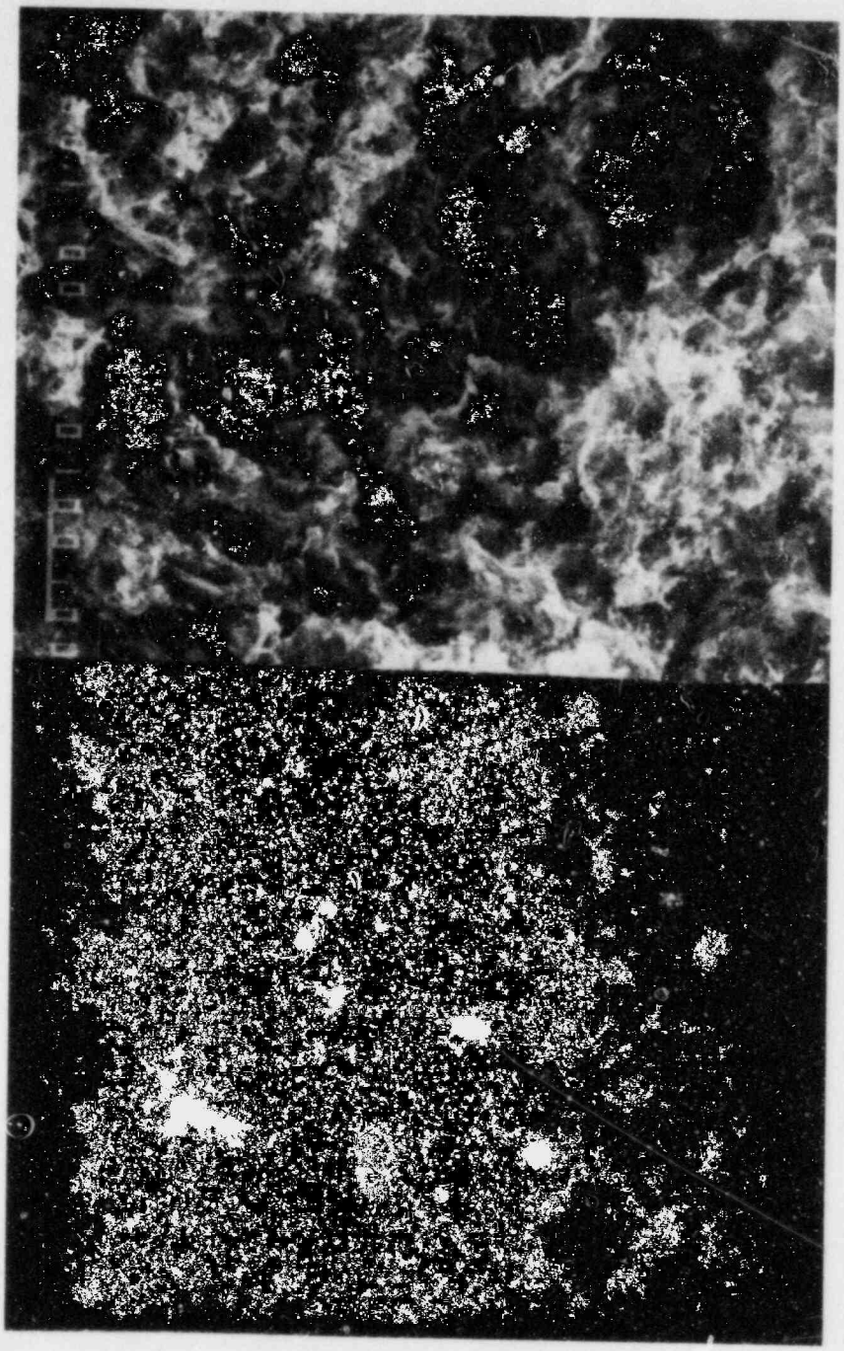

Figure 1.1.3 a) SEM Micrograph of the Inside of the Spalled Skin from S-2020 Medium Sized Sample.
b) X-Ray Map for Fe of the Area Shown in a).

One of the samples will be profiled to study oxidation gradient. The elastic moduli of the rest of the samples will be measured by ultrasonic wave velocity mesurement techniques. Compressive strength will be measured in a destructive way after that.

This medium term oxidation experiment under realistic condition will be continued with PGX samples. The oxidation condition will be reevaluated before initiating the oxidation of new samples.

1.2 Fission Product Migration (B. S. Lee, J. H. Heiser, III, and C. C. Finfrock)

1.2.1 Fission Product Migration by an Aerosol Formation

The study on fission product migration by an aerosol formation was continued this quarter. The objectives for this study is a determination of major parameters that affect aerosol formation and an identification of aerosol formation mechanisms for different fission products.

It was reported in the previous progress report that the amount of silver collected by a filter seems proportional to the flow rate of the coolant (B. S. Lee, 1983). In this quarter, the aerosol particle size for each run was measured by taking photomicrographs of the aerosol particles with a scanning electron microscope, and some results are shown in Figure 1.2.1. It can be seen that the particle size increases as the coolant velocity increases.

The particle sizes were also measured at different temperatures ranging from 1400 - 1800°C. More results will be reported and analyzed in the next quarterly report.

1.2.2 Integrated Fission Product Transport Experiments

As reported in the previous quarterly report, the two experimental runs with Mo_2C at 3000 and 3200°C showed blockages of the cooling channel which is located at the center of the mock-up fuel block above the susceptor. The diagram of the experimental set-up is shown in Figure 1.2.2. The filters showed a trace amount of Mo and small amounts of Na, K and Cl.

Since both runs showed extensive blockages of the cooling channel even though He gas was pulled by a mechanical pump which was connected after a filter, it was suspected that due to negative gauge pressure in the coolant channel, air entered the system to oxidize the graphite and that this could have lead eventually to block the cooling channel with the graphite particles generated by the oxidation. To remove this possibility, two very sensitive pressure gauges (sensitivity; 2.5 N/m^2) were installed to aid in keeping the pressure inside the cooling channel 12.44 N/m^2 (1.2×10^{-4} atm) above atmospheric pressure.

After these two runs, it was decided to study the mechanism(s) for the cooling channel blockage more in detail because of its potential importance in the course of UCHA's.

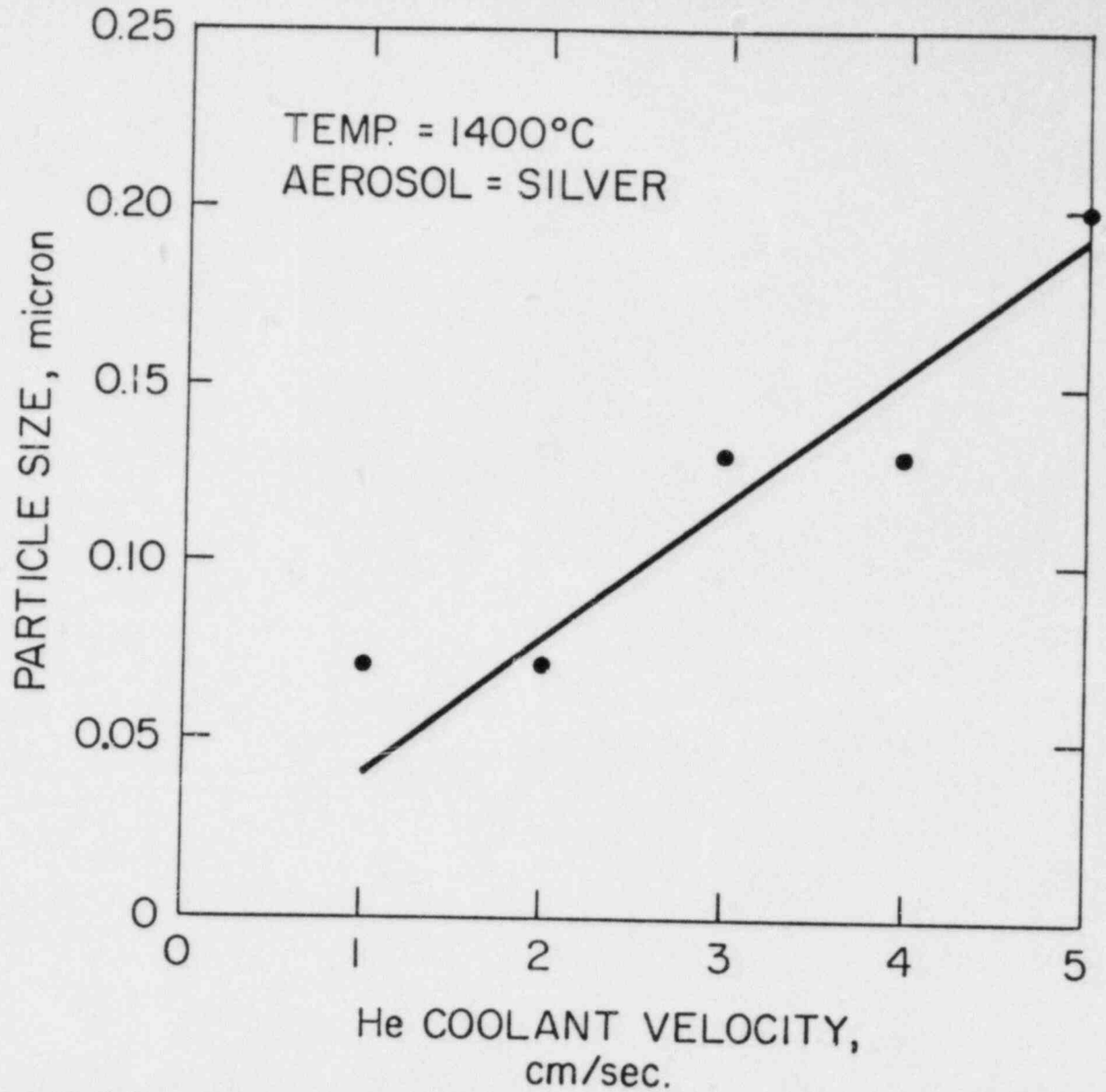

Figure 1.2.1 Silver Aerosol Particle Size as a Function of He Coolant Velocity at 1400 °C (Crucible Temperature).

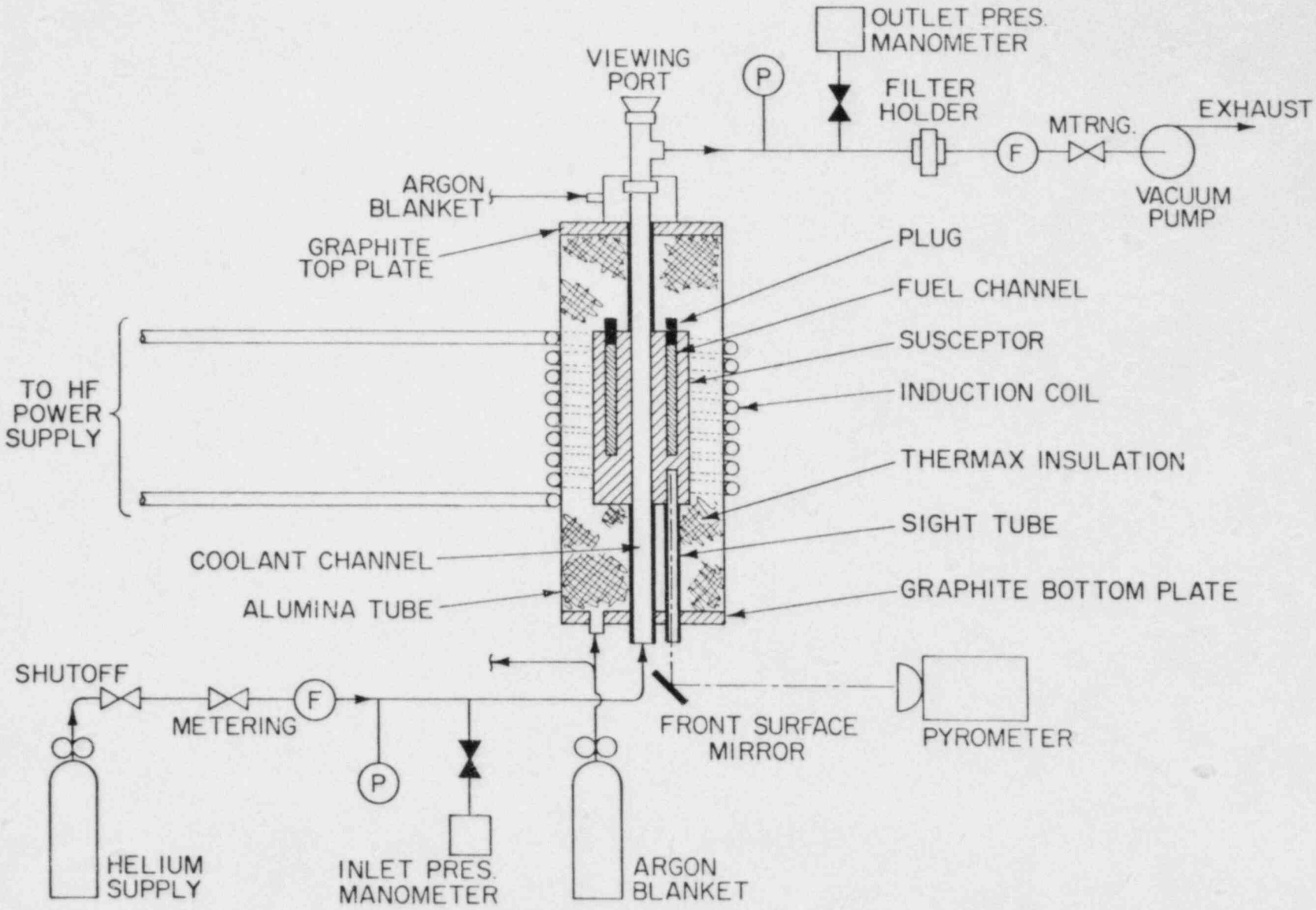

Figure 1.2.2 Experimental Set-Up for Integrated Fission Product Migration Study.

A blank H-451 susceptor (without Mo_2C) was heated at 2400°C for 6 hours (Run #13184) and no blockage was observed. The filter collected small amounts of NaCl and KCl.

It was believed that observing the blockage of the cooling channel (chimney) in situ should give us more information on blockage mechanism and flexibility in conducting experiments. Thus, the experimental set-up was modified so that the inner walls of the chimney/susceptor could be viewed on a video monitor of a video camera equipped with a telescopic lens and a quartz window attached to the top of the chimney. Argon flow through the thermax insulation was also added to minimize the oxidation of thermax.

In the run with 1.39% SiC (Run #31384) at 2400°C, the EDAX results from the filter showed the peaks from Si, S, Na, K, Cl and Ca. Sulfur is believed to be from the SiC used for the experiment, and Na and Cl exists in a crystalline form of NaCl. It took 2 hours to block more than half of the cross-section of the chimney. The chimneys will be split and examined by a SEM and TEM, and the results will be reported in the next progress report.

1.2.2.1 Temperature Gradient in the Susceptor

A 8.26 cm diameter by 15.2 cm long cylindrical susceptor was fabricated for the purpose of observing any temperature gradient in axial direction. Four sight tube holes were bored longitudinally around the coolant channel to depths of 2.54, 5.08, 7.62 and 10.16 cm measured up from the bottom of the susceptor. They were spaced at 60° intervals around the circumference of a circle with radius 2.17 cm.

The susceptor was heated to a temperature of 2400°C measured at the 7.62 cm depth. A flow of helium through the coolant channel was maintained at 600 cc/min at the inlet. Shortly after stabilizing at 2400°C for 1 1/2 hours on the 7.62 cm hole, the temperatures for the other holes were measured, and the results are shown in Table 1.2.1.

Table 1.2.1
Temperatures of the Susceptor at Different Depths

Depth (cm)	Temperature (°C)
2.54	2360
5.08	2380
7.62	2400
10.16	2415

As shown in this table, temperature gradient does exist even though the temperature variation is ~2%. For the integrated fission product migration experimental runs, the temperatures are measured at 2.54 cm. More temperature gradient runs are planned at higher temperatures, to evaluate the uncertainties due to lack of thermal uniformity.

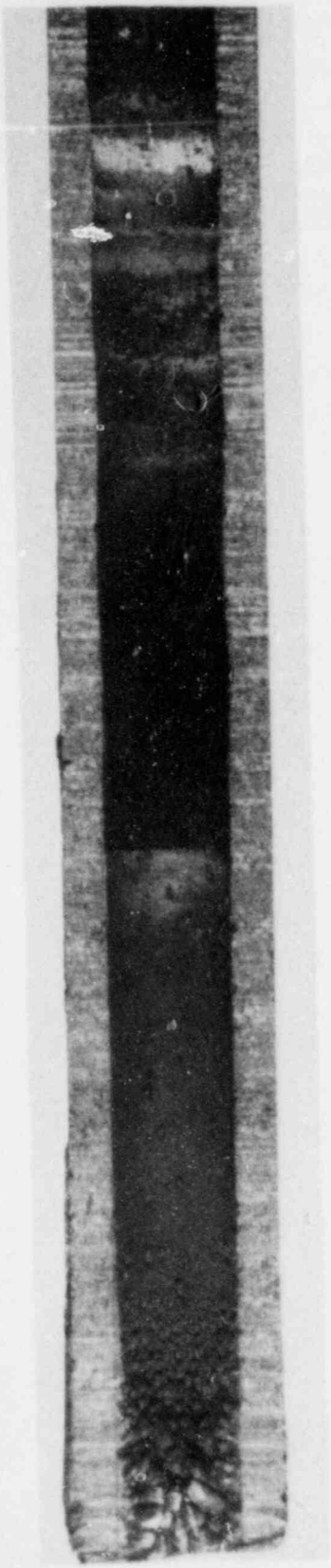

REMARKS

6 — high peaks of Si, Ca

5 — Si, Fe

4 — Si, V, no Fe

3 — high V, Ti

2

1 — graphite deposits

Figure 1.2.3 Cross Section of a Chimney from the Run 11184. Mag. 14x at 3200^{0}C.

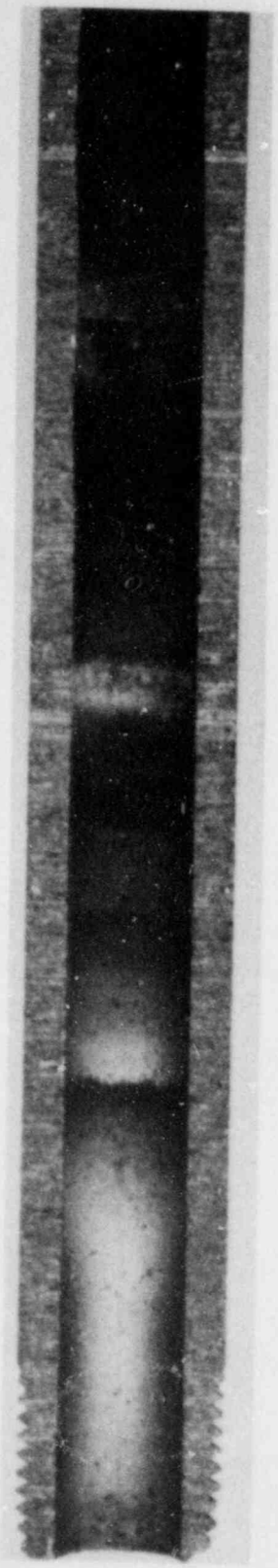

REMARKS

salt crystals

6 — Si

7 — high Si, high Ca, high Fe

8 — high Si, high Fe (Si increasing, Fe decreasing)

9 — high V, little Ti, no Si

10 — Small amount of Si

Figure 1.2.4 Cross Section of a Chimney from the Run 13184 with a Blank Susceptor at 2400°C. Mag. 14x.

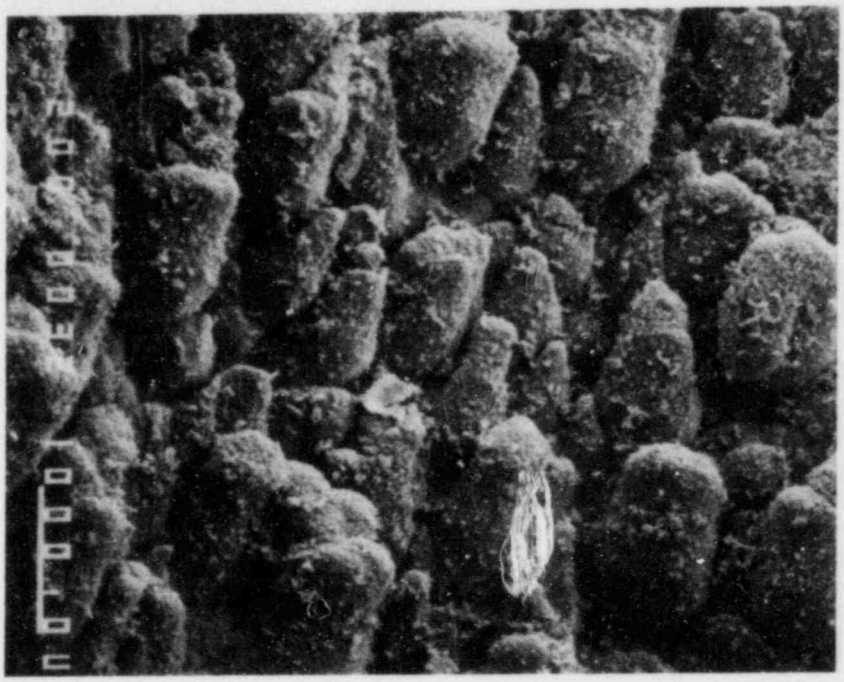

Figure 1.2.5 Graphite Particles Deposited at the Blockage of the Chimney, Section 1 in Figure 1.2.3. Mag. 20x.

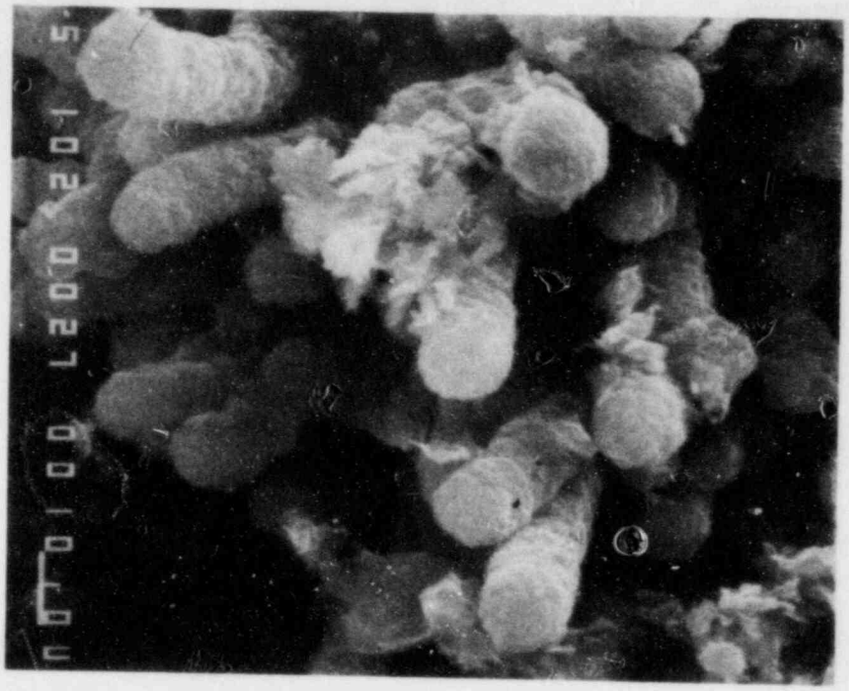

Figure 1.2.6 Fiber Shaped Graphite Growing in Section 3 of Figure 1.2.3. This Area Showed X-Ray Peaks of V and Ti. Mag. 1000x.

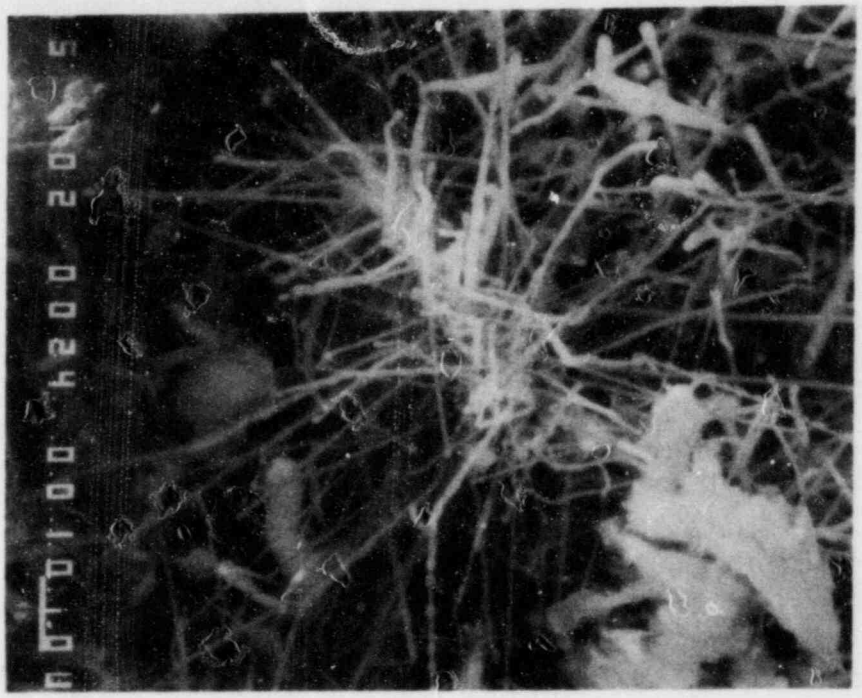

Figure 1.2.7 The Treads are Believed to be SiC from Section 5 in Figure 1.2.3. X-Ray Peaks of Si and Fe were Observed. Mag. 1000x.

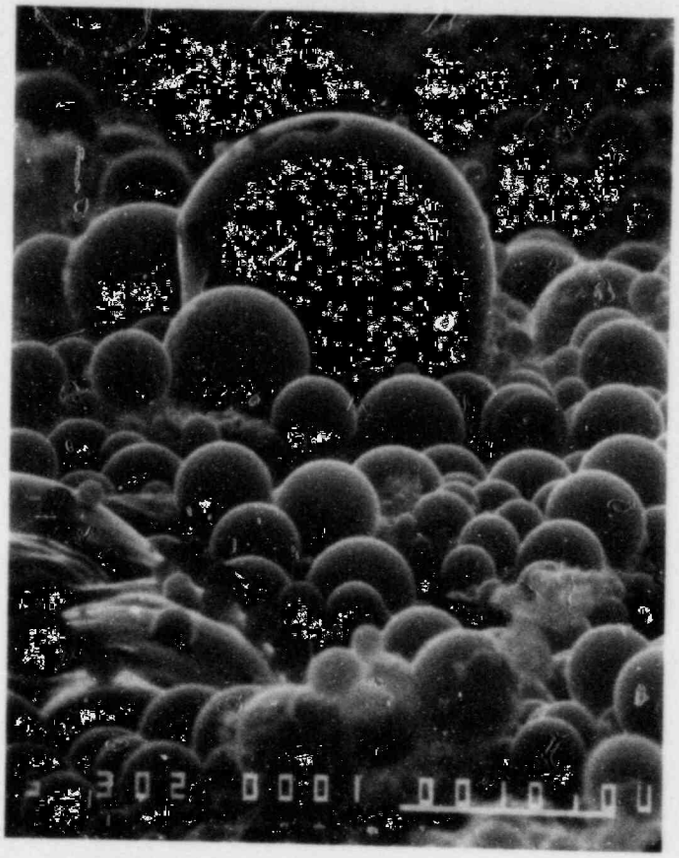

Figure 1.2.8 From Section 6 of Figure 1.2.3. The Balls Showed High X-Ray Peaks of Si and Ca. Possibly Silicate Glass Beads. Mag. 3000x.

1.2.2.2 Elemental Analysis of H-451 Graphite and Thermax

Since the upper part of the chimney (see Figure 1.2.3) and the filters showed small amounts of NaCl and KCl crystals, it was decided to analyze the H-451 graphite and thermax for Na and K to find the source of these elements. H-451 graphite and thermax, 10 grams each, were ashed with low temperature asher from LFE Corporation* for 5 days. This apparatus oxidizes the graphite by generating O_3 through inductive coupling and reaches temperatures in the range of ~200°C. After the ashing, atomic absorption spectrophotometry technique was used to analyze for Na and K, and the results are shown in Table 1.2.3. The detailed procedure for the analysis is described in our earlier progress report (BNL-NUREG-51454, 1981).

After 2 hrs run at 2800°C of a blank H-451 susceptor (Run #2984), the inner wall of the chimney was plated with compounds apparently made of graphite impurity elements. However, the chimney was not blocked. The filter showed small amounts of NaCl and KCl.

In the next run (Run #21584) it was observed through the video camera described above that small globular clusters began to grow at 2850°C on the inner chimney wall surface that was close to the susceptor. After 1 1/2 hours at 3000°C, the chimney was ~98% (in cross-section) blocked. The filter again showed NaCl and KCl.

The chimneys were split and sectioned after the experiments and optical and electron microscopes were used to examine the inner wall surfaces.

Earlier BNL studies on sublimation of H-451 graphite (Soo, 1978) showed that Si, Fe, S, Cl, and Ca are the major impurities that evaporated from the graphite and deposited on the walls of the sight tube. Those experiments were conducted at ~3800°C.

The impurities from the current runs are similar to those mentioned above except that V also deposited in significant amount. Figure 1.2.3 and 1.2.4 show the inner walls of the chimneys from the 3200 and 2400°C run, respectively, and the EDAX analysis results are also shown.

In both experiments, the order of the plated-out elements are identical, and the morphologies of the depositing compounds are the same. Some of the representative morphologies of the deposits are shown in Figures 1.2.5 through 1.2.8.

It was noticed that Si deposited on the inner surface of the chimney over a wide range of temperature gradients. In addition, the morphology of the deposits suggest that Si compounds plate-out in liquid form and work as a particle getter, which may explain why the filter did not collect aerosol particles. At cold regions (upper part of the chimney), Figure 1.2.8, the Si compound deposited in the form of glass balls due to the higher cooling rate than the lower part.

*Waltham, Ma.

In a core heat-up accident situation, the SiC coatings in fuel particles fail and the silicon is one of the elements that would migrate to the cooling channel. The amount of Si from the fuel is orders of magnitude higher than that from the graphite impurities. The approximate amount of SiC per fuel lock is calculated to be ~2.3% by weight. Thus, two experimental runs were conducted at 2400°C with 3.7% and 1.39% of SiC by weight, respectively, filling the fuel channels. Pure graphite powder was mixed with SiC powder, and the mixture was poured into the fuel channels.

In the run with 3.7% SiC (Run #3184), the chimney began to show initiation of a blockage at 2400°C, and after about 15 minutes it was almost completely blocked.

Table 1.2.3

Na and K Contents in H-451 Graphite and Thermax[a]

	Na (ppm)	k (ppm)
H-451 Graphite	4	<1
Thermax	46	7

a. Tradename for thermal carbon (Vanderbilt Co.)

1.3 Analytical

1.3.1 Containment Building Atmosphere (P. G. Kroeger, B. C. Chan)

Previous analyses of the containment building (CB) atmosphere under UCHA conditions (App. F of Reilly et al, 1984) did not include the capability to compute gas and structure temperatures, and were based on rough estimates of these temperatures.

An initial assessment of heat transfer conditions in the CB during UCHA without LCS, i.e., with ingress of concrete decomposition gases from the PCRV, indicates that significant natural circulation will occur in the upper hemisphere of the CB with the natural circulation mass flow rate being approximately five to ten times larger than the incoming mass flow from te PCRV. At the same time,the hot incoming gases are strongly radiating due to their CO_2 and H_2O content.

The details of heat transfer by simultaneous natural circulation and gas radiation in a strongly non-isothermal cavity would be difficult to analyze. However, under the prevailing conditions approximate limiting analyses, considering either the natural circulation heat transfer alone, or considering gas radiation alone, show that in either case the bulk gas temperature will be close to the CB inside wall surface temperature, and that the conduction transient into the solid structures dominates the CB atmosphere temperature evolution.

Therefore, a simplified model has been formulated and coding is currently in progress. The model includes a transient lumped solution of mass and energy conservation for the gas atmosphere, with convective heat transfer from the gas to the CB structures using a turbulent natural convection boundary layer model. Radiation heat transfer from the hot incoming gas and through the bulk of the gas to the structures is considered using the optically thick limit. Heat conduction into the CB walls and into the outside of the PCRV structure is modeled as one-dimensional transient conduction. Condensation is currently being considered as a net energy removal from the system, due to condensation on the solid surfaces. The expected earlier condensation on particles in the gas stream (cloud condensation) will be considered later. While it has no significant effect on the temperature evolution, it does effect the potential settling of fission product aerosols.

1.3.2 Vapor Migration in Concrete (P. G. Kroeger, Y. Shiina)

The full model of vapor migration in concrete permitting time varying boundary conditions and temperature dependent concrete properties has been completed and debugged. Initial results have been obtained. The model solves the one-dimensional transient energy and mass conservation equations in a porous concrete structure, being heated at the thermal barrier surface. The Darcy porous flow approximation is used for the fluid velocities. The presence of a non-condensable gas is included and is found to be of significant effect. During a typical transient, as the heat-up of PCRV concrete progresses and the outer concrete surface temperature reaches the water saturation temperature, a "dry region" is being formed at the outer surface, and a "front" separating this dry region from the cooler "wet region" begins to pass through the porous concrete. The dry region contains only vapor, generally in the superheated state. The wet region contains water as liquid and as saturated vapor, and non-condensables (air), but the latter are generally not found close to the front.

Typical results for a sample transient are shown in Figures 1.3.1 and 1.3.2. The thermal barrier heat-up transient, which is a boundary condition for this code is taken from previous core heat-up analyses (App. F of Reilly et al, 1984). The concrete properties used are best estimate data for PCRV concrete, except that the liquid phase flow rate was artificially reduced by three orders below the best data available. Reduced liquid flow will increase the gas pressure in the concrete behind the liner, and will decrease the width of the dry region which is being formed during the initial PCRV heat-up.

Figure 1.3.1(a) shows the heat-up of concrete for a typical UCHA scenario with thermal barrier in place but without operating liner cooling system. At about 3 hrs the dry region begins to be formed, as the liner surface and front temperatures separate. The front position and velocity are shown in Figure 1.3.1(b). After about 40 hrs a 30 cm dry region containing only superheated vapor has been formed. Figure 1.3.1(c) shows the front temperature and pressure. It should be noted that the dry region pressure is essentially constant and equal to the front pressure as long as the liner remains intact and the outer surface is thus impermeable. Thus, for this case of reduced liquid

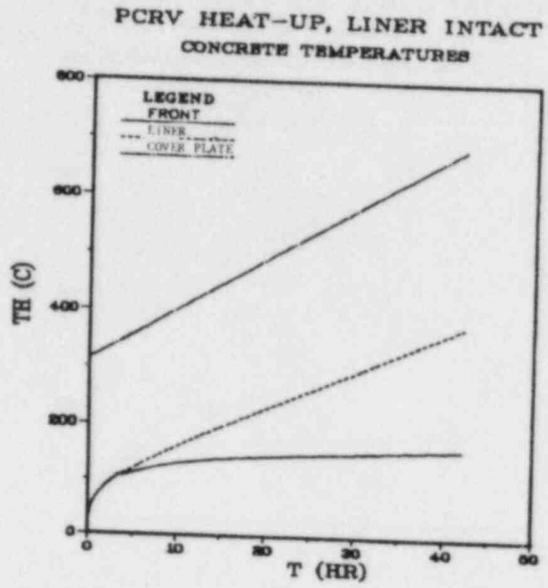

(a)

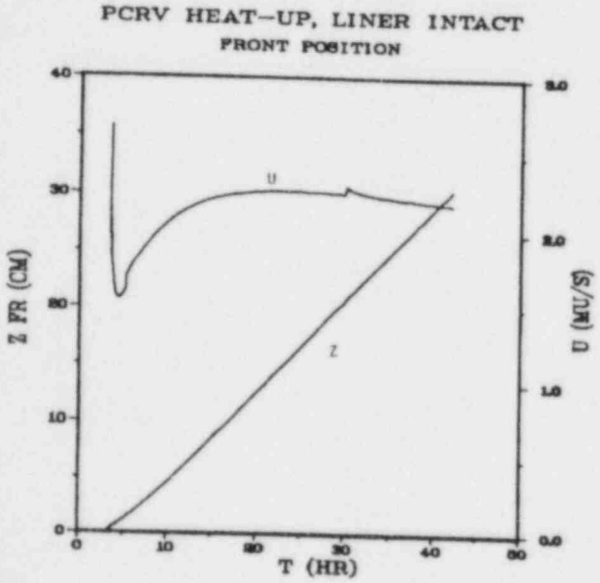

(b)

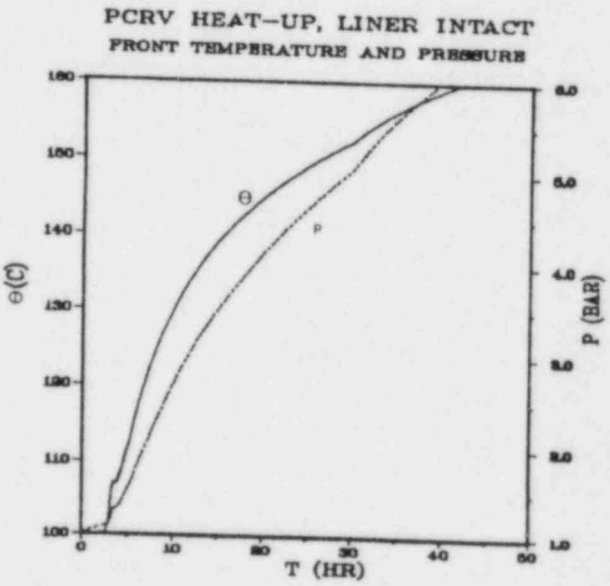

(c)

Figure 1.3.1 Concrete Vapor Migration During PCRV Heat-Up Prior to Liner Failure.

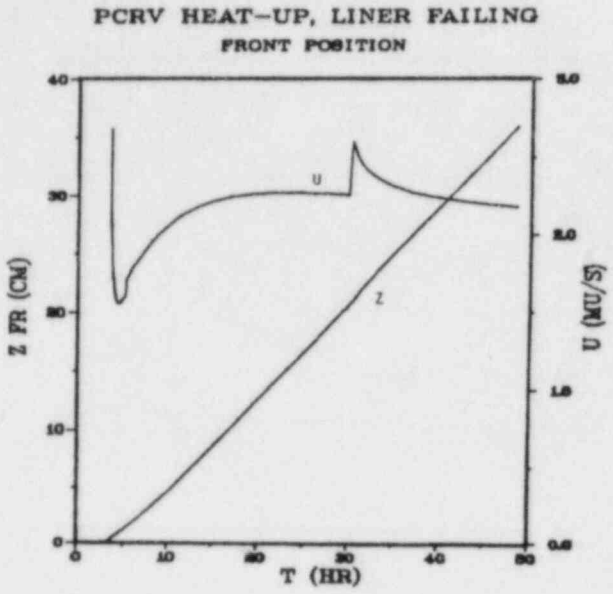

(a)

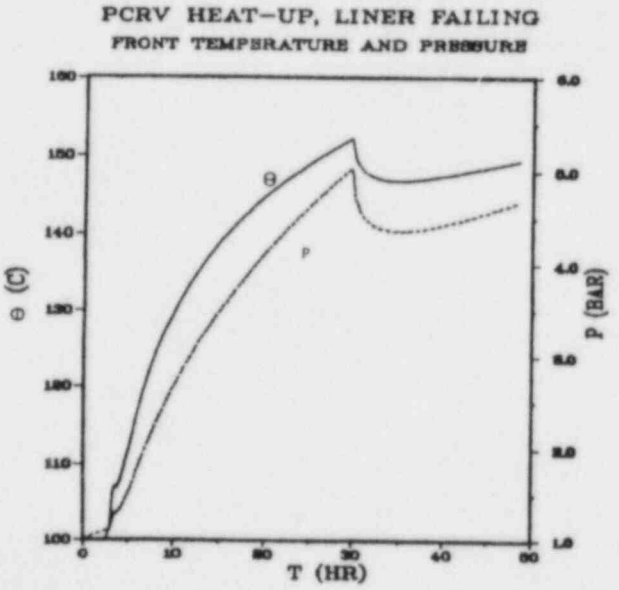

(b)

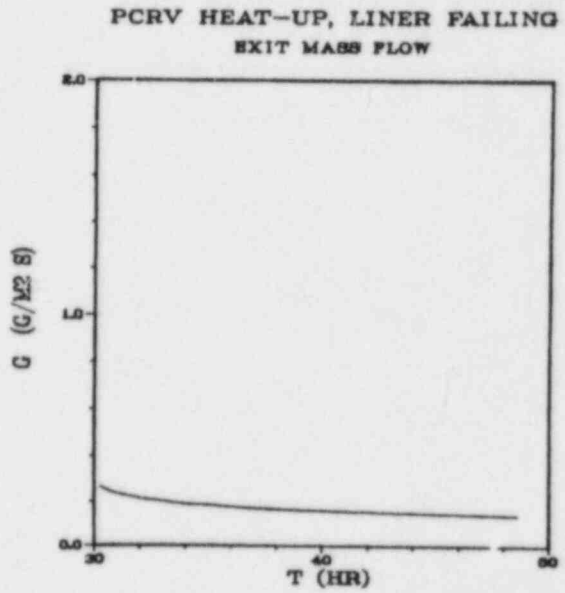

(c)

Figure 1.3.2 Concrete Vapor Migration During PCRV Heat-Up with Thermal Liner Failure at 30 hr.

flow, a pressure behind the liner of about 5 bar would be reached around 30 hrs, at a liner temperature of 290°C (550°F). At higher liquid flow rates, the pressures would be significantly lower, and the dry region would be wider due to faster advance of the front.

The above results show that in this extreme case of low liquid mobility significant pressures behind the liner could arise, causing potentially earlier liner failures. Assuming that liner failure were to occur as early as 30 hrs, the resulting front progression is shown in Figure 1.3.2(a), i.e., its progression continues as prior to failure. This is, however, due to another conservative assumption in this sample application, of not accounting for the loss of the thermal insulation at liner failure time. Actually that loss of insulation would cause faster concrete heat-up and result in faster front travel, increasing the dry region width. The resulting front temperatures and pressures are shown in Figure 1.3.2(b). Note that after failure the dry region pressure gradually decreases from its peak at the front, to core atmosphere pressure at the liner position. The resulting mass flow of superheated vapor into the core cavity after liner failure is shown in Figure 1.3.2(c). This mass flow into the core cavity even though computed for an extreme case of low liquid mobility is about one order lower than the water ingress rates used previously (App. F of Reilly et al, 1984).

Thus, first results indicate that in actual UCHA scenarios, due to the gradual concrete heat-up with liner failure only after days, most of the PCRV moisture is driven into cooler regions of the concrete, and actual water ingress into the PCRV after liner failure appears to be at least one order lower than previously assumed. This would significantly enhance the safety margin towards CB failure from overpressurization or deflagration burning.

Other scenarios remain to be investigated. The code in its current form is usable, but with difficulty (inefficient and unnecessarily long computer run times). Code improvements are in progress and are expected to be completed during the current quarter. While our original plans called for this code to be part of our core thermal analysis code (THATCH) it appears now to be more efficient to leave this vapor migration code (VAPMIG) as a separate code.

REFERENCES

1. LEE, B. S., Quarterly Progress Report Oct. - Dec. 1983, BNL-NUREG-51454 Vol. 3., No. 4.

2. REILLY et al, "Preliminary Evaluation of HTGR Severe Accident Source Terms, EG&G Idaho National Engineering Laboratory, EGG-REP-6565, April 1984.

3. SOO, P., Quarterly Progress Report, July - Sept. 1978, BNL-NUREG-50931.

4. SOO, P., Quarterly Progress Reports, BNL-NUREG-51454, Vol. 1, No. 3, pp. 9, 1981 and Vol. 1, No. 4, pp. 12, 1981.

2. SSC Development, Validation and Application (J.G. Guppy)

The Super System Code (SSC) Development, Validation and Application Program deals with advanced thermohydraulic codes to simulate transients in liquid metal-cooled reactors (LMRs). During this reporting period, work continued on three codes in the SSC series. These codes are: (1) SSC-L for simulating short-term transients in loop-type LMRs; (2) SSC-P which is analogous to SSC-L except that it is applicable to pool-type designs and (3) SSC-S for long-term (shutdown) transients occurring in either loop- or pool-type LMRs. In addition to these code development and application efforts, validation of these codes is an ongoing task. Reference is made to the previous quarterly progress report (Guppy, 1983) for a summary of accomplishments prior to the start of the current period.

2.1 SSC-L Code (W.C. Horak)

2.1.1 SSC-L Modeling of the SNR-300 Power Limiter Control and Temperature Limiter Control (W.C. Horak)

During this quarter, two additional control systems were developed and tested for incorporation into the SSC-L model of the SNR-300 plant. These two systems, the power limiter control (PLC) and the temperature limiter control (TLC), are designed to minimize scrams during long transients but do not hinder any PPS action. These controllers, which are unique to the SNR-300 plant, were developed at the request of the Gesellschaft fur Reaktorsicherheit (GRS), in Cologne, FRG.

The PLC ensures that the reactor power becomes no greater than 107% (103% $\pm$ 4% measurement error) for a long period. The PLC is designed to limit the decay heat and to avoid scram during slow transients. No plant protection system (PPS) actions are affected by the PLC.

An increase of reactor power, which might cause the activation of the PLC, can occur during three types of disturbances:

1) Reactivity insertion caused or not controlled by the PPS (e.g., malfunction of reactor power control)

2) A reduction of reactor inlet temperature (e.g., reduction of feedwater temperature through loss of a major portion of the preheater capacity)

3) An increase of the sodium flow rate in the primary system (e.g., malfunction of primary pump control)

In cases 2) and 3), the plant control system (PCS) increases the reactor power to keep the reactor outlet temperature constant.

The TLC system ensures that the hot sodium temperatures in the primary and secondary loops cannot remain at higher than design level for long periods, even if the PCS fails. The TLC avoids unnecessary reactor scrams during milder transients, but it does not hinder any PPS action.

TLC actions may take place during the following disturbances:

1) Uncontrolled withdrawal of a control rod

2) A stuck control rod during power reduction

3) Uncontrolled slowdown of a secondary sodium pump, which can lead to secondary sodium temperatures higher than the design values in those loops

4) Constant secondary pump speeds during an increase of power.

Events 1) and 2) cause the reactor power generation to be higher than the plant load which leads to a storage of heat and thereby to an increase of temperatures.

In events 3) and 4), the power generation is controlled so that the reactor outlet temperature remains constant (if not a scram takes place), but the poor heat removal in the secondary loops leads to an increase of the secondary temperature above design limits ($T_{design\ second}$ = 530°C, $T_{vessel\ outlet\ max.}$ = 546°C).

If either the TLC or PLC is activated, the following actions occur:

- The control rods are stopped, whether a drive signal is given or not.
- Two trim rods receive a drive-in signal.
- The setpoint of thermal power in the supervisory control system remains unchanged.
- After completion of the PLC or TLC action, the control rods can be moved.

These controllers were incorporated into SSC by adding calls in the subroutine PPCS8T to two new subroutines, PLC8T and TLC8T. Control rod block logic was also added to PCON8T.

A ramp insertion of .005 $/s for 50(s) was used to test the power limiter control (PLC). The transient was started from a 100% power condition.

The PLC was monitored to determine if the following functions were performed:

1) Time delay of the reactor flux
2) PLC activation
3) Control rod blockage
4) Trim rod insertion
5) PLC deactivation
6) Control rod activation.

Figure 2.1 shows the flux and delayed flux. The PLC activates when the delayed flux exceeds a value of 1.03 and the error in the instantaneous flux versus a setpoint exceeds .03. The flux peaks at 50(s) when the ramp insertion terminates and then starts to decrease due to the insertion of the primary control rods. The delayed flux peaks at about 70(s). At this time, both the flux and delayed flux are slightly greater than 1.03. The PLC is activated at 60(s) and remains active until 90(s).

Figure 2.2 shows the trim rod insertion distance. The trim rods are inserted only over the time period 60-90(s); they are not withdrawn after that time.

Figure 2.3 shows the reactivity of the primary control rods. As can be seen, the primary reactivity decreases (i.e., the control rods are inserted) in response to the ramp insertion until the delayed flux exceeds 1.03 at 60(s) into the transient. At that time, the control rod motion is blocked and remains blocked through the rest of the transient since the delayed flux which controls the blocking logic never decreases to the release value of 1.0.

As a test of the temperature limiter control (TLC), the IHX secondary coolant outlet temperature was step-changed from its 100% power steady-state value of 793°K to 810°K, held at that value for 15(s), and then allowed to decay back to its calculated value. All other parameters were held at their steady-state values.

The TLC was monitored to determine if the following functions were performed:

1) Measurement time delay of the IHX secondary outlet temperature.
2) TLC activation
3) Control rod blockage
4) Trim rod insertion
5) TLC deactivation
6) Control rod activation.

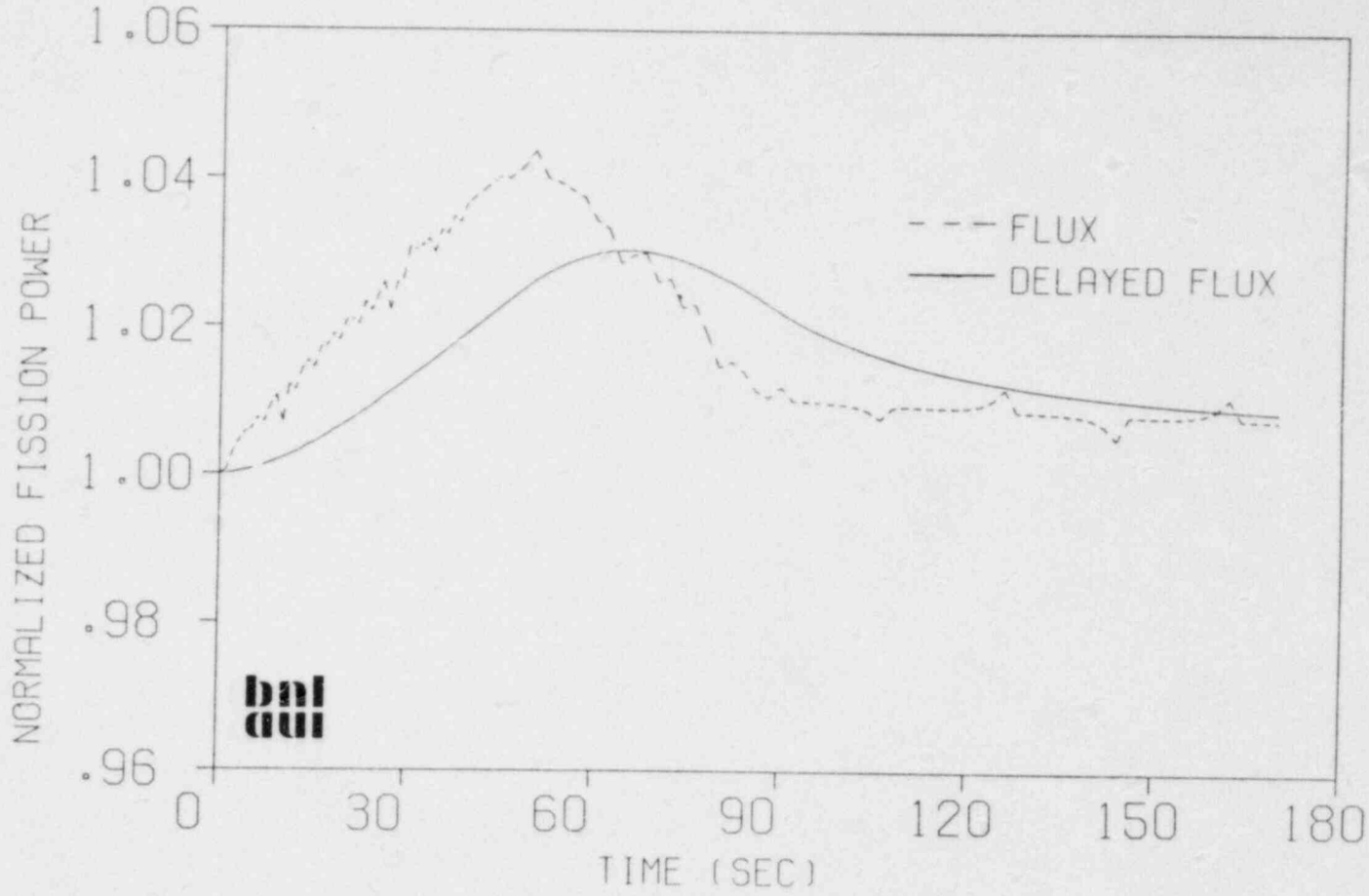

Fig. 2.1 Normalized Fission Power

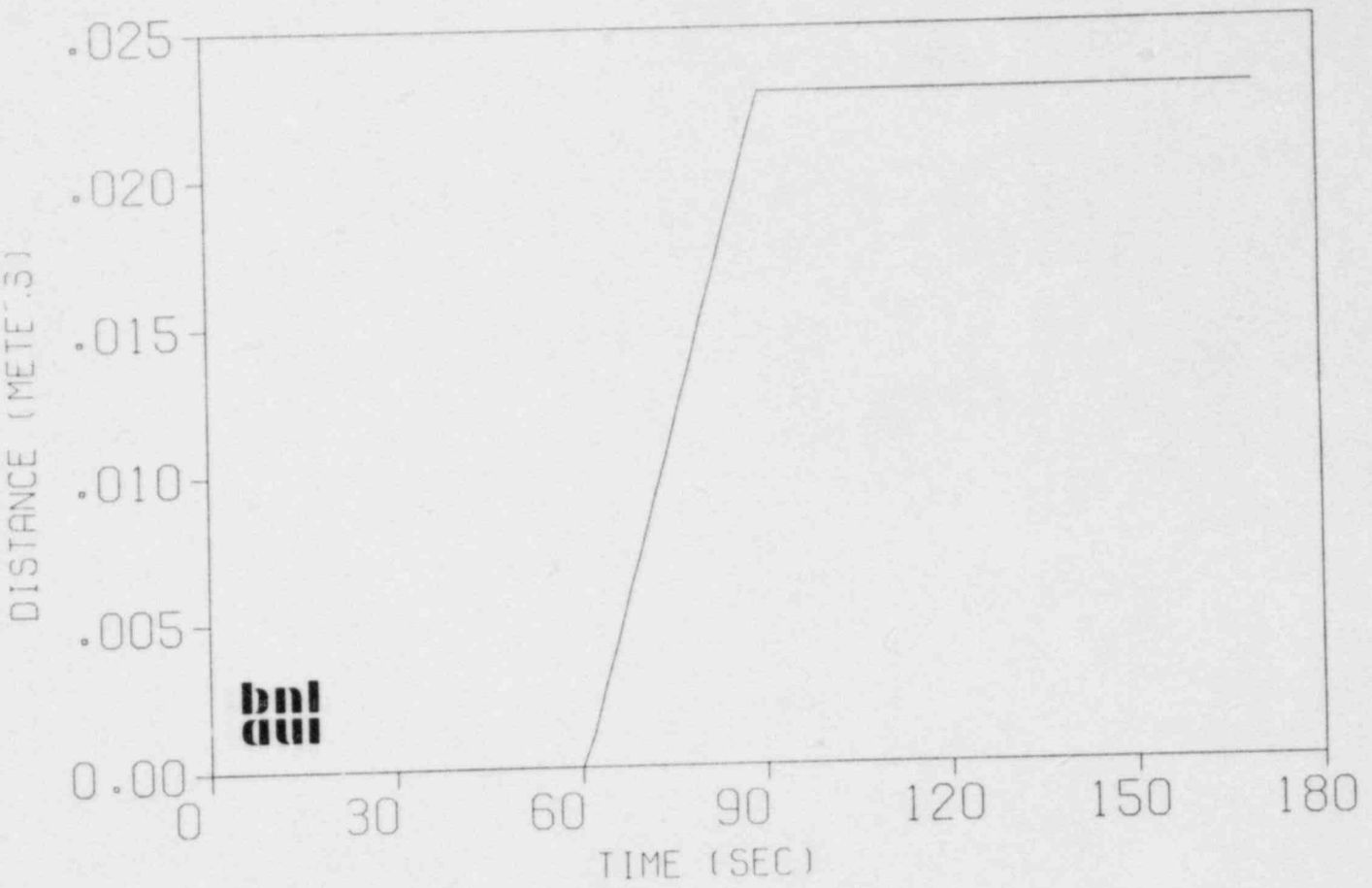

Fig. 2.2 Trim Rod Insertion

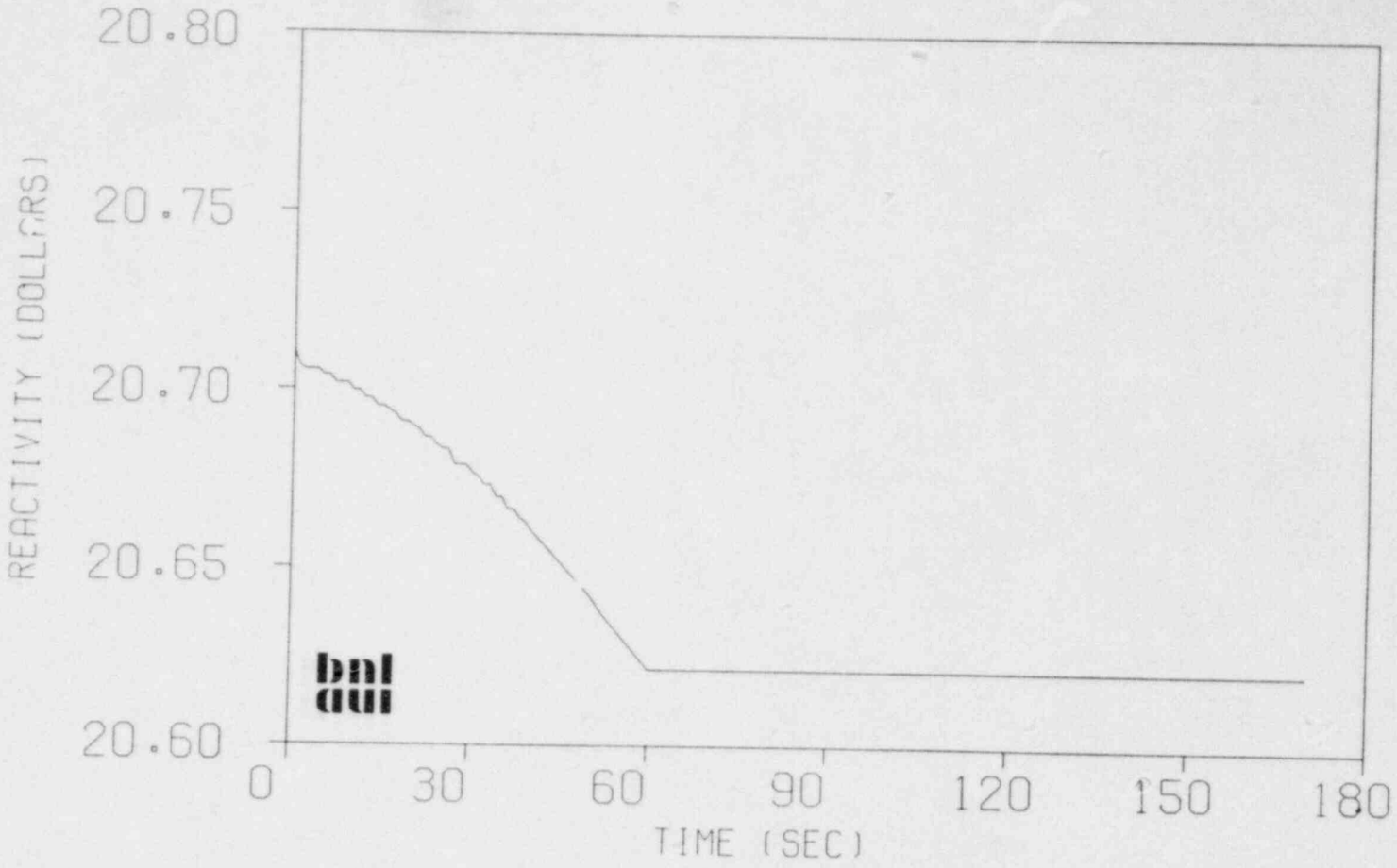

Fig. 2.3 Control Rod Reactivity

Figure 2.4 shows the IHX secondary outlet temperature and the time delayed "measured" IHX secondary outlet temperature which control the TLC action. As is shown, the IHX secondary outlet temperature is step-changed from 793°K to 810°K at time, t=0. The temperature is held at 810°K for 15(s) and then allowed to decay back to its steady-state. The "measured" temperature is simulated using a simple time delay with a time constant of 1(s).

Figure 2.5 shows the trim rod insertion distance. As can be seen, the trim rods are inserted when the TLC is activated (4(s) - 16(s)) and they are not withdrawn upon completion of TLC activity. Moreover, because the time delayed temperature remains above 793° K, control rod movement is still blocked at the conclusion of the transient. This is shown in Figure 2.6, where the reactivity worth of the control rods is shown to be constant except at the initial stages of the transient.

In summary, two additional controls, the Power Limiter Control (PLC) and the Temperature Limiter Control (TLC) have been developed for the SSC representation of the SNR-300 reactor system. These two controllers have been modeled by including two additional subroutines, PLC8T and TLC8T, and making slight modifications to three existing SSC subroutines. These controllers were tested on two sample transients and found to perform as expected.

2.1.2 Inter-Assembly Heat Transfer (W.C. Horak, R.J. Kennett)

Work this quarter has concentrated on the development of appropriate numerical schemes for inter-assembly heat transfer analysis. Several finite-difference method based schemes and nodal schemes have been developed and are currently being evaluated.

The intra-assembly code is now being prepared for a series of nodalization studies. These studies will be helpful in determining the degree of detail necessary to correctly calculate the duct temperature, which controls the inter-assembly heat transfer rate.

2.2 SSC-P Code (E.G. Cazzoli)

2.2.1 Modeling for EBR-II Transient Analysis (J.G. Guppy)

An improved input deck for the EBR-II (cold pool) plant representation was prepared. Additionally, code modifications were implemented to better simulate the primary system hydraulics. In particular, given the way that SSC presently handles the primary loop hydraulics, the calculation of the vessel inlet and outlet pressures had to be revised because the free surface in the EBR-II (cold pool design) can only be used relative to the pump inlet pressure calculation. Vessel and loop pressure drops and calculations of absolute pressures were made consistent. A null transient was performed.

2.2.2 Generic Pool Subroutine (W.C. Horak)

A subroutine is being developed that will permit modeling of the thermal balance in a pool system. This subroutine will be accessed as an option in the SSC base program library. The hydraulic modeling for such a pool option is still under development.

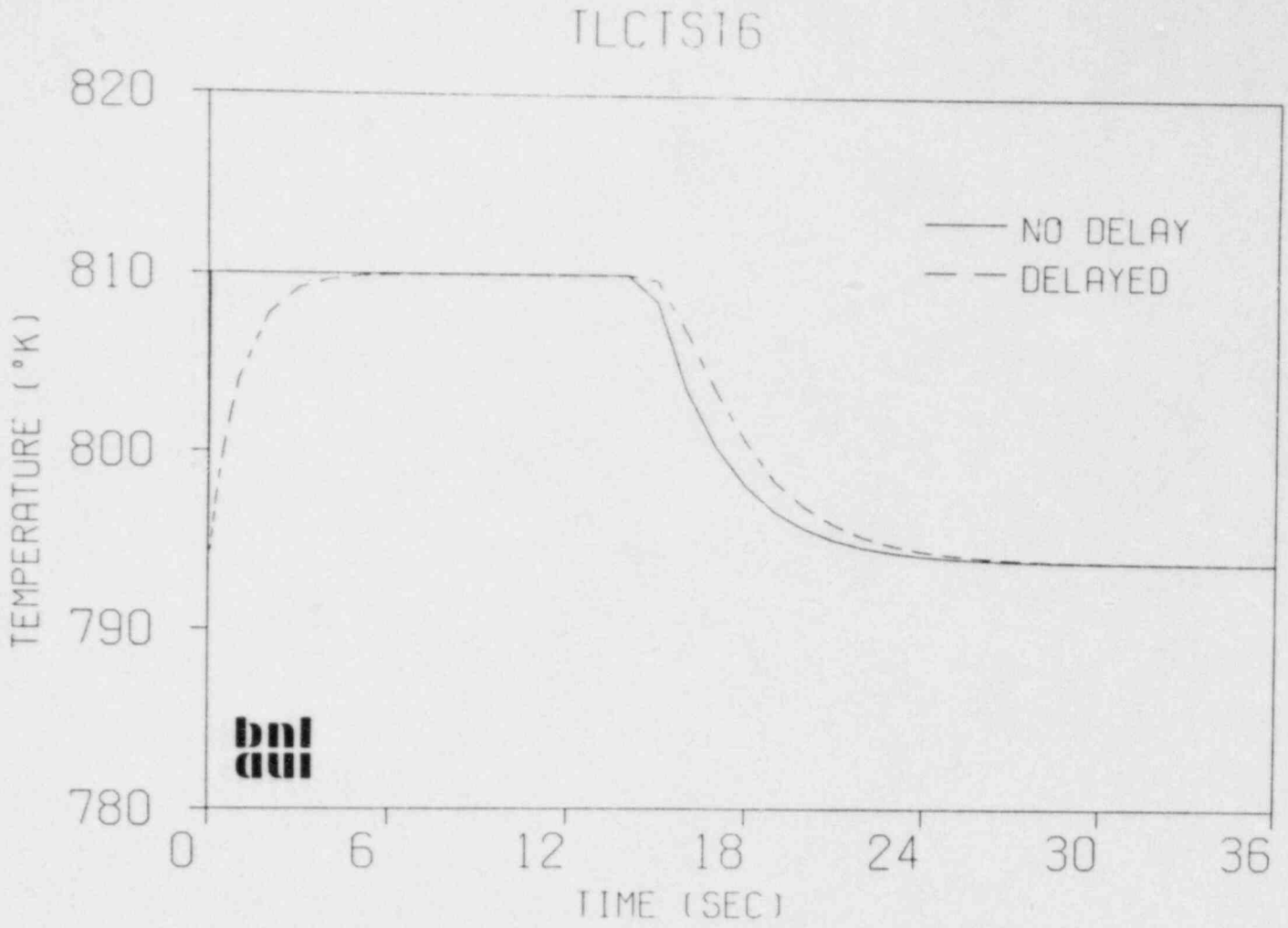

Fig. 2.4 IHX Sec Outlet Temperature

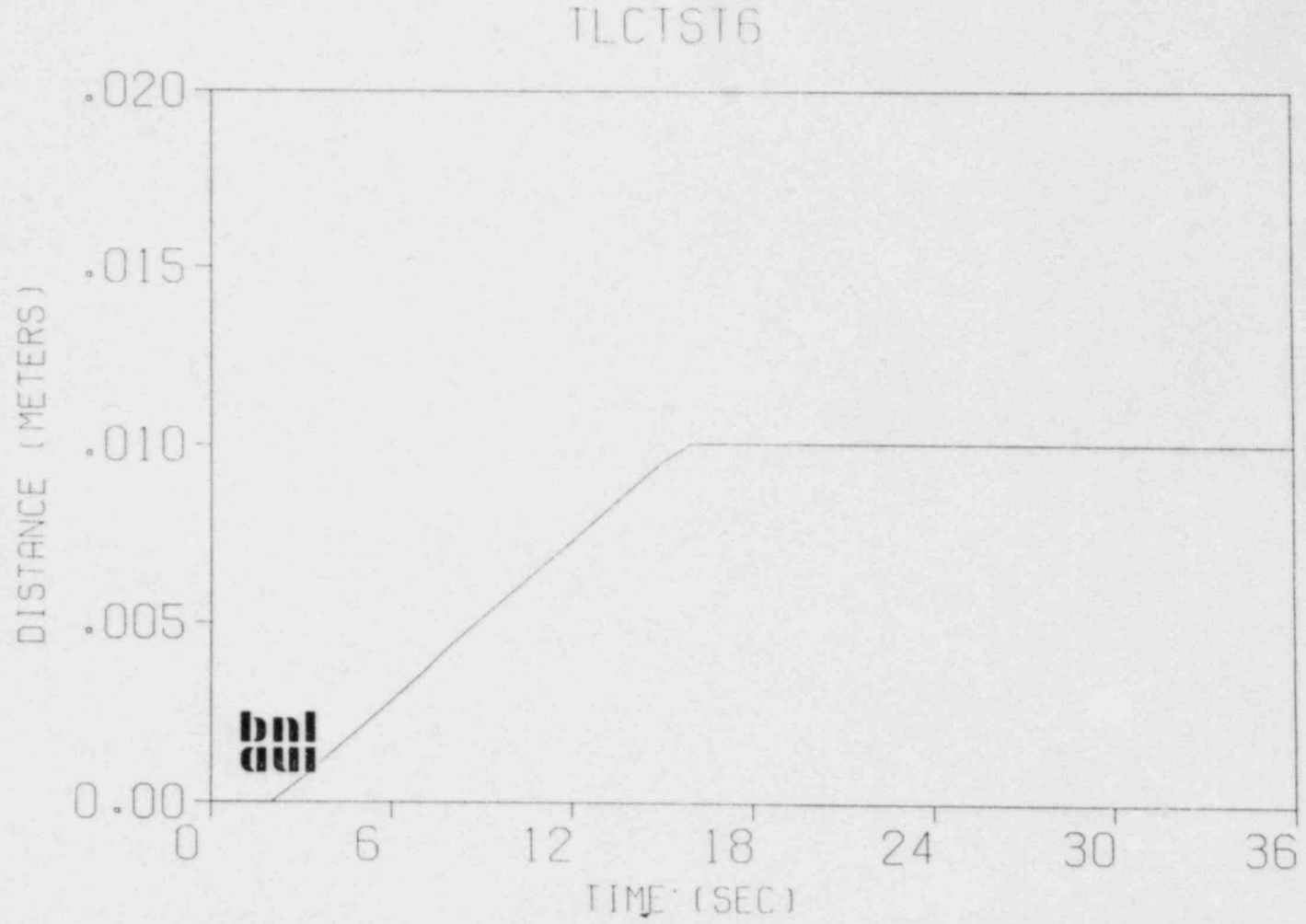

Fig. 2.5 Trim Rod Insertion

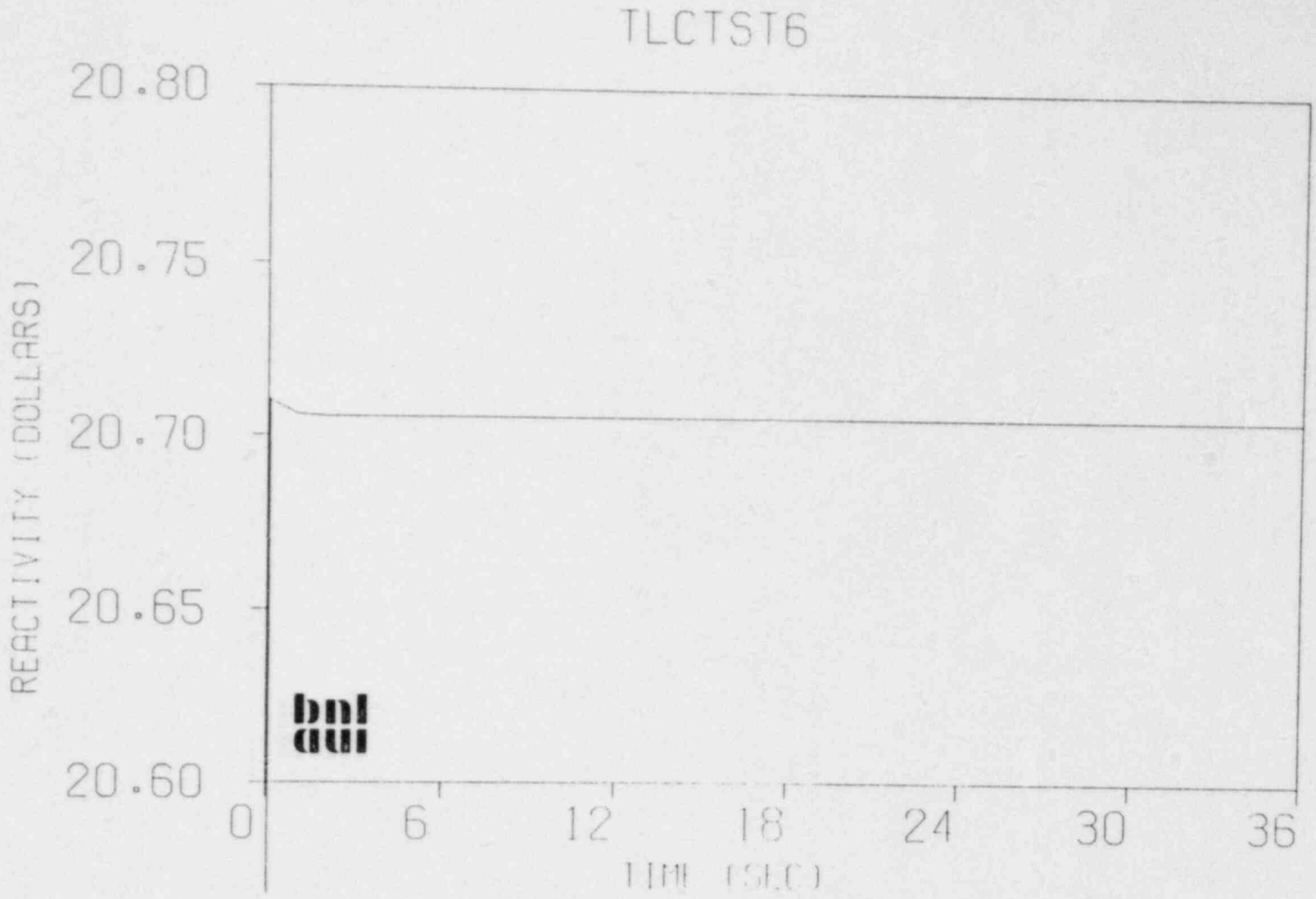

Fig. 2.6 Control Rod Reactivity

2.2.3 Code Maintenance (E.G. Cazzoli)

The pool version of SSC is under review and is being modified in the latest cycle of the program library, in order to take advantage of recent improvements in SSC-L. In order to check that the updated version of SSC-P incorporating the revisions is correct, previously simulated plant transients performed for Phenix will be repeated and comparisons made for consistency.

2.3 SSC-S Code (B.C. Chan)

2.3.1 Improved Upper Plenum Modeling (B.C. Chan)

The FFTF upper plenum simulation using the upper plenum stand-alone code has been extended to 300.0 seconds of transient simulation time. The results show that at the initial steady-state isothermal operating conditions, heated sodium enters the plenum from the reactor core and, after completely mixing within the plenum, exits through the outlet nozzles. Following reactor scram and pump coastdown, the plenum experiences an abrupt decrease in both entering sodium temperature and flow rate. The entering sodium increases in density and decreases in momentum as a result of temperature and flow rate decreases. The denser and lower momentum sodium has insufficient inertia entering the plenum to overcome the negative buoyancy force. The incoming sodium is forced downward and flows outward toward the exit nozzle. This created a stratified flow pattern within the plenum; the sodium in the stagnant upper zone of the plenum is relatively warm and the sodium in the lower zone is relatively cool. Subsequently, after 200 seconds following reactor scram, the incoming sodium temperature increases. This positive buoyancy force together with the momentum of the entering sodium is sufficient to provide full penetration and results in complete mixing again.

2.4 Code Validation (W.C. Horak)

2.4.1 Validation of New Cycle (W.C. Horak, R.J. Kennett)

Given the success of the comparisons of SSC results to FFTF experimental data, the development of a fourth test problem is being pursued. This problem, based on an FFTF-type plant, is designed to detect asymmetries that may be unintentionally introduced at new cycles. The test problem contains two identical core channels and two identical thermal loops. During the transient, the response of the two channels should be identical, as should the two loops. The output format, along with an appropriate set of plots, is now being standardized. The test problem, along with accompanying documentation, will be distributed with the next cycle of SSC.

As part of the continuing validation of SSC, the current cycle of SSC-L (CY-41) along with the current update set (CHNG-42) was tested using standard problem No. 1, a steady-state transient. The updated cycle performed well on this test problem.

The gap conductivity model in SSC is being examined to see if any revisions are needed. Current efforts are focused on various new user options, such as a fixed input value. An improved closed gap contact conductance is also being evaluated.

REFERENCE

GUPPY, J. G., et al., (1983), "SSC Development, Validation and Application," Safety Research Programs Sponsored by Office of Nuclear Regulatory Research Quarterly Progress Report, Oct. 1 - Dec. 31, 1983, Brookhaven National Laboratory Report to be published.

PUBLICATIONS

CHAN, B. C., "A Buoyancy-Dominated Model for LMFBR Upper Plenum Flows," Brookhaven National Laboratory, BNL report to be published, 1984.

CHAN, B. C., KENNETT, R. J., GUPPY, J. G., "A Numerical Investigation of Buoyancy-Induced Flow Stratification in the LMFBR Upper Plenum," Brookhaven National Laboratory, BNL report to be published, 1984.

GUPPY, J. G., HORAK, W. C., VAN TUYLE, G. J., "Independent Assessment of the Natural Circulation Capability of the Heterogeneous Core CRBR," Trans. Am. Nucl. Soc. 45, 416, (1983).

HORAK, W. C., et al., "Short Term Post Test Analysis of the FFTF Scram to Natural Circulation Transients Using SSC," Brookhaven National Laboratory, ANS Meeting, June 1984.

HORAK, W. C., KENNETT, R. J., GUPPY, J. G., "Long Term Post-Test Simulation of the FFTF Natural Circulation Tests," Brookhaven National Laboratory, BNL report to be published, 1984.

KHATIB-RAHBAR, M., CAZZOLI, E. G., "Two-Dimensional Modeling of Intra-Subassembly Heat Transfer and Buoyancy-Induced Flow Redistribution in LMFBRs," Brookhaven National Laboratory, NUREG/CR-3498, BNL-NUREG-51713, 1983.

KHATIB-RAHBAR, M., "Core Coolability Following Loss-of-Heat Sink Accidents," Trans. Am. Nucl. Soc. 45, 365, (1983).

KHATIB-RAHBAR, M., "Intra-Assembly Flow Redistribution in LMFBRs: A Simple Computational Approach," Trans. Am. Nucl. Soc. 45, 816, (1983) also see 1st Proc. of the T&H Division, 13-20 (1983).

MADNI, I.K., "Modeling Considerations for the Primary System of the Experimental Breeder Reactor - II, Brookhaven National Laboratory Report to be published, 1984.

3. Generic Balance of Plant Modeling (J.G. Guppy)

The Balance of Plant (BOP) Modeling Program deals with the development of safety analysis tools for system simulation of nuclear power plants. It provides for the development and validation of models to represent and link together BOP components (e.g., steam generator components, feedwater heaters, turbine/generator, condensers) that are generic to all types of nuclear power plants. This system transient analysis package is designated MINET to reflect the generality of the models and methods, which are based on a momentum integral network method. The code is to be fast-running and capable of operating as a self-standing code or to be easily interfaced to other system codes. Reference is made to the previous quarterly progress report (Guppy, 1983) for a summary of accomplishments prior to the start of the current period.

3.1 Balance of Plant Models (G. J. Van Tuyle)

Models for Version 1 of MINET have been completed and tested, and are currently being documented in the MINET Code Documentation (Van Tuyle et al., 1984). New models will be incorporated in Version 2, which is to include a generic package of control system models. Some of the functions developed for the SNR-300 control system modeling effort will be utilized.

Models for pumps and turbines are currently available in MINET. An interface between these modules, through the rotor (speed), is under development, so that a turbine driven pump can be modeled. Various approaches have been considered, and we are now working to determine the optimum combination of accuracy, flexibility, and user convenience.

3.2 MINET Code Improvements (G.J. Van Tuyle, T.C. Nepsee)

Code additions and modifications have been made to implement a generalized interface to another code for boundary module data. This is now in the test/debug phase. A minor error in the Global Container Manager Utility has been identified and corrected.

A 1000-node test case has been successfully completed. Because of the large amount of data storage required, it was necessary to make use of the CDC 7600 Large Core Memory to augment the Small Core Memory. This was easily accomplished because of the inherent flexibility of the Data Abstraction approach to data management as implemented in MINET.

An error has been identified in the MINET Version 1.6 EVENTTIMES function. Incorrect SAVE time values are returned after restarting a simulation from a CONTEXT SAVE file. A code revision correcting the error has been tested and will appear in the next version.

A new internal utility, TABLE, has been designed to perform data management and interpolation for tabular boundary condition and internal driving functions. It is intended to provide for uniform handling of tabular functions from both MINET input data and host code interface.

Until recently, the time step size taken in the MINET calculations was determined from the smallest time constant in the heat exchanger tube temperature computations, the time constant generally most limiting in terms of stability. With the computational portion of MINET, Version 1, now completed, the opportunity was taken to include other potentially limiting time constants. These include time constants associated with valve movement, adjustments in pump and turbine speed, heat exchanger structure temperatures and observed changes in key parameters, such as segment inlet enthalpy.

3.3 MINET Standard Input Decks (G.J. Van Tuyle)

For Version 0 of MINET, executing with Cycle 41 of SSC, the standard input decks currently in use are: a version of deck E1 which is maintained for use in a combined representation of the whole EBR-II system, and is known to give the same results as the version of deck E1 used with MINET Version 1, the stand-alone code; and MINET deck S3 for the SNR-300 plant, which has recently been used extensively in testing the SNR-300 control system models.

Several decks are currently utilized for MINET Version 1, including example decks X1 and X2, helical coil heat exchanger deck H1, and EBR-II plant deck E1. Two new standard input decks have been documented, deck I1 for simulating Integral Economizer Once-Through Steam Generators (IEOTSGs) and deck U1 for representing U-Tube Steam Generators (UTSGs).

3.4 MINET Validation and Applications (G.J. Van Tuyle, E.G. Cazzoli)

Control system models for the SNR-300 plant steam generator system were incorporated in Version 0 of MINET, as part of an effort to simulate the entire SNR-300 heat transport system using SSC/MINET. Two tests have been performed, a null transient and a post-scram transient. In the null transient, the system conditions held near the steady state conditions for the six minute simulation. However, the feedwater pump speed and valve position and the drain valve position exhibited a tendency to drift due to windows in the control system setpoints, e.g., the drum water level drifts between 2.0 and 3.0 meters (setpoints). For the post scram transient, the control system model performed as German engineers specified, and the system response seemed quite reasonable, at least for the first six minutes. The results of the effort are being documented (Van Tuyle, 1984a).

Further parametric tests were performed on the helical coil test transient, with comparisons made against the test data provided by PNC (Japan). It was found that the sodium outlet temperature is relatively sensitive to the amount of structure that is assumed. Five test transients were performed, with the structural mass varied from zero to an essentially infinite mass. It was determined that a near perfect match with experimental data results from a structural mass equivalent to an outer tube of twice the thickness of the tube separating the water/steam and the sodium. Documentation of this effort is in progress (Van Tuyle, 1984b).

Work is progressing on the interfacing between the RAMONA code (Wulff et al., 1984) and MINET, as part of the Boiling Water Reactor (BWR) Severe Accident Sequence Analysis (SASA) Program. The RAMONA code has been studied to determine the most efficient places to call the MINET driver subroutines, and RAMONA variables important to the interface have been identified. A means of performing the interface with minimal impact on the programming of either code has been worked out, and awaits implementation. A simple MINET input deck, to be used for the initial test, has been developed and tested.

Two input decks to RAMONA-3B were finalized, describing a prescribed SASA accident for the Browns Ferry BWR, one representing 12 channels, quarter core symmetry, and one with 8 channels, one-eighth core symmetry. Comparisons were made with geometrical and nuclear data provided by the FSARs as well as on-site and INEL's RELAP-5 and TRAC input descriptions for the Browns Ferry plant. Steady-state calculations were satisfactorily performed to ensure a match to the prescribed initial conditions.

3.5 EBR-II 44 Minute Transient

The EBR-II test transient analyzed was a coastdown from 36% full power and 39% full primary flow (Van Tuyle, 1983; 1984c). Transient boundary conditions, determined from test results, included secondary flow and IHX outlet temperature, feedwater flow and temperature, and drain flow. The auxiliary flow and the turbine bypass (throttle was closed) valve characteristics were obtained from a previous simulation (Mohr and Feldman, 1981). Specifically, the secondary, feedwater, and auxiliary flows decreased, the drain flow was shut off quickly, the feedwater temperature held nearly constant, the IHX outlet temperature decreased steadily, and the bypass valve closed in response to reduced steam pressure. Fourteen system parameters were compared, including temperatures, pressures, flows, and drum level. Figure 3.1 compares two such parameters, the superheater inlet and outlet sodium temperatures. Evaporator inlet and outlet temperatures are shown in Figure 3.2. As can be seen, MINET yields results in good agreement with the experimental data. The tendency of the MINET calculated temperatures to lead the measured values was traced to thermocouple response times, which ranged from 10 seconds to 1 minute (Mohr and Feldman, 1981).

3.6 Integral Economizer Once-Through Steam Generator (IEOTSG)

Babcock and Wilcox have conducted experiments on a 19-tube IEOTSG test facility (Loudin and Oberjohn, 1976) in support of the full scale units currently utilized. Two of these test transients were simulated using MINET, and calculational results were compared against experimental data.

In simulating the step reduction in steam flow rate, from 65 to 55 per cent of rated load, measured feedwater and steam flow rates were input as transient boundary conditions. Feedwater temperature, as well as primary inlet flow rate and temperature and primary outlet pressure were held constant. MINET calculated steam pressure (Fig. 3.3) and primary outlet temperature (Fig. 3.4) were in close agreement with the data throughout the 20 second transient. MINET simulation of the second transient, a step reduction in steam flow rate, was equally accurate (Van Tuyle, 1984d).

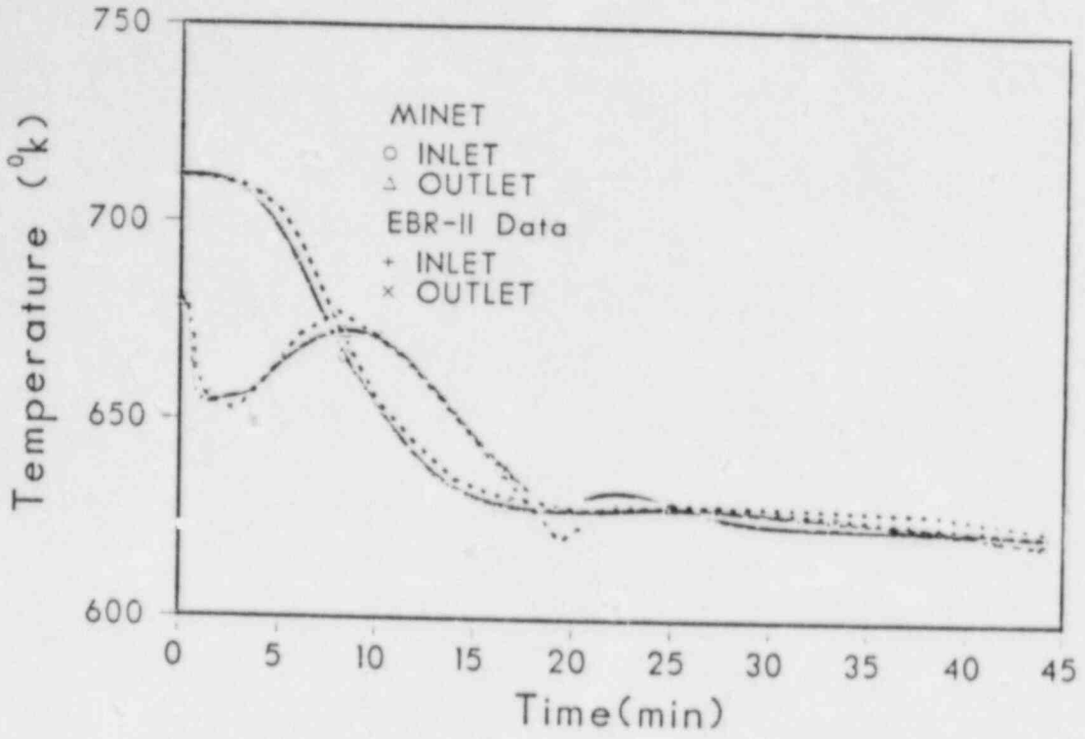

Fig. 3.1 Superheater Sodium Temperatures

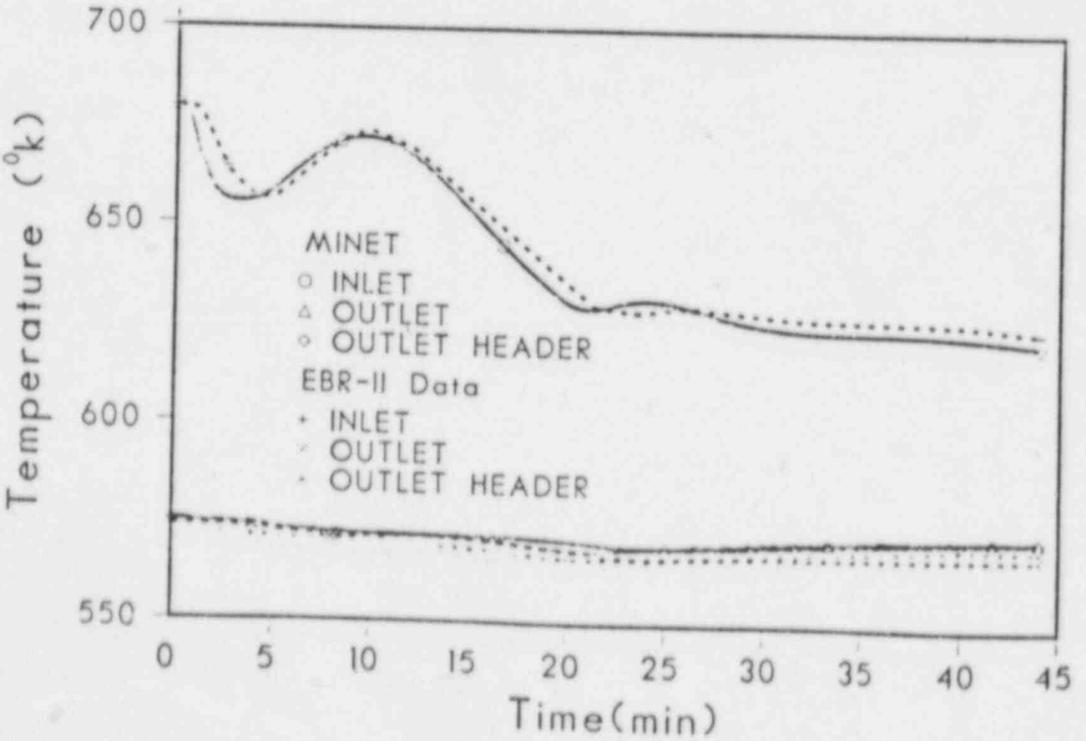

Fig. 3.2 Evaporator Sodium Temperatures

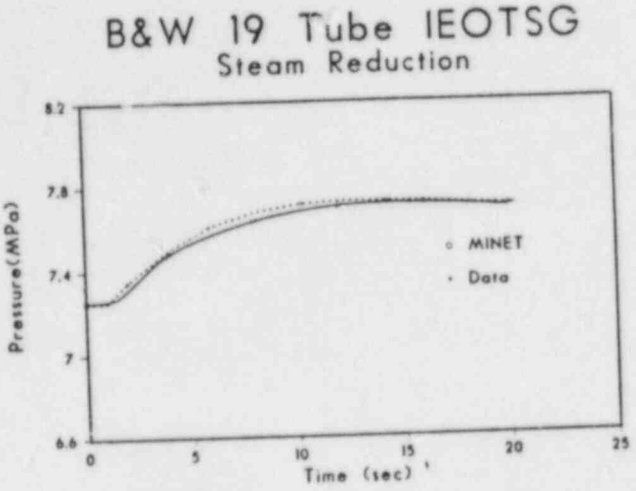

Fig. 3.3 Steam Outlet Pressures for IEOTSG Case

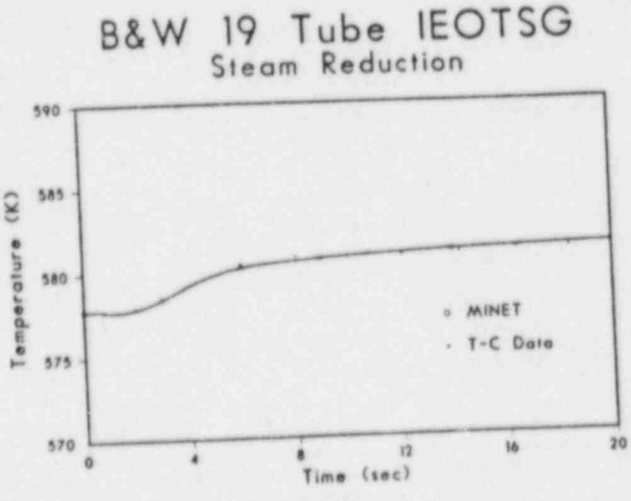

Fig. 3.4 Primary Outlet Temperature for IEOTSG Case

3.7 U-Tube Steam Generator (UTSG)

Test data for a UTSG were obtained during startup testing of Unit 1 of the Donald C. Cook Nuclear Station (Indiana and Michigan Power Co., 1976). The MINET representation used in simulating the UTSG is shown in Figure 3.5. Note that parallel and countercurrent heat exchanger modules are used to simulate the U-shaped flow path of the primary fluid, while pipe and volume modules are used to represent the steam dome, feed chamber, downcomer, and other parts of the unit.

In simulating the turbine trip transient (Indiana and Michigan Power Co., 1976), plant data were used to determine MINET transient boundary conditions for the feedwater and steam flow rates, as well as the primary inlet temperature and pressure. Primary outlet mass flow rate and feedwater temperature were held constant.

The feed chamber water levels calculated by MINET and by the TRANSG code (Lee et al., 1980), a steam generator transient analysis code, and the level measured during the first 10 seconds, are shown in Figure 3.6. This level is the vertical distance from the bottom of the feed chamber volume to the top of the water region in the steam dome (see Figure 3.5). The two computer codes are in excellent agreement with each other, and with the measured level, except around 2 seconds into the transient where there is a small disagreement. Similar agreement was found in the calculated steam pressure, where MINET and TRANSG agreed closely with one another, and relatively well with the measured pressure (Van Tuyle, 1984d).

3.8 User Support (G.J. Van Tuyle, T.C. Nepsee, J.G. Guppy)

Work in modeling the SNR-300 steam generator system controllers is in direct support of German usage of SSC/MINET for the analysis of the SNR-300. Studies regarding the helical coil steam generator transient simulation are supportive of using SSC/MINET for simulating the Japanese MONJU plant.

The initial draft of the MINET code documentation has been completed, and editing is in progress. The current version of MINET, Version 1.6 is actually described, but the format is such that it can easily be updated to be compatible with the most current version.

Several validation studies have been completed recently, including the extended EBR-II study, and the helical coil, once-through, and U-tube steam generator studies. The process of documenting these studies and making them available to potential users is well along, and we expect to have the various reports available for export with the completed MINET Code Documentation in the coming months.

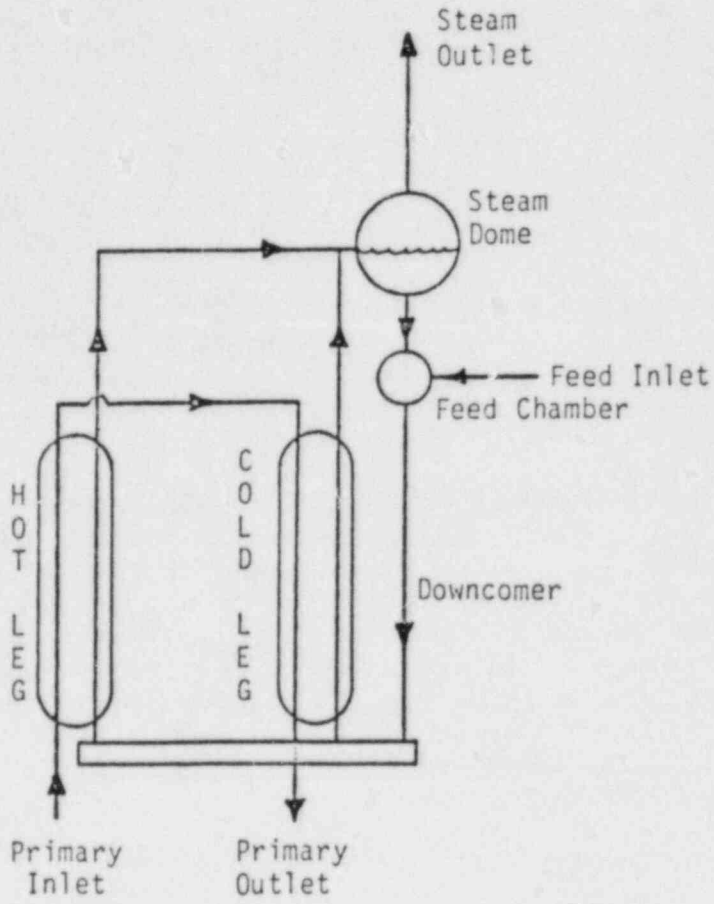

Fig. 3.5 MINET Deck U1, U-Tube Steam Generator

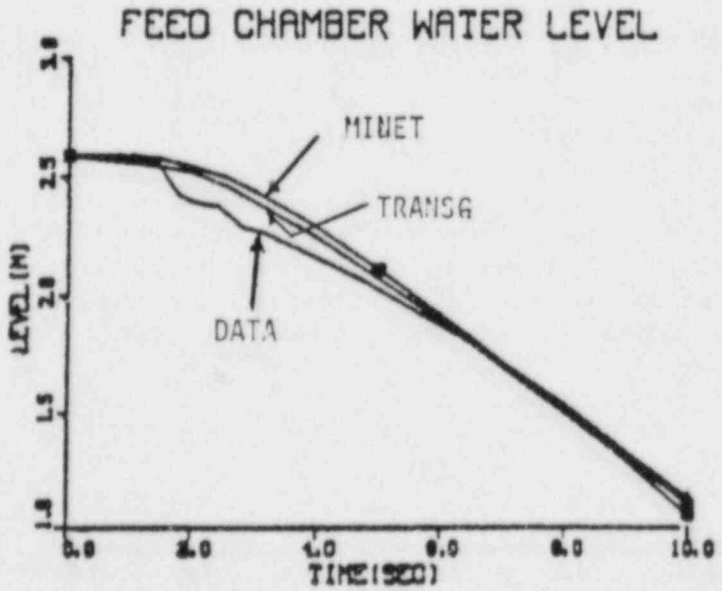

Fig. 3.6 Water Level for U-Tube Test Transient

REFERENCES:

GUPPY, J. G., et al., (1983), "Balance of Plant Modeling," Safety Research Programs Sponsored by Office of Nuclear Regulatory Research Quarterly Progress Report, Oct. 1 - Dec. 31, 1983, Brookhaven National Laboratory Report to be published.

LOUDIN, G.W. and OBERJOHN, W.J., (1976), "Transient Performance of a Nuclear Integral Economizer Once-Through Steam Generator (OTSG)," Alliance Research Center Report 4679, Babcock and Wilcox, January 1976.

MOHR, D. and FELDMAN, E.E., (1981), "A Dynamic Simulation of the EBR-II Plant During Natural Convection with the NATDEMO Code," Published in Decay Heat Removal and Natural Convection in Fast Breeder Reactors, Agrawal and Guppy, Hemisphere Publishing Corporation, New York, 1981.

WULFF, W., et al., (1984), "A Description and Assessment of RAMONA-3B: A Computer Code with Three-Dimensional Neutron Kinetics for BWR System Transients," Brookhaven National Laboratory Report, NUREG/CR-3664, BNL-NUREG-51746, January 1984.

VAN TUYLE, G.J., (1983), "MINET Validation Study Using EBR-II Test Data," Brookhaven National Laboratory, NUREG/CR-3603, BNL-NUREG-51733, November 1983.

VAN TUYLE, G.J., NEPSEE, T.C., GUPPY, J.G., (1984), "MINET Code Documentation, Brookhaven National Laboratory, NUREG/CR-3668, BNL-NUREG-51742, February 1984.

VAN TUYLE, G.J., (1984a) "Implementation of SNR-300 Steam Generator System Controller Models Into SSC/MINET," Brookhaven National Laboratory Report to be published.

VAN TUYLE, G.J., (1984b), "Simulation of a Helical Coil Sodium/Water Steam Generator, Including Structural Effects," Brookhaven National Laboratory Report to be published.

VAN TUYLE, G.J., (1984c), "MINET Validation Study Using EBR-II Transient Data," Thermal-Hydraulics Division Proceedings, Summer 1984, American Nuclear Society Meeting, June 1984.

VAN TUYLE, G.J., (1984d), "MINET Validation Study Using Steam Generator Transient Data," Brookhaven National Laboratory Report to be published.

PUBLICATIONS

VAN TUYLE, G.J., "MINET Validation Study Using EBR-II Test Data," Brookhaven National Laboratory, NUREG/CR-3603, BNL-NUREG-51733, November 1983.

VAN TUYLE, G.J., NEPSEE, T.C., GUPPY, J.G., "MINET Code Documentation, Brookhaven National Laboratory, NUREG/CR-3668, BNL-NUREG-51742, February 1984.

VAN TUYLE, G.J., "Simulation of a Helical Coil Sodium/Water Steam Generator, Including Structural Effects," Brookhaven National Laboratory Report to be published.

VAN TUYLE, G.J., "Implementation of SNR-300 Steam Generator System Controller Models Into SSC/MINET," Brookhaven National Laboratory Report to be published.

VAN TUYLE, G.J., "MINET Validation Study Using EBR-II Transient Data," Thermal-Hydraulics Division Proceedings, Summer 1984, American Nuclear Society Meeting, June 1984.

VAN TUYLE, G.J., "MINET Validation Study Using Steam Generator Transient Data," Brookhaven National Laboratory Report to be published.

4. Thermal-Hydraulic Reactor Safety Experiments

4.1 Core Debris Thermal-Hydraulic Phenomenology: Ex-Vessel Debris Quenching (T. Ginsberg, J. Klein, J. Klages, and C. E. Schwarz)

This task is directed towards development and experimental evaluation of analytical models for prediction of the rate of steam generation during quenching of core debris under postulated LWR core meltdown accident conditions. This program is designed to support development of LWR containment analysis computer codes.

4.1.1 Background

A major source of containment pressurization during degraded core accidents in LWRs would result from the ex-vessel thermal interaction between molten core debris and water available in the region beneath the reactor vessel. It has been suggested (Ginsberg, 1982) that the thermal interaction would occur in two stages: (i) the melt fall period during which the melt mixes with water, breaks up and transfers energy to the coolant, and (ii) the debris bed or molten pool quench period during which the core debris rests on the concrete beneath the vessel and is cooled by an overlying pool of water. The above sequence of events is represented schematically in Figure 4.1. It is noted that steam explosions are possible during the core melt fall period.

Prior ex-vessel debris quench research reported in previous quarterly reports dealt with the second stage of the melt-water thermal interaction, in particular the quench characteristics of superheated debris beds (e.g., Ginsberg, 1984). The objective of the work described here is to develop and evaluate models to predict the mixing dynamics of core debris with water and the rate of steam generation during the melt fall period of the thermal interaction process.

Several models have been proposed to characterize the extent of mixing of melt and water during the premixing stage of energetic melt-water interactions. These models, although based upon differing principles, predict that the extent of mixing is limited either by availability of water (Fauske, 1983) or, if water is available, by the dispersiveness of the fuel-water system due to efficient heat transfer and rapid steam generation (Bankoff, 1984).

Experiments have been designed to simulate the process of mixing core melt and water in order to evaluate the principles involved in the models. The experiments are described below.

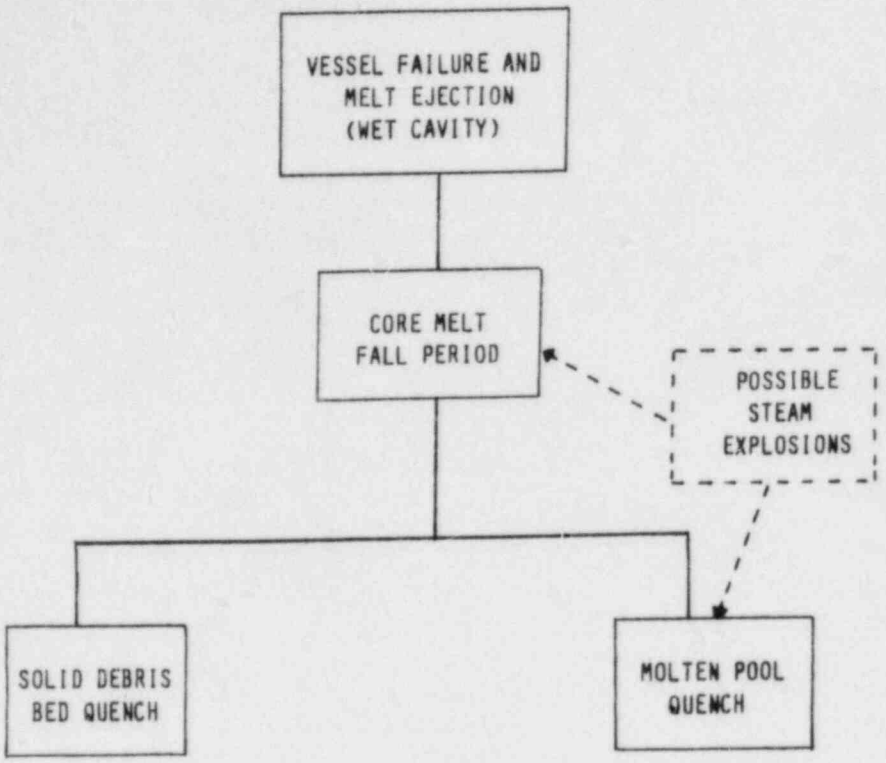

Figure 4.1 Thermal Interactions Between Core Debris and Water: LWR Accident Sequence.

4.1.2 Apparatus

Experiments are being conducted in the debris quench apparatus described previously (Ginsberg, 1983), with some modification to permit high-speed motion pictures to be taken. The experiments involve dropping kilogram quantities (thus far up to 20 kg) of hot stainless steel particles into a pool of water at its saturation temperature. The experimental test vessel is shown in Figure 4.2. The lower glass section is a quartz pipe which contains the hot particulate after it settles to the bottom of the test column. The diameter of the test column is approximately 100 mm. Both the water pool and the column of spheres which are dropped into the water are constrained to this diameter.

Measurements which are made during an experiment include:

(i) instantaneous steam generation rate,
(ii) pressure at the base of the column,
(iii) speed of the leading edge of particles,
(iv) initial particle and water temperatures.

In addition, high-speed motion pictures are taken of the thermal interaction.

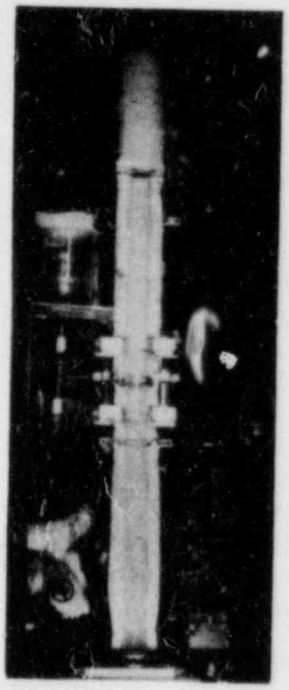

Figure 4.2 Photograph of Test Vessel.

4.1.3 Preliminary Results

Preliminary experiments have been performed with 3-mm diameter spheres, preheated to 977K (1300F). Five- and ten-kilogram masses of this shot have been dropped into pools of water of 0.5- and 1.0-meter depths. The results of Run No. 108, conducted with 10 kg of steel shot, are described below.

The steam generation results for this run are shown in Figure 4.3. The time scale in Figure 4.3 is measured from initiation of data acquisition. Contact between particles and water and, hence, steam generation, began at approximately 14.7 s. The speed of the leading edge of particles was approximately 4.9 m/s just prior to contact with water. Data taken from the motion picture indicate that the leading edge of spheres passed through the water and reached the bottom of the column at about 0.2 s following contact with water. This corresponds to a speed of 2.5 m/s for the passage of the leading edge through water.

The motion pictures indicate that approximately one-third of the particles entered the water pool and generated steam. The steam flux was so great, however, that the remaining particles above those that were submerged were fluidized and were dispersed in the upward direction. These dispersed particles, therefore, could not participate effectively in the initial interaction. This dispersal event was visually observed to take place at approximately 15.3 s in Figure 4.3, or 0.6 s following initial contact. The first peak observed in Figure 4.3 is probably attributable to this dispersal event.

Steam generated by the particles which were submerged and continued to fall through the pool, also fluidized much of the water from the initial pool. This water was also ejected upwards. Since the experimental column is quite long (7 m) it is likely that the water and steel which were ejected upward were not in very good contact, and probably did not produce much steam while they were suspended. Eventually both the water and the particles were seen to fall back into the view of the camera. At about this time, i.e., 16.7 s in Figure 4.3, signs of a second interaction were observed visually. This event was only mildly dispersive. The second peak observed in Figure 4.3 is probably due to this event. Nearly all the particles were settled into a bed configuration at about 5.3 s following the initial contact between water and steel.

The results thus far, while preliminary, indicate that there are limits to the extent of particle-water mixing if the initial heat transfer process is very efficient in producing vapor. The current one-dimensional apparatus tends to force water into the interaction region and leads to efficient heat transfer. It is speculated that this relatively efficient heat transfer process led, in Run No. 108, to the observed dispersal of particulate away from the interaction region. Similar results have been observed using 6-mm diameter steel particles.

An analytical effort is under way to model the sequence of events which are characterized above.

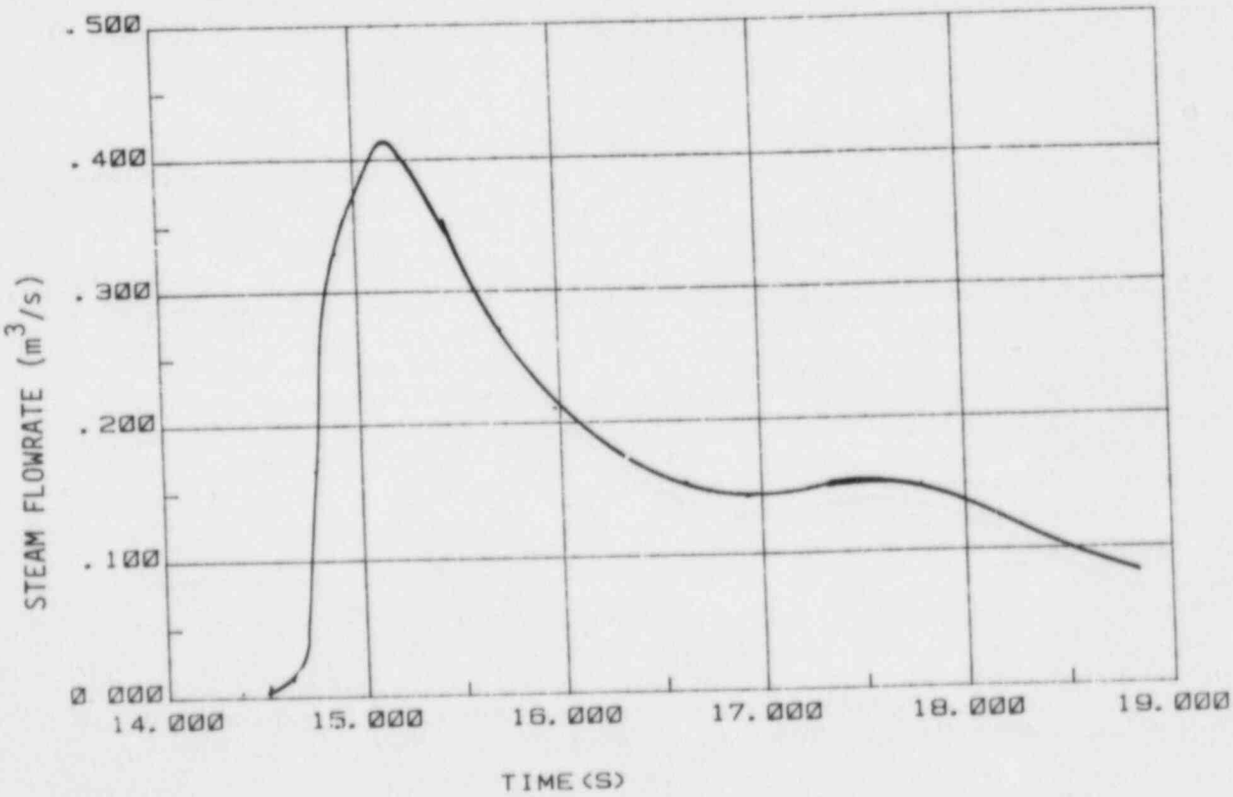

Figure 4.3 Steam Flow Rate Transient During Particle-Water Thermal Interaction.

4.2 Core Debris Thermal-Hydraulic Phenomenology: In-Vessel Debris Quenching (N.K. Tutu, T. Ginsberg, J. Klein, J. Klages, and C.E. Schwarz)

The purpose of this task is to develop an understanding of the transient quenching of in-vessel debris beds (formed in the reactor core region) when the coolant is injected from below. The experimental results would, in addition, generate a data base for verifying the transient thermal-hydraulic models for the quenching process. The present experimental and model development effort is directed towards the case where the coolant is being injected at a constant rate.

4.2.1 Model Development

The quasi-steady 1-D debris bed quenching model developed earlier (Tutu et al., 1983) assumes the existence of a "heat transfer layer" traveling up the bed at a constant speed. The model is valid only after the heat transfer layer has been formed and has begun to propagate at a constant speed. From the moment of coolant injection until this time, the model is invalid, and the model becomes invalid again once the top of the heat transfer layer reaches the top of the debris bed. For deep beds (heat transfer layer thickness $<<$ bed height), this initial and final quench period is only a small part of the total quench duration, and if details of the initial period are not required, the quasi-steady model is quite adequate. However, when the heat transfer layer thickness is of the same order as the bed height (shallow bed), the quasi-steady assumption is likely to break down for most of the quench duration. In this case the governing partial differential equations must be solved directly. To reduce the numerical computation time and yet retain the essential physics of thermal interaction, we shall now make a few assumptions. This is being done primarily to interpret our experimental results and to demonstrate the main features of the problem. It must be emphasized that we are still considering the problem where the liquid is being injected at a constant rate from below.

We make the following assumptions:

(i) the liquid enters at saturation temperature T_{sat} and remains at T_{sat},

(ii) the solid-vapor heat transfer is neglected,

(iii) molecular heat conduction through the solid is negligible compared to the boiling heat transfer,

(iv) the absolute liquid velocity of a liquid element within the bed remains constant,

(v) the vapor is produced at the film temperature, $(T_{solid} + T_{sat})/2$.

A discussion of these assumptions, the partial differential equations representing the mass and energy balances, and the detailed results is presented elsewhere (Tutu et al., 1984). Numerical computations show that for shallow beds the results are very sensitive to the heat transfer coefficients used. With proper choice of the parameters describing the heat transfer coefficients reasonable agreement with the experimental data can be obtained. Figure 4.4 shows the calculated and experimental values of the instantaneous vapor flux at the top of the debris bed as a function of time for one of the experimental cases. As can be seen, the agreement is qualitatively reasonable and demonstrates both the effectiveness of the simple model, and more importantly, the value of modeling the heat transfer coefficients accurately.

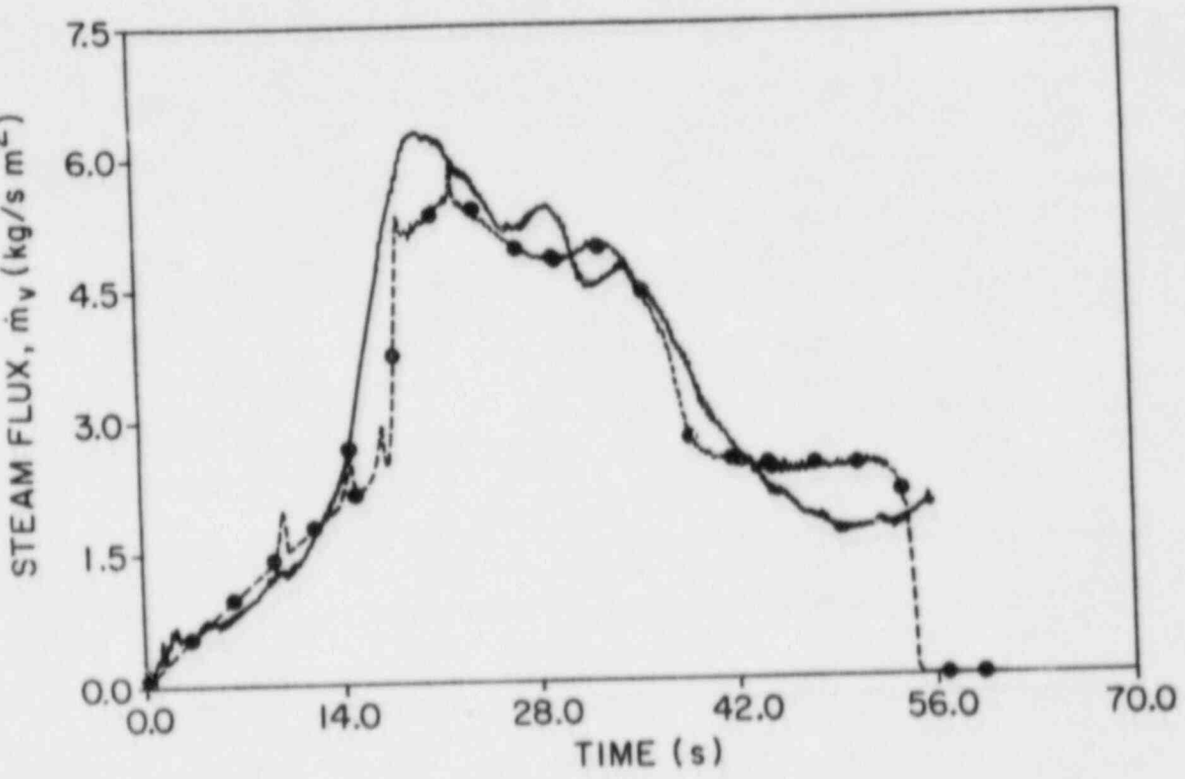

Figure 4.4 Instantaneous Steam Flux at the Top of Debris Bed. ——— : Experimental Data; –●– : Transient Model Prediction. Initial debris bed temperature = 775 K, Inlet Water Temperature = 373 K, Water Injection Superficial Velocity = 7.4 mm/s, Bed Height = 422 mm.

4.3 Core-Concrete Heat Transfer Studies: Coolant Layer Heat Transfer

(G. A. Greene and T. F. Irvine, Jr. (SUSB))

The purpose of this task is to study the mechanisms of liquid-liquid boiling heat transfer and its effect on the ex-vessel attack of molten core debris on concrete. This effort is in support of the CORCON development program at Sandia National Laboratories.

4.3.1 Experimental Facility Improvements

In the first series of liquid-liquid film boiling tests with noncondensable gas flux, it was observed that the gas flux would decrease during the test as the liquid metal melt temperature decreased. This was due to induced freezing of the melt on the gas injection coil. This difficulty was overcome by the addition of an in-line high temperature 1/2-inch pipe heater to preheat the noncondensable gas to the initial melt temperature. This would also prevent the gas from acting as a heat sink if injected into the hot melt at room temperature. It was found possible to maintain the gas melt temperature to within $\pm$20C of the liquid metal bulk temperature throughout the transient boiling quench simply by overshooting the initial melt temperature and then manually adjusting the power to the pipe heater during the run.

4.3.2 Experimental Modeling

Detailed thermophysical properties data have been gathered and curve-fit for the range of liquid metals and boiling fluids expected to be used in these tests. The properties are necessary to perform the melt energy balance, as well as calculate the expected boiling heat transfer and perform necessary hydrodynamic instability calculations. Property data for the liquid metals (bismuth, lead, Wood's metal, and mercury) include specific heat, density, surface tension, and latent heat. Property data for the boiling fluids (R-11, water, and methyl alcohol) include density, viscosity, thermal conductivity, heat of vaporization, specific heat, and surface tension for the saturated liquid and superheated vapor.

4.3.3 Test Apparatus Reconstruction

During the testing procedure, an unexpected high voltage arc caused by a malfunction of the circuitry protection system for the power supply arced to the test apparatus, melting through the 1/2-inch steel base. The damage to the apparatus was substantial, requiring reconstruction of the test vessel. At this time, other desirable design modifications were incorporated into the new test section. This work was completed during the quarter and the experiments were resumed.

4.3.4 Experimental Observations

A total of 21 R11/liquid metal film boiling experiments with noncondensable gas flux were performed this quarter. In addition, 6 R11 liquid metal boiling experiments without gas flux, two conventional R11 film boiling experiments on a solid horizontal surface, and 7 R11 heat balance tests were performed.

The R11/liquid metal liquid-liquid film boiling tests with gas injection from below were performed over a range of superficial gas velocity from 0.6 cm/s to 5.0 cm/s. An example of the transient thermal behavior of the liquid metal pool during film boiling with gas injection is shown in Figures 4.5(a-b) for Run 219 (J_G = 5.0 cm/s). Seven thermocouples are submerged in the liquid metal pool; TC5 is closest to the free surface while TC11 is closest to the base. The depths of the thermocouples below the free surface are indicated in parentheses on the figure.

The data indicate that the liquid metal pool is well-mixed over its entire eight centimeter depth, both due to the film boiling above as well as the gas injection from below. The pool appears to cool isothermally (0-210 s) until it reaches its fusion temperature (Pb fusion temperature = 600K). The pool remains isothermal throughout its depth at the fusion temperature as a bubbling slurry (210-280 s) until almost all the latent heat is removed by the boiling layer above. As the slurry concentration increases, its viscosity increases until convection can no longer be sustained to keep the pool well-mixed. At this point, the pool is essentially completely frozen (280 s) and a temperature gradient develops across the now solidified pool, indicating a transition from convection to conduction as the mechanism of heat transfer within the metal layer.

In addition to the observation that slurry freezing is the dominant mode of solidification of a bubbling liquid metal pool (no conclusions are being made concerning oxidic pools), it was found that the solidified mass was porous even after freezing was complete. The gas injection flow rate remained constant and the pressure drop across the metal pool remained constant during the entire time of the test.

A third observation was that at even the highest gas injection superficial velocity ($J_G \approx 5.0$ cm/s), there were observed no R11/liquid metal vapor explosions such as occurred with water. This indicates that R11 is highly stable in liquid-liquid film boiling, as compared to water which was found to be unstable; an understanding of why may shed some light on the mechanisms of pool-geometry vapor explosions in the future.

4.3.5 Experimental Results

Several of the liquid-liquid film boiling tests have been analyzed and the results are presented in Figures 4.6-4.8.

Figure 4.6(a-b) presents the results of Bismuth/R11 Film Boil Run 130 without gas injection from below. The trend of the data is seen to agree well with the Berenson film boiling model (solid line). However, the magnitude of the heat flux for liquid-liquid boiling is seen to lie above the Berenson model by approximately a factor of two.

In Figure 4.7(a-b) are presented the results for Pb/R11 Film Boil Run 212 with superficial gas velocity equal to 0.77 cm/s. Once again, the trend of the data is the same as the Berenson model; however, even at such a low gas flow rate as 0.77 cm/s, the bubbling enhancement of the film boiling heat flux is evident. In this case, the measured heat flux is 2.5 times greater

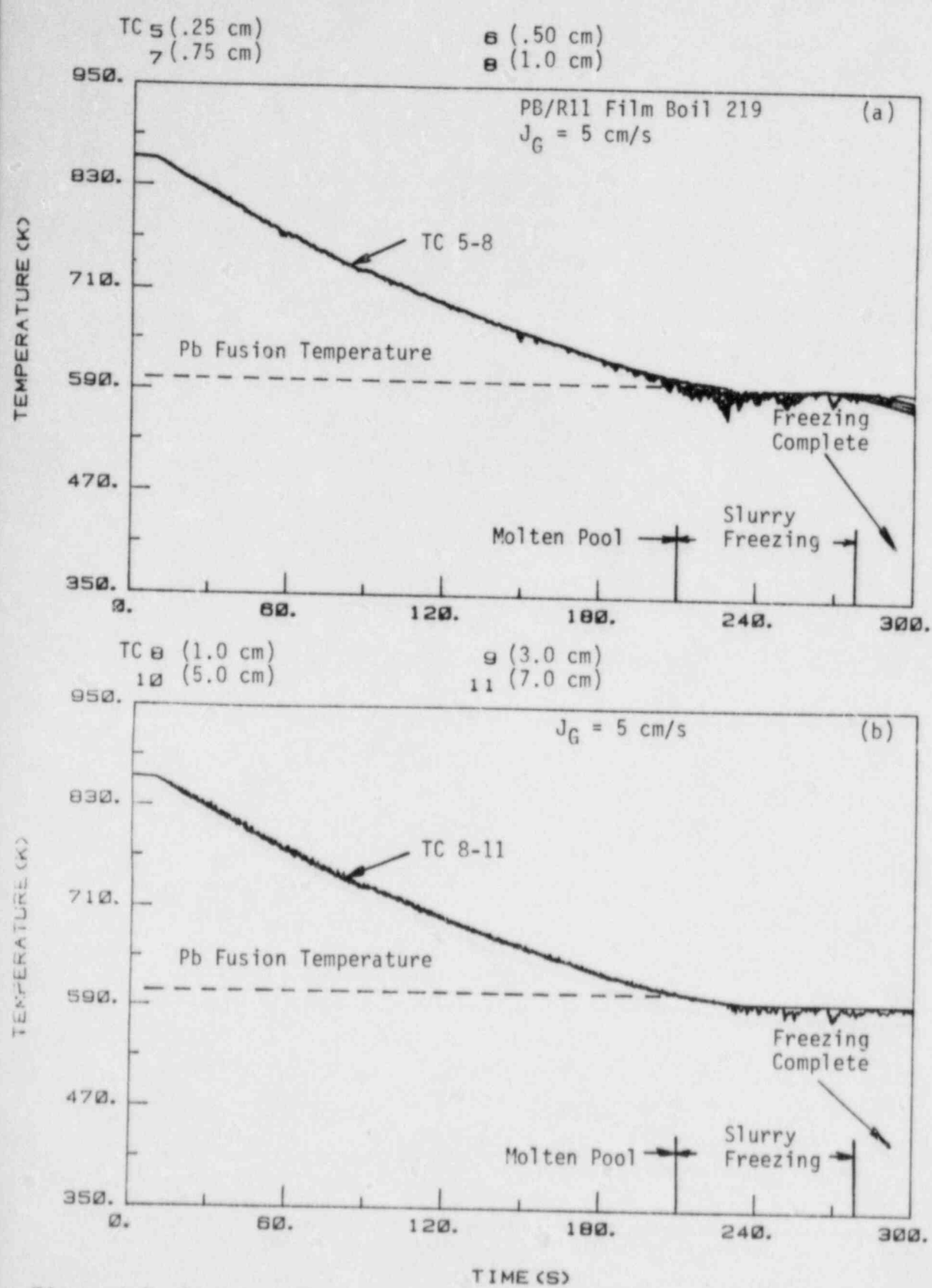

Figure 4.5 Transient Thermal Response of Molten Lead Pool During Liquid-Liquid Film Boiling: Run No. 219.

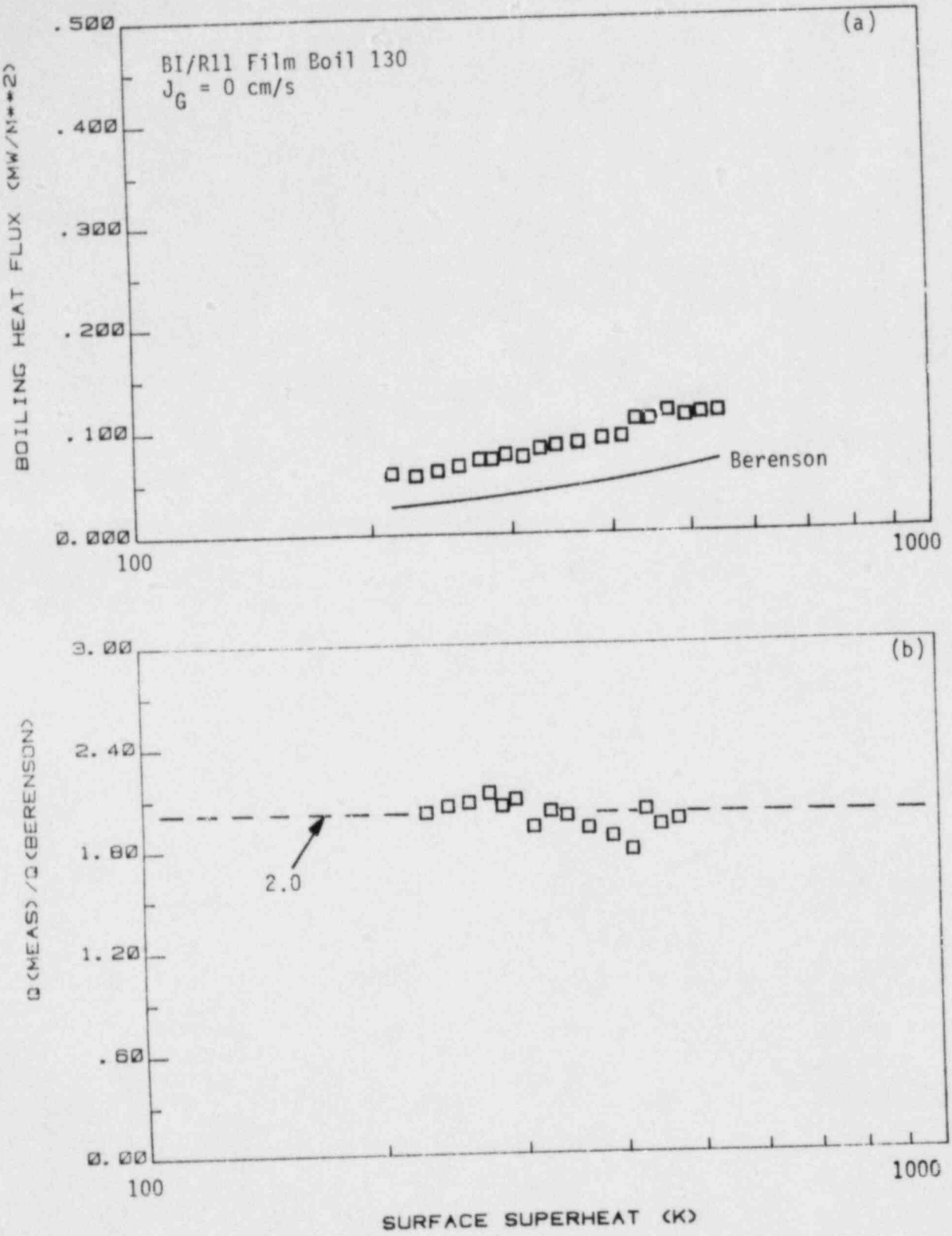

Figure 4.6 Liquid-Liquid Film Boiling Run 130: J_G = 0 cm/s.

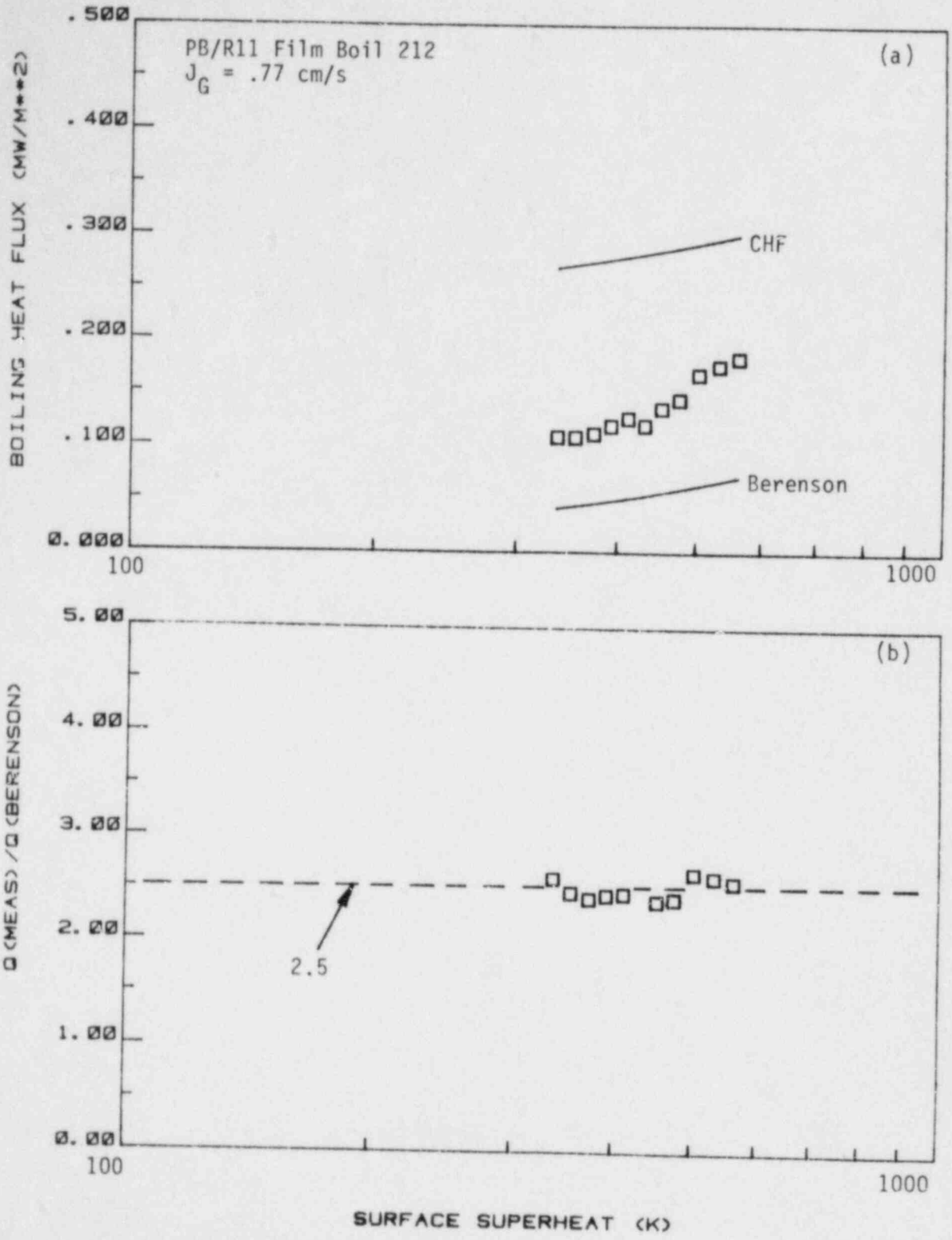

Figure 4.7 Liquid-Liquid Film Boiling Run 212: J_G = .77 cm/s.

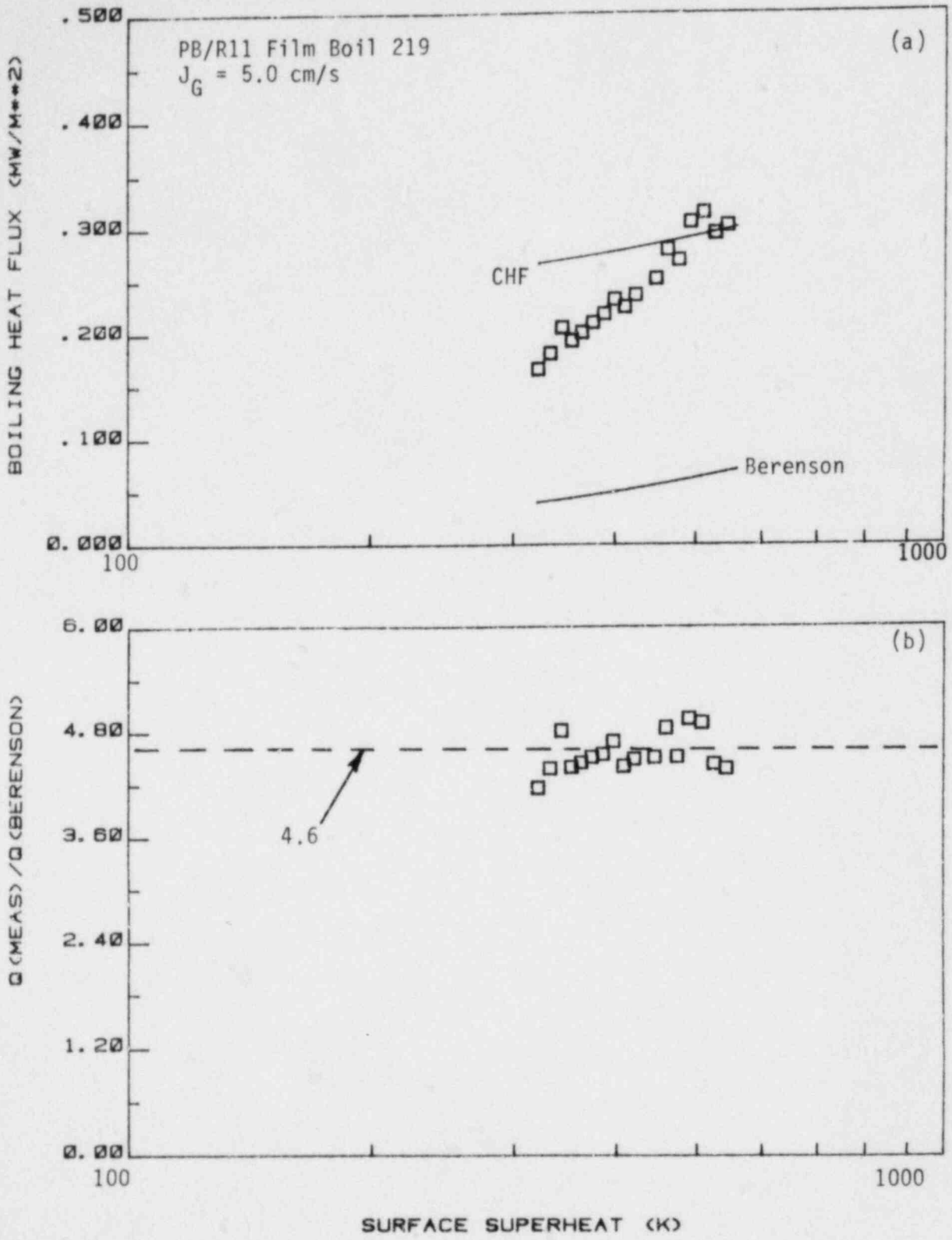

Figure 4.8 Liquid-Liquid Film Boiling Run 219: J_G = 5.0 cm/s.

than the Berenson model. This represents a 25% increase over the zero gas flux case.

In Figure 4.8(a-b) are presented the results for Pb/R11 Film Boil Run 219 with superficial gas velocity equal to 5.0 cm/s. This represents the highest gas flux achieved in these tests. Here we see the measured heat flux approaches the critical heat flux for R11. The critical heat flux shown in the figure is calculated based upon physical properties at the local boiling film temperature, i.e., $T = (T_{surface} + T_{sat})/2$. For this case, the measured heat flux is almost 5 times greater than the Berenson model prediction. This represents an increase over the zero gas flux case of a factor of 2.3.

For the case of R11 liquid-liquid film boiling, the bubbling enhancement to the film boiling heat flux appears to be due to an increase in the interfacial surface area between the R11 and the liquid metal. Reasons for the increase in heat flux for the case of no gas injection, as well as the gas injection enhancement, are currently under investigation. These results should be considered preliminary and may be subject to change.

REFERENCES

BANKOFF, S. G. and S. H. HAN, "Mixing of Molten Core Material and Water," Nuclear Science and Engineering (1984).

BERENSON, P. J., "Film Boiling Heat Transfer From a Horizontal Surface," J. Heat Transfer, 83, pp. 351-358 (1961).

FAUSKE, H. K. and R. E. HENRY, "Interpretation of Large-Scale Vapor Explosion Experiments with Application to LWR Accidents, "Proceedings of International Meeting on Light Water Reactor Severe Accident Evaluation, 1, 6.5-1 (August 1983).

GINSBERG, T., et al., "LWR Steam Spike Phenomenology: Debris Bed Quenching Experiments," NUREG/CR-2857, BNL-NUREG-51571 (June 1982).

GINSBERG, T., et al., Chap. 4 in "Safety Research Programs Sponsored by Office of Nuclear Regulatory Research, Quarterly Progress Report, July 1 - September 30, 1983; compiled by Allen J. Weiss, NUREG/CR-2331, BNL-NUREG 51454, Vol. 3, No. 3, 1984.

GINSBERG, T., et al., Chap. 4 in "Safety Research Programs Sponsored by Office of Nuclear Regulatory Research, Quarterly Progress Report, October 1 - December 31, 1982; compiled by Allen J. Weiss, NUREG/CR-2331, BNL-NUREG 51454, Vol. 2, No. 4, 1983.

TUTU, N. K., et al., Ch. 4 in "Safety and Research Programs Sponsored by Office of Nuclear Regulatory Research, Quarterly Progress Report, April 1 - June 30, 1983; compiled by Allen J. Weiss, NUREG/CR-2331, BNL-NUREG-51454, Vol. 3, No. 2, 1983.

TUTU, N. K., et al. (1984), "Debris Bed Quenching Under Bottom Flood Conditions," NUREG/CR-3850, to be published.

5. Development of Plant Analyzer
(W. Wulff)

5.1 Introduction

This program is being conducted to develop an engineering plant analyzer, capable of performing accurate, real-time and faster than real-time simulations of plant transients and Small-Break Loss of Coolant Accidents (SBLOCAs) in LWR power plants. The engineering plant analyzer is being developed by utilizing a modern, interactive, high-speed, special-purpose peripheral processor, which is designed for time-critical systems simulations. The engineering plant analyzer supports primarily safety analyses, but it serves also as the basis of technology development for nuclear power plant monitoring, for on-line accident diagnosis and mitigation, and for upgrading operator training programs and existing training simulators.

There were three activities related to the LWR Plant Analyzer Development Program; namely, (1) the assessment of the capabilities and limitations in existing simulators for nuclear power plants, (2) the selection and acquisition of a special-purpose, high-speed peripheral processor suitable for real-time and faster than real-time simulation of power plant transients, and (3) the development of mathematical models and the software for this peripheral processor.

(1) One each of operating PWR and BWR power plants and their simulators had been selected to establish the status of current real-time simulations with respect to modeling fidelity for the thermohydraulics in the Nuclear Steam Supply System (NSSS). The assessment consisted of establishing the modeling assumptions in the process descriptions for the NSSS, and of comparing NSSS-related simulator results with results from RETRAN calculations. The evaluation was performed to determine the current simulator capabilities and limitations of providing engineering predictions for operational transients and for transients caused by loss of coolant injection, by a loss of feedwater or feedwater heaters, by a loss of heat sink (steam generator failure), or by a mismatch between fission power and cooling rate.

(2) The AD10 of Applied Dynamics International (ADI) of Ann Arbor, Michigan, had been selected earlier as the special-purpose, high-speed peripheral processor on the basis of its capacity to execute faster and more efficiently the operations which are currently being performed in training simulators by general-purpose computers. Specifically, the special-purpose processor was selected for efficient, high-speed integration of ordinary differential equations and for direct, on-line interactions with the user, with instrumentation, with both digital and analog signals from other computers and with graphic devices for continuous, on-line display of a large number of computed parameters.

(3) The software development for the new peripheral processor is carried out in two phases. One phase was the implementation of an existing thermohydraulics model for a BWR system to simulate operational transients on the new

processor. This phase served to compare the computing speed and accuracy of the AD10 processor with those of the CDC-7600 mainframe computer, and thereby to demonstrate in principle the feasibility of computing realistic transients at faster than real-time computing speeds. The second phase is the modeling of the primary loop outside of the vessel and its controls, neutron kinetics and thermal conduction for the complete BWR simulation and the formulation and implementation of a thermohydraulic model for the faster than real-time analysis of operational and SBLOCA transients in PWR power plants. This is supplemented by implementation of multicolor graphics displays.

Below is a brief summary of previously obtained results and a detailed summary of achievements during the current reporting period.

5.2 Assessment of Existing Simulators (W. Wulff and H. S. Cheng)

The assessment of current simulator capabilities consisted of evaluating qualitatively the thermohydraulic modeling assumptions in the simulator and of comparing quantitatively the predictions from the simulator with results from the detailed systems code RETRAN.

The results of the assessment have been published earlier in three reports (Wulff, 1980; Wulff, 1981a; Cheng and Wulff, 1981). It had been found that the reviewed training simulators were limited to the simulation of steady-state conditions and quasi-steady transients within the parameter range of normal operations. Most PWR simulators delivered before 1980 cannot simulate two-phase flow conditions in the primary reactor coolant loops, nor the motion of the two-phase mixture level beyond the narrow controls range in the steam generator secondary side. Most BWR simulators delivered before 1980 cannot simulate two-phase flow conditions in the recirculation loops or in the downcomer and lower plenum, nor can they simulate coolant level motions in the steam dome, the lower regions of the downcomer (below the separators), or in the riser and core regions. These limitations arise from the lack of thermohydraulic models for phase separation and mixture level tracking (Wulff, 1980; 1981a).

The comparison between PWR simulator and corresponding RETRAN results, carried out for a reactor scram from full power, showed significant discrepancies for primary and secondary system pressures and for mean coolant temperatures of the primary side. The discrepancies were found even after the elimination of differences in fission power, feedwater flow and rate of vapor discharge from the steam dome. Good agreement was obtained between simulator and RETRAN calculations for only the early part (narrow control range) of the water level motion in the steam generator. The differences between simulator and RETRAN calculations have been explained in terms of modeling differences (Cheng and Wulff, 1981).

5.3 Acquisition of Special-Purpose Peripheral Processor (A. N. Mallen and R. J. Cerbone)

The AD10 had been selected earlier as the special-purpose peripheral processor for high-speed, interactive systems simulation. A brief description of

the processor has been published in a previous Quarterly Progress Report (Wulff, 1981b). A PDP-11/34 DEC computer serves as the host computer.

Two AD10 units, coupled directly to each other by a bus-to-bus interface and equipped with a total of one megaword of memory, have been installed with the PDP-11/34 host computer, two 67 megabyte disc drives, a tape drive and a line printer. On-line access is facilitated by a model 4012 Tektronix oscilloscope terminal and a 28-channel signal generator. The system is accessed remotely via four ADDS CRT terminals and two DEC Writer terminals, one also equipped with a line printer. An IBM Personal Computer will also be used to access the PDP-11/34 host computer but is now used primarily to generate labelled, multicolored graphs from AD10 results. An advanced multicolor graphics terminal is needed, however, for extensive on-line display of simulated parameters generated by the AD10 at real-time or faster computing speeds.

5.4 Software Implementation on AD10 Processor

A four-equation model for nonhomogeneous, nonequilibrium two-phase flow had been formulated and supplemented by constitutive relations from an existing BWR reference code, then scaled and adapted to the AD10 processor to simulate the Peach Bottom-2 BWR power plant (Wulff, 1982a). The resulting High-Speed Interactive Plant Analyzer code (HIPA-PB2) has been programmed in the high-level language MPS-10 (Modular Programming System) of the AD10. After implementing the thermohydraulics of HIPA-PB2 on the AD10, we compared the computed results and the computing speed of the AD10 with the results and the computing speed of the CDC-7600 mainframe computer, to demonstrate the feasibility of achieving engineering accuracy at high simulation speeds with the low-cost AD10 minicomputer (Wulff, 1982b).

It has been demonstrated (Wulff, 1982b) that (i) the high-level, state equation-oriented systems simulation language MPS-10 compressed 9,950 active FORTRAN statements into 1,555 calling statements to MPS-10 modules, (ii) the hydraulics simulation occupies one-fourth of available program memory, (iii) the difference between AD10 and CDC-7600 results is only approximately $\pm$ 5% of total parameter variations during the simulation of a severe licensing base transient, (iv) the AD10 is 110 times faster than the CDC-7600 for the same transient, and (v) the AD10 simulates the BWR hydraulics transients ten times faster than they progress in real-time. It has been demonstrated now that even after the inclusion of models for neutron kinetics, conduction, balance of plant dynamics and controls, the AD10 still achieves ten times real-time simulation speed for all transients reported earlier (Wulff, 1983c).

The HIPA-PB2 hydraulics program used earlier for the feasibility demonstration has been expanded to simulate neutron kinetics (point kinetics), thermal conduction in fuel elements and the thermohydraulics of the components shown in Figure 5.1. The expanded version is called HIPA-BWR/4.

The stand-alone program modules for neutron kinetics with feedback simulation and scram control, for thermal conduction in fuel elements, for compressible flows in the steam line and for the control logic for operating the

safety and relief valves tested earlier (Wulff, 1982c; 1983a) have been implemented in HIPA-BWR/4. Models had been formulated and tested separately for the control systems and the plant components forming the loop through turbines, condensers and the feedwater trains. They have been implemented during the previous reporting period.

Specific accomplishments of the current reporting period are described below.

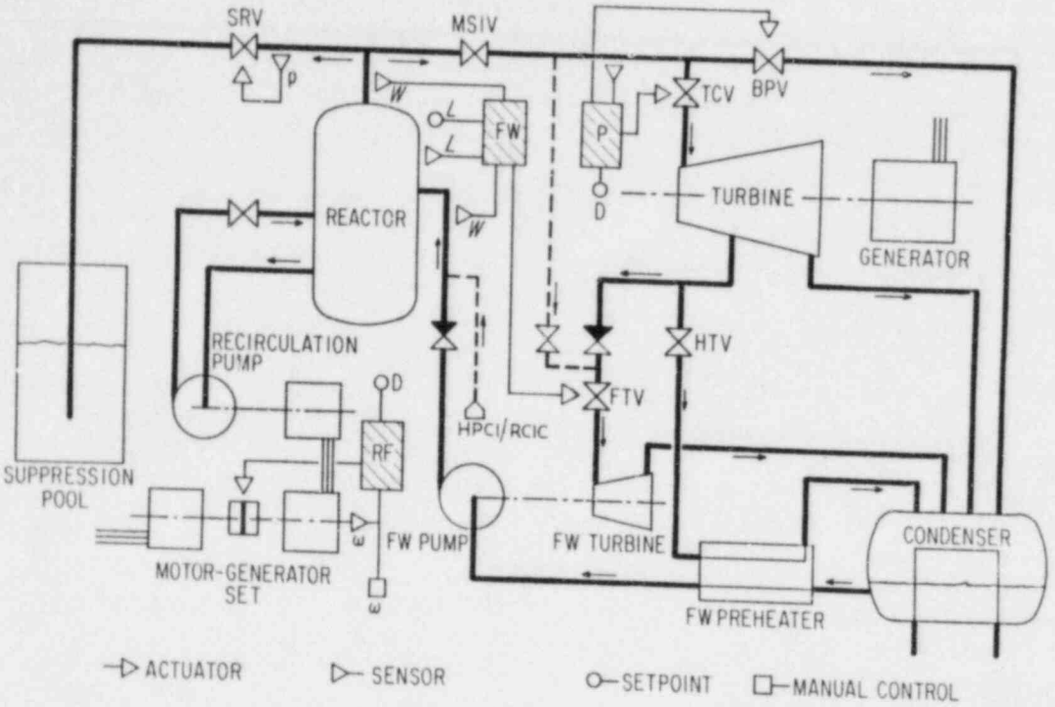

Figure 5.1 Flow Schematic and Control Blocks for BWR Simulation; FW - Feedwater Controller, P - Pressure Controller, RF - Recirculation Flow Controller.

5.4.1 Program Improvements (H.S. Cheng, A.N. Mallen and W. Wulff)

During the previous reporting period we reported on a numerical instability problem which was perceived to be caused by the limit of the dynamics range associated with computing the wall friction for the steam line flow. The problem has been resolved. The actual source of the instability was an error of logic. The dynamic range of the wall shear has been expanded by three decades.

An additional vapor mass balance has been added to predict the vapor mass in the upper portion of the downcomer, bounded at the top by the moving mixture level. This additional mass balance permits the prediction of the mixture level in the upper downcomer portion within the framework of the existing hydraulics model. It replaces the equation for the motion of the mixture level, based on the mass jump condition if there is no liquid above the mixture level.

5.4.2 Developmental Assessment

The thermohydraulics model had been assessed earlier by comparison with power plant test data (Wulff, 1981c). This assessment had been carried out with the CDC-7600 computer, prior to the model implementation as HIPA-BWR in the AD10 processor. The assessment will be repeated after the previously used slip flow model is replaced by the drift flux model.

To assess the plant analyzer capabilities in simulating the entire plant response, including the responses of the balance of plant components and of the control system, we compared plant analyzer results with available data on severe transients. The first set of available data are computed results published by GE (1981).

These reference results are obtained from generic analyses on General Electric BWR-4 power plants. The control system parameters and many plant data used in these generic analyses were not published by GE and should be expected to differ from the plant-specific data taken for the plant analyzer from the Final Safety Analysis Report (FSAR, Philadelphia Electric Company, 1971) of Peach Bottom II and from the EG&G Report by James D. Milton (1982). Consequently, it cannot be expected that the GE data agree completely with the plant analyzer results. However, the comparisons should reveal, whether or not the control functions are simulated in the plant analyzer so as to activate valves and trips in the protection system in the proper sequence, and whether or not main engineering parameters vary as in the GE predictions.

Differences between plant analyzer data and results from GE predictions should be attributable to differences in control system set points, signal transmission delay times, pump, turbine and actuator responses, and possibly to differences in valve flow capacities. For the plant analyzer results presented, these data are plant-specific for Peach Bottom II and the best data available at this time. For the GE calculations, the data were not completely defined and are claimed to represent BWR-4 power plants generically. Differences which cannot be attributed to the differences in plant data would indicate modeling differences. The purpose of comparing the GE predictions with plant analyzer simulations is to identify the sources of their differences either as plant data differences or modeling differences.

Below are presented the first 10 transients simulated so far. They are anticipated transients without scram, initiated by eight different events and accompanied by four alternate circumstances as follows:

(i) Main Steam Isolation Valve Closure

(ii) Loss of AC Power

(iii) Loss of Condenser Vacuum

(iv) Loss of Feedwater Flow

(v) Loss of Feedwater Heaters

(vi) Turbine Trip with Bypass Flow

(vii) Turbine Trip without Bypass Flow

(viii) Pressure Regulator Failure at Zero Demand

(ix) Pressure Regulator Failure at Maximum Demand

(x) Feedwater Controller Failure at Maximum Demand.

Shown are the plant analyzer results as printed via the IBM Personal Computer, with GE predictions plotted by hand onto the same diagrams.

Discussion of Comparisons

The comparisons show in general that the plant analyzer produces results similar to the GE predictions. There are minor differences in parameter variation, of amplitudes and timing that are directly related to the differences in plant data as discussed above. The major differences recognized from the comparisons are in the relief valve cycling frequency. GE predictions (1981) show four to five times slower depressurization rates than the plant analyzer results. However, plant analyzer results concerning the valve action are in very good agreement with the predictions from the RAMONA-3B code and they fall between GE predictions and predictions from TRAC-BD1 (Saha, 1984) as shown in Table. 5.1 below.

Table 5.1 Periods of Relief Valve Action during ATWS after MSIV Closure

	Cycling Period
Plant Analyzer	14 seconds
GE Predictions	75 seconds
TRAC-BD1	5 seconds
RAMONA-3B	12 seconds

The valve cycling period is only slightly affected by valve action set points. It depends strongly upon the rate of pressure change which is a consequence of modeling and of valve capacity data. A simple global analysis, independent of plant analyzer modeling assumptions,* yields for the rate of change of volume-average vessel pressure

$$\dot{\langle p \rangle} = \frac{(W_{fw}-W_{s\ell})(h_f v_g - h_g v_f) - v_{fg}(W_{fw}h_{fw} - W_{s\ell}h_g + \dot{Q}) - \dot{F}_\ell}{v_{fg}(V - M_f h_f' - M_g h_g') + h_{fg}[M_g v_g' + M_f v_f']} , \qquad (1)$$

where

$$\dot{F}_\ell = \dot{M}_\ell[v_{fg}(h_f - h_\ell) - h_{fg}(v_f - v_\ell)] + M_\ell \left(h_{fg}\frac{dv_\ell}{dh} - v_{fg}\right)\dot{h}_\ell \qquad (2)$$

represents the contributions from the subcooled liquid in the vessel, and W_{fw} and $W_{s\ell}$ designate, respectively, the feedwater and steam line mass flow rates. Q is the rate of heat addition to the coolant and h_{fw} is the feedwater enthalpy. M_ℓ, M_f and M_g are the masses of subcooled liquid, saturated liquid and saturated vapor, respectively, h and v stand for enthalpy and specific volume, respectively, and V is the vessel volume. The superscript dot designates differentiation with respect to time and the primes designate differentiation with respect to pressure along the saturation line. Subscripts f, g, ℓ and fg indicate saturated liquid, saturated vapor, subcooled liquid and phase change, respectively.

Since the subcooled liquid is primarily in the adiabatic downcomer, $\dot{h}_\ell \approx 0$ in Eq. 2. Also, as the level changes very little under quasi-steady valve cycling and under HPCI injection at a constant rate, one can set $\dot{M}_\ell \approx 0$ and conclude that F_ℓ contributes nothing to $\dot{\langle p \rangle}$ in Eq. 1.

Equation 1 implies equilibrium phase change in regions occupied by saturated liquid M_f and/or saturated vapor M_g. Since the depressurization rate is small ($\approx$0.5 bar/s) and the heating power is low ($\approx$25% of full power), the actual phase change should be close to equilibrium.

Equation 1 was evaluated at a particular instant during the depressurization phase of the valve action cycle (approximately 120 seconds after MSIV closure, cf. Figure 5.1). Equation 1 was evaluated with W_{fw}, $W_{s\ell}$, h_{fw}, Q, (M_f+M_ℓ) and M_g as printed out from the plant analyzer. The subcooled liquid mass M_ℓ was taken to be the mass in the downcomer nodes where the liquid temperature was observed to be below saturation temperature. Also printed out from the plant analyzer was the depressurization rate. The results are as follows:

---

*The equation in HIPA corresponding to Eq. 1 contains the nonequilibrium evaporation rate.

	Depressurization Rate (bar/s)
Equation 1 (equilibrium phase change)	-0.568
Plant Analyzer, printed	-0.577
graph slope	-0.576

It can be seen that the plant analyzer (and also RAMONA-3B and TRAC-BD1) follow, as expected, the thermodynamic equilibrium phase change.

Equation 1 reveals also that the slow depressurization rate predicted by GE could have been caused by a combination of

(i) assuming that all the liquid in the vessel is saturated,

(ii) producing a slightly larger fission power at the same condititons.

Treating all the liquid in the vessel as saturated liquid, one finds that the depressurization rate becomes smaller by a factor of 2.5 relative to the rate obtained by accounting for the subcooled liquid. The factor of 2.5 is not enough to explain the five times smaller depressurization rate predicted by GE.

On the other hand, if only the rate of heat addition to the coolant were kept at 28% of full power during quasi-steady valve cycling (cf. Figure 5.2), instead of the 22% predicted by the plant analyzer, then the depressurization rate predicted by Eq. 1 would decline by the needed factor of five. The heat transfer to the coolant is shown in the GE report to be higher than the plant analyzer results (as is the fission power), but the graphs are unsuitable to pinpoint the exact difference between heat transfer rates as the fluctuations are too irregular.

Each transient below is shown with four curves in two diagrams generated by the IBM PC printer. GE results are superimposed by hand. The selected parameters were chosen to characterize the particular transients.

(i) ATWS Induced by MSIV Closure

Figures 5.2 show the comparison between plant analyzer and GE code predictions. The system pressure predictions agree well except for the differences in cycle amplitude and frequency. The amplitude differences are clearly a consequence of pressure set point differences in relief valve control specifications (unspecified in the GE document). The frequency differences are caused by modeling differences (compressibility of subcooled liquid and/or void feedback reactivity and fission power) as discussed above.

The fission power reaches a spike after approximately five seconds of 5.3 times normal power in the GE calculations and 3.5 times normal power in the

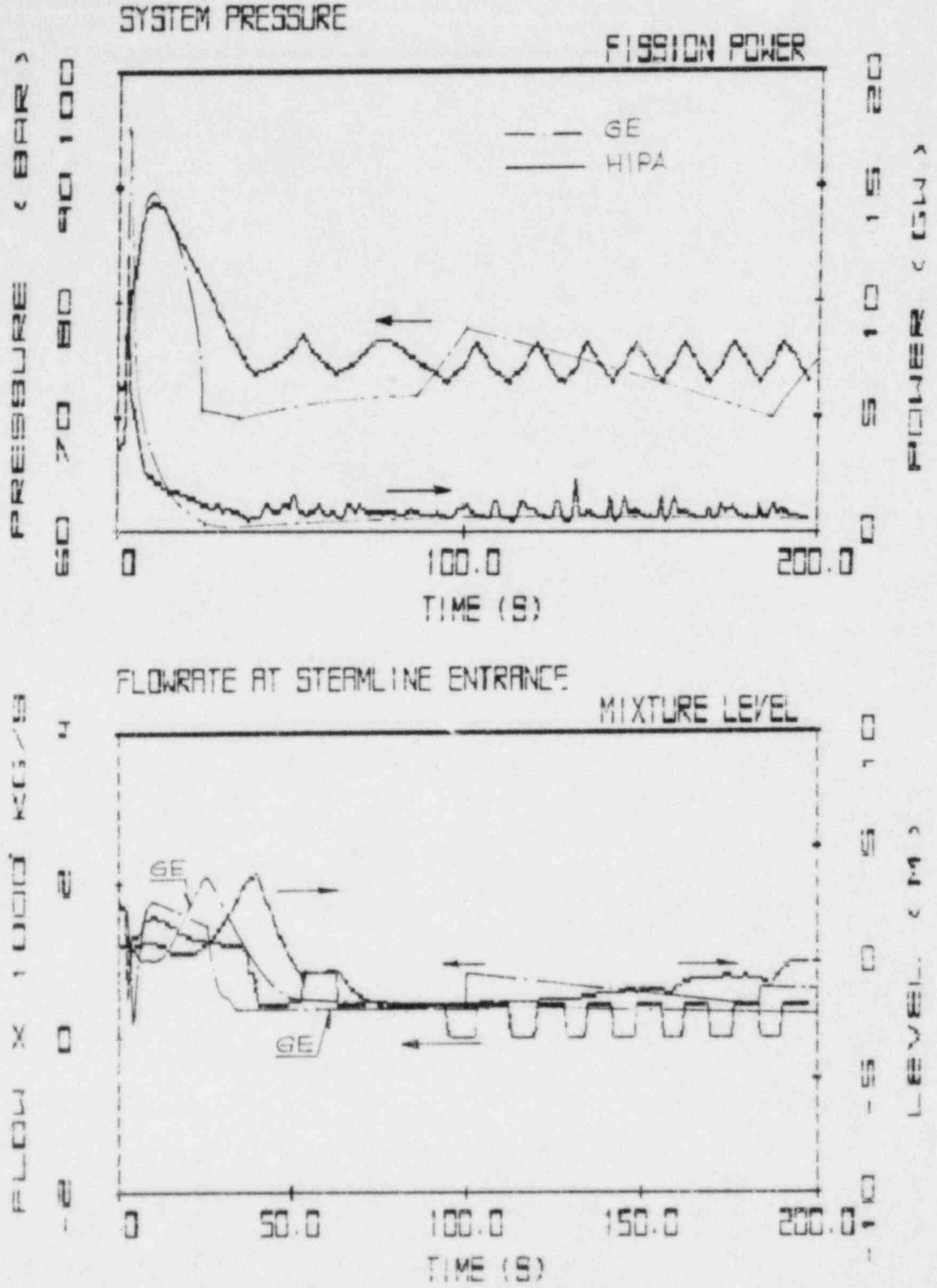

Figures 5.2 HIPA-GE Comparisons for MSIV-Initiated ATWS. —— HIPA, -·- GE. Top graph shows vessel pressure and fission power, bottom graph steam line flow and mixture level in downcomer.

plant analyzer. The power spike is proportional to the pressurization rate. The plant analyzer shows a slower fission power decrease after the spike and, correspondingly, a slower depressurization. One minute after MSIV closure the fission powers from GE and plant analyzer predictions agree. It should be noted that detailed (3-dimensional) RAMONA-3B simulations predict a power spike of 2.4 times normal fission power. Plant analyzer predictions, therefore, fall between GE and RAMONA-3B predictions.

The mixture level in the downcomer reaches its peak approximately 15 seconds earlier in the plant analyzer simulation than in the GE prediction. This difference is clearly due to differences in plant data defining the feedwater pump and control systems. Both the maximum levels and the levels reached long after the initial disturbance are predicted by the plant analyzer in good agreement with GE predictions.

The differences in the prediction of the mass flow rates through the safety and relief valves are small (cf. Fig. 5.2) and reflect the valve responses to the system pressures shown in the top of the figure.

(ii) Loss of AC Power and Scram Failure (ATWS)

This transient is shown in Figures 5.3. The transient is similar to the ATWS initiated by MSIV closure. The loss of AC power trips the main steam isolation valve closure, the recirculation pumps and the feedwater pump. The fission power and pressure peaks are lower than for the MSIV-induced ATWS because the main steam isolation valves close after the turbine has tripped or after the recirculation pumps have been tripped, that is, after some fission power reduction.

The agreement between GE predictions and plant analyzer results is about the same as for the MSIV-induced ATWS simulation. The plant analyzer predicts an initial fission power peak of 2.2 times normal power, compared with the GE power rise by the factor of 2.7. This is caused by different valve closing rates as reflected consistently in the corresponding pressure rise.

(iii) ATWS after Loss of Condenser Vacuum

Loss of condenser vacuum causes first a turbine trip with bypass opening and then MSIV closing approximately two seconds after turbine trip.

The plant analyzer predicts a fission power increase by 362%, GE predicted 403%. The plant analyzer predicts a slower depressurization rate after reaching the peak pressure. Therefore, the vapor void fraction in the core remains low for longer times, causing the fission power to exceed that predicted by GE and consequently to maintain the relief valves open even before the bypass and main steam isolation valves close. With the relief valve open in the plant analyzer prediction, the MSIV closure produces a much weaker pressure rise than predicted by GE with its MSIV closure started while all safety and relief valves are closed. The long-term predictions are governed by pressure set point specifications for the relief valves. Notice that the long-term depressurization rates from the plant analyzer (slopes of pressure curves) agree with the GE predictions.

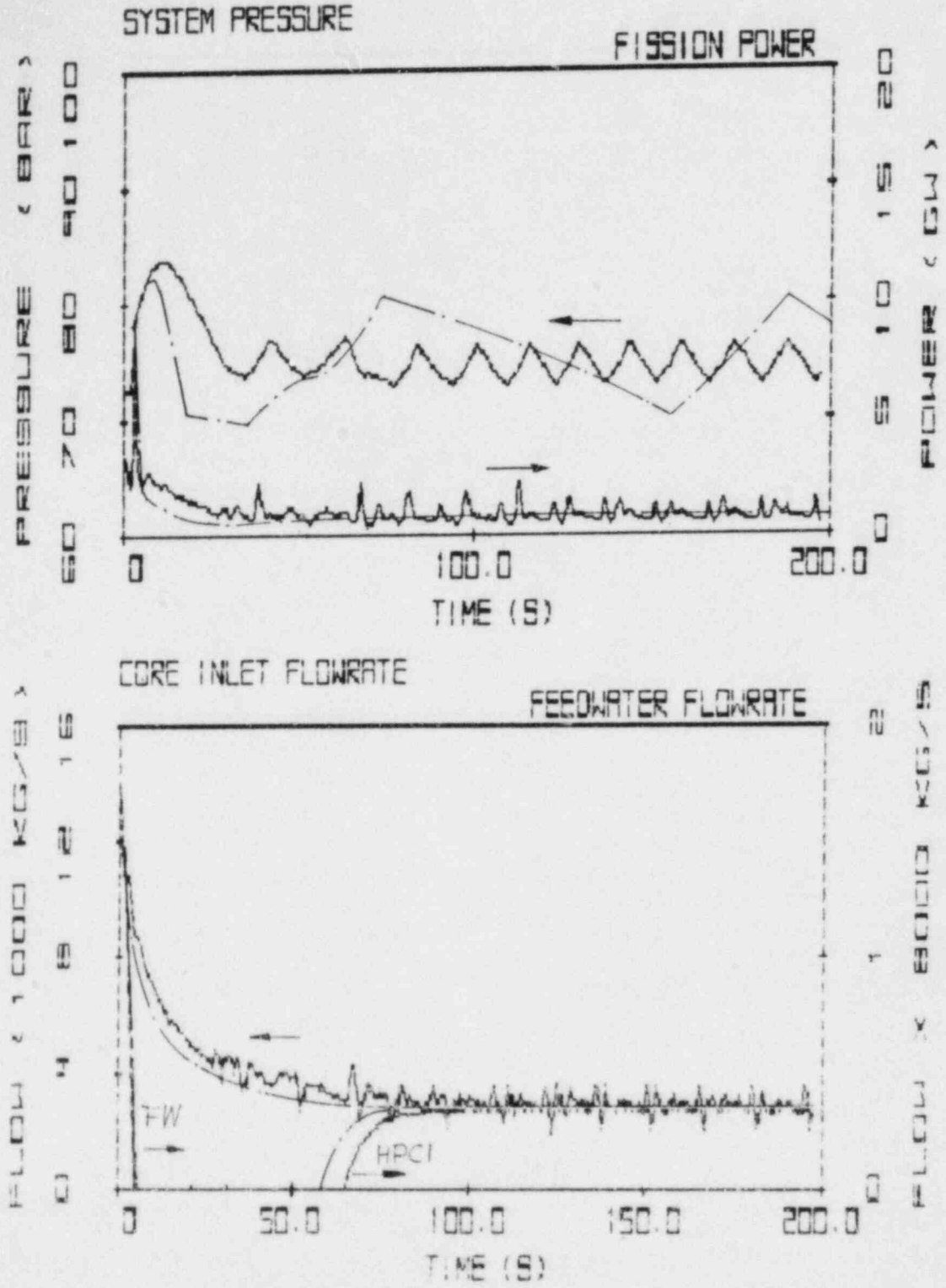

Figures 5.3 HIPA-GE Comparisons for ATWS after Loss of AC Power. —— HIPA, -·- GE. Top graph shows vessel pressure and fission power, bottom graph mixture mass flow rate at core entrance, feedwater and HPCI flows.

The feedwater flow simulation by the plant analyzer agrees well with the GE prediction. The High Pressure Core Injection is predicted to come on 24 seconds earlier in the plant analyzer than in the GE code. This results from differences in set point specifications as do the differences in mass flow rate predictions for the steam lines (top curve in lower diagram of Figures 5.4).

(iv) ATWS Induced by Loss of Feedwater Flow

This transient occurs when the feedwater turbine trips or if the feedwater regulator fails at zero demand. The results of the comparison are shown in Figures 5.5.

The plant analyzer predictions for system pressure, fission power, mixture level position in downcomer, feedwater flow and high-pressure injection agree well with the GE results. High-pressure injection is initiated earlier in the GE simulation, leading to a level recovery earlier than that of the plant analyzer. This timing difference is caused by differences in set point specifications.

(v) ATWS Caused by Loss of Feedwater Heaters

This transient is caused by a loss of extraction steam to all five heaters in a heater train. As show in Figures 5.6, pressure and fission power remain nearly unaffected as the control system, primarily the recirculation flow controller, compensates for the reactivity insertion due to the decrease in feedwater temperature.

GE reports that the fission power increases by 10% of full power and that the pressure remains constant. The plant analyzer predicts the same. The feedwater temperature drop predicted by GE is 36°C, the temperature drop predicted by the plant analyzer is 37°C.

The feedwater regulator in the plant analyzer responds to the early dropping of the mixture level in the downcomer as can be seen in the top of the lower diagram in Figures 5.6. The level position drops because feedwater with lower density is injected, causing the liquid in the downcomer to contract. The feedwater regulator increases temporarily the feedwater flow to restore the level position. This response is not shown in the GE results.

(vi) ATWS Following a Turbine Trip with Bypass Flow

Figures 5.7 show the comparisons between plant analyzer predictions and GE calculations. GE calculations lead to a fission power peak of 3.92 times normal full power, the plant analyzer produced a peak of 3.31 times normal full power. After the peak, the plant analyzer's fission power remains higher during the following hundred seconds, leading to higher pressures and to a higher combination of relief valve and bypass valve steam flow rates (cf. bottom graph in Figures 5.7). The reason for the high fission power is the feedwater flow rate prediction. There is more feedwater injected in the plant analyzer simulation than in the GE calculations, causing the moderator density

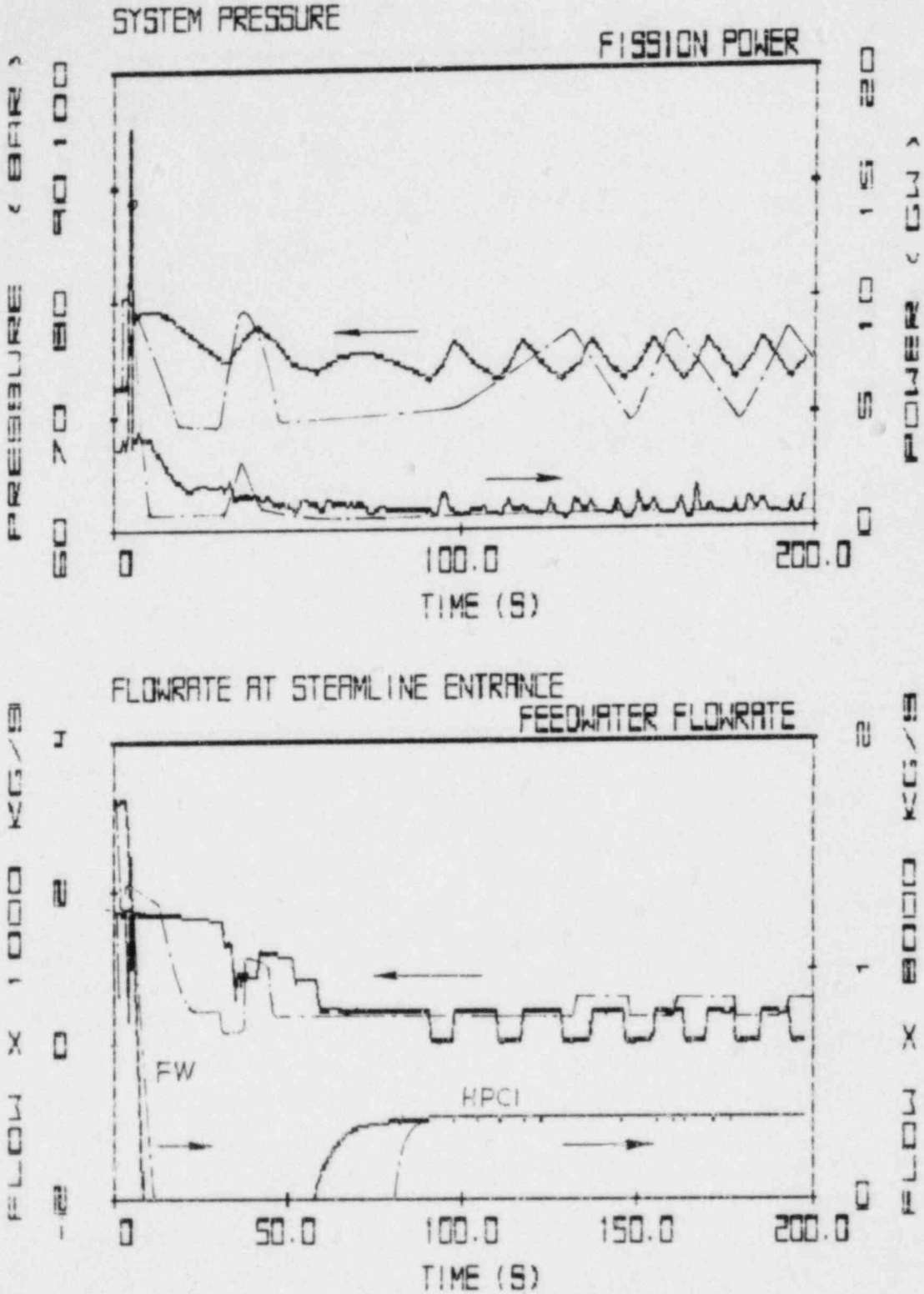

Figures 5.4 HIPA-GE Comparisons for ATWS after Loss of Condenser Vacuum. — HIPA, -·- GE. Top curve shows vessel pressure and fission power, bottom graph feedwater, HPCI flows and steam flow into steam line.

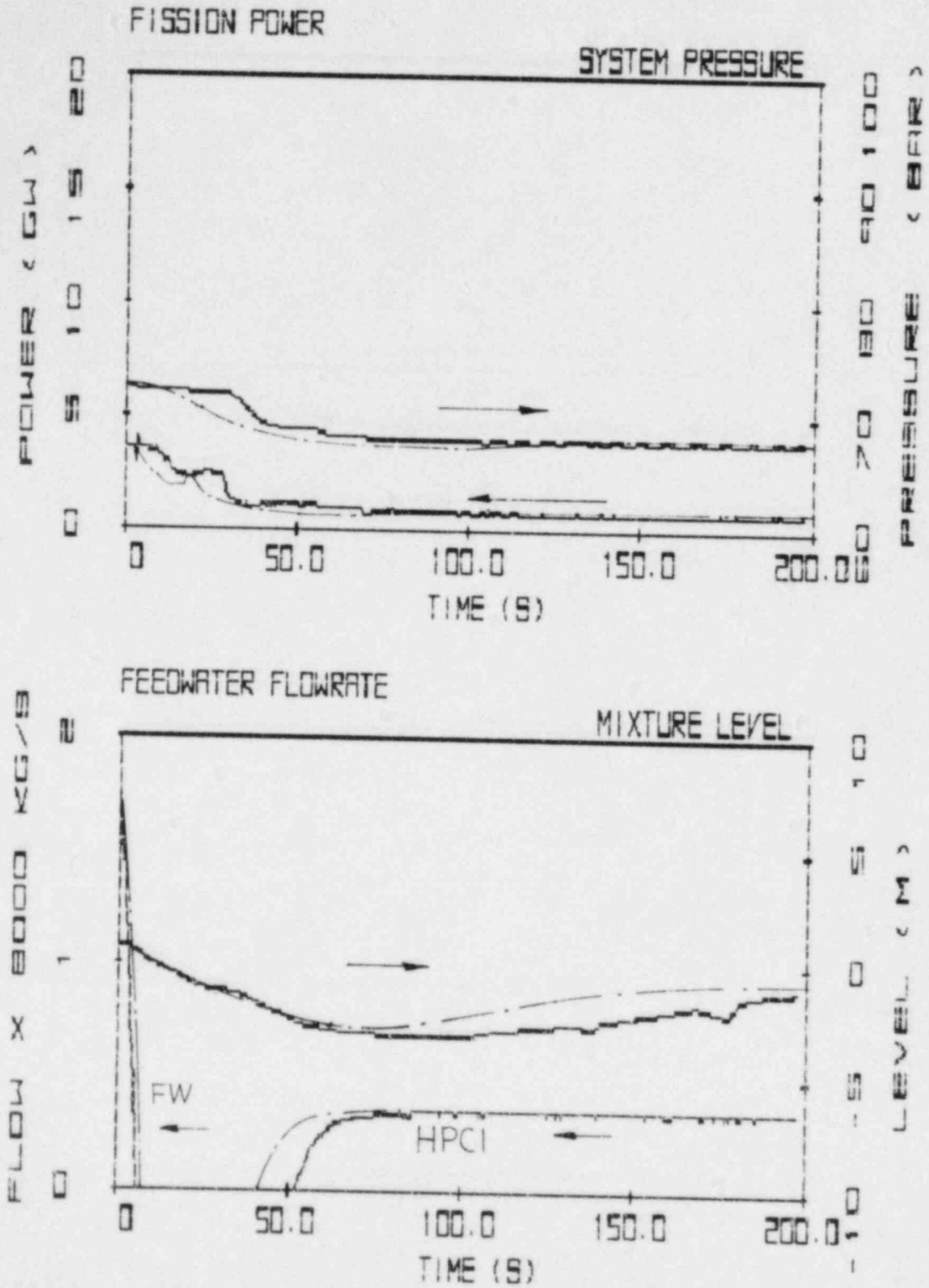

Figures 5.5 HIPA-GE Comparisons for ATWS after Loss of Feedwater Flow. —— HIPA, - - - GE. Top graph shows vessel pressure and fission power, bottom graph mixture level in downcomer, HPCI and feedwater flows.

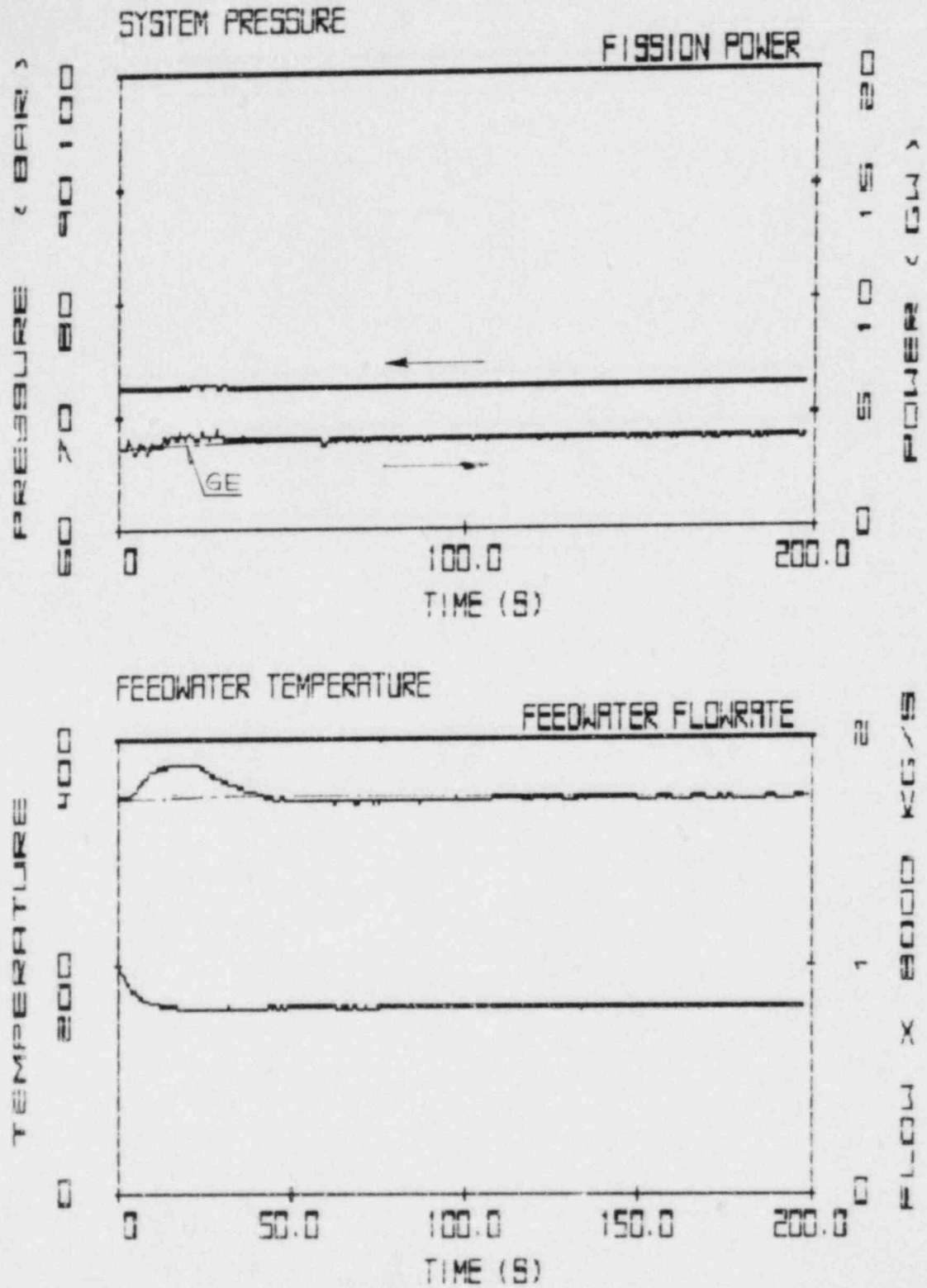

Figures 5.6 HIPA-GE Comparisons for ATWS after Loss of Feedwater Preheaters. — HIPA, -·- GE. Top graph shows fission power and vessel pressure, bottom feedwater flow rate and temperature. (No temperature data from GE).

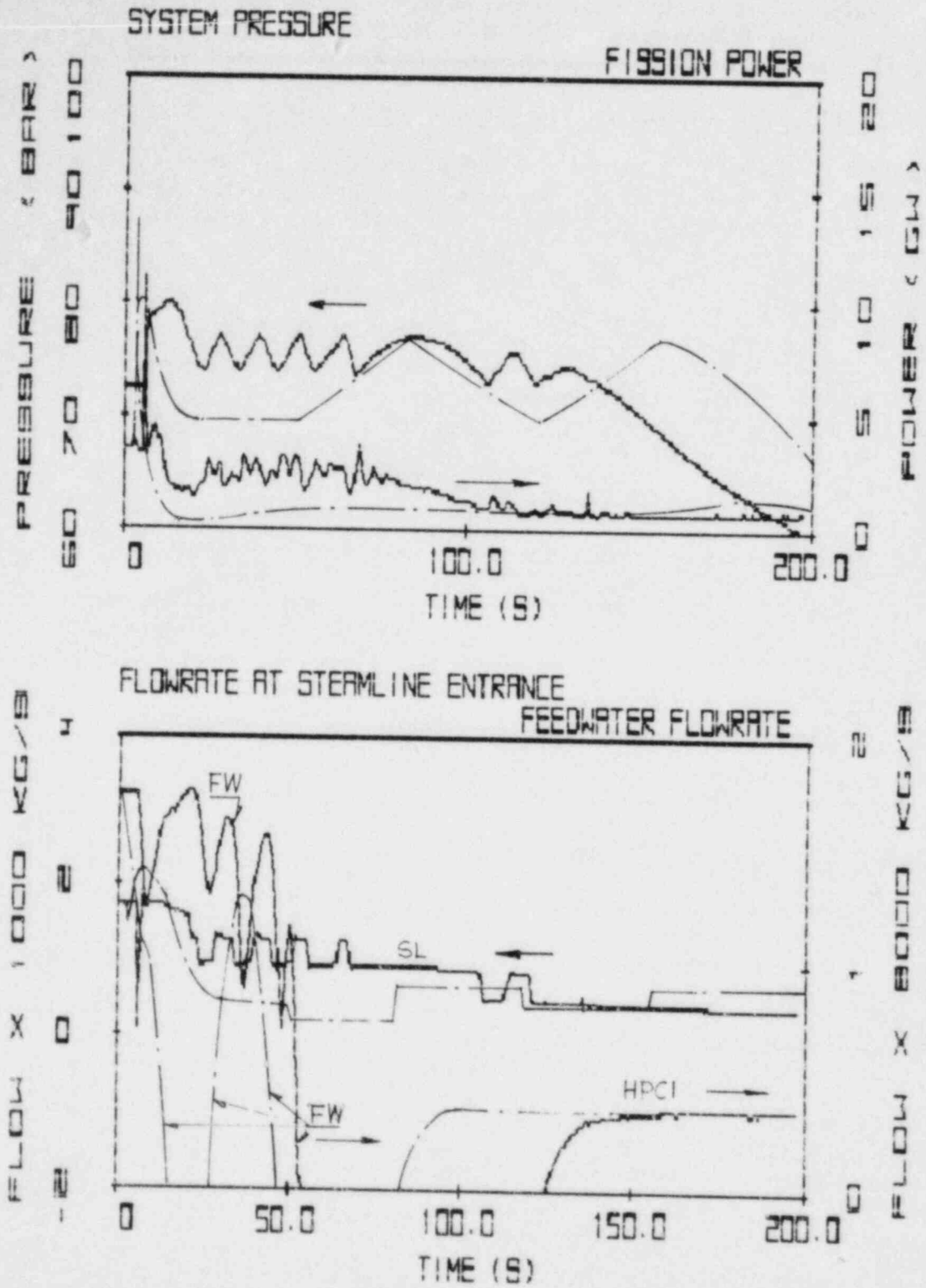

Figures 5.7 HIPA-GE Comparisons for Turbine Trip with Bypass Flow and Without Scram. —— HIPA, -·- GE. Top graph shows vessel pressure and fission power, bottom graph flows in steam line, feedwater and HPCI nozzles.

and the fission power to increase. The difference between the predictions of feedwater injection is due to differences in the control system specifications, particularly for the feedwater regulator.

(vii) ATWS Following a Turbine Trip Without Bypass Flow

This transient is shown in Figures 5.8. Shown are only the plant analyzer results because GE's report does not contain any graphs for this transient. The GE report lists characteristic data which are compared in the table below.

	Plant Analyzer	GE
Peak to normal fission power	5.60	6.55
Maximum vessel pressure	89 bar	87 bar

(viii) ATWS Initiated by Pressure Regulator Failure at Zero Demand

This transient starts with the closing of turbine control valves, responding (slowly) to the zero demand signal at the pressure regulator. Recirculation and feedwater pumps are tripped. Fission power is reduced through core voiding and the pressure is controlled via relief and bypass valves.

There are no GE results available for this transient. The plant analyzer results, however, show consistent responses of the control systems and of the engineered safety systems as can be seen from Figure 5.9.

(ix) ATWS Initiated by Pressure Regulator Failure at Maximum Demand

This transient starts from the signal to open the turbine control valves fully. This in turn causes the system pressure to drop and the MSIVs to close at low pressure set points. The comparisons between plant analyzer results and computed GE data are shown in Figure 5.10.

The plant analyzer predicts a power peak of 4.8 times full power. GE results show a peak of 5.6 times full power. The differences in depressurization rates and pressure amplitudes during valve cycling are due to the modeling differences discussed earlier and due to differences in pressure set point specifications. The core flow rate comparison shows good agreement. The collapsed liquid level in the downcomer rises earlier in the GE calculations due to the earlier recirculation pump trip. The level position predicted in the plant analyzer approaches the position calculated by GE.

(x) ATWS Initiated by the Failure of the Feedwater Controller at Maximum Demand

The comparisons for this transient are presented in Figures 5.11. Excessive feedwater injection causes the water level to rise. The rising water level trips the turbines and the feedwater pumps.

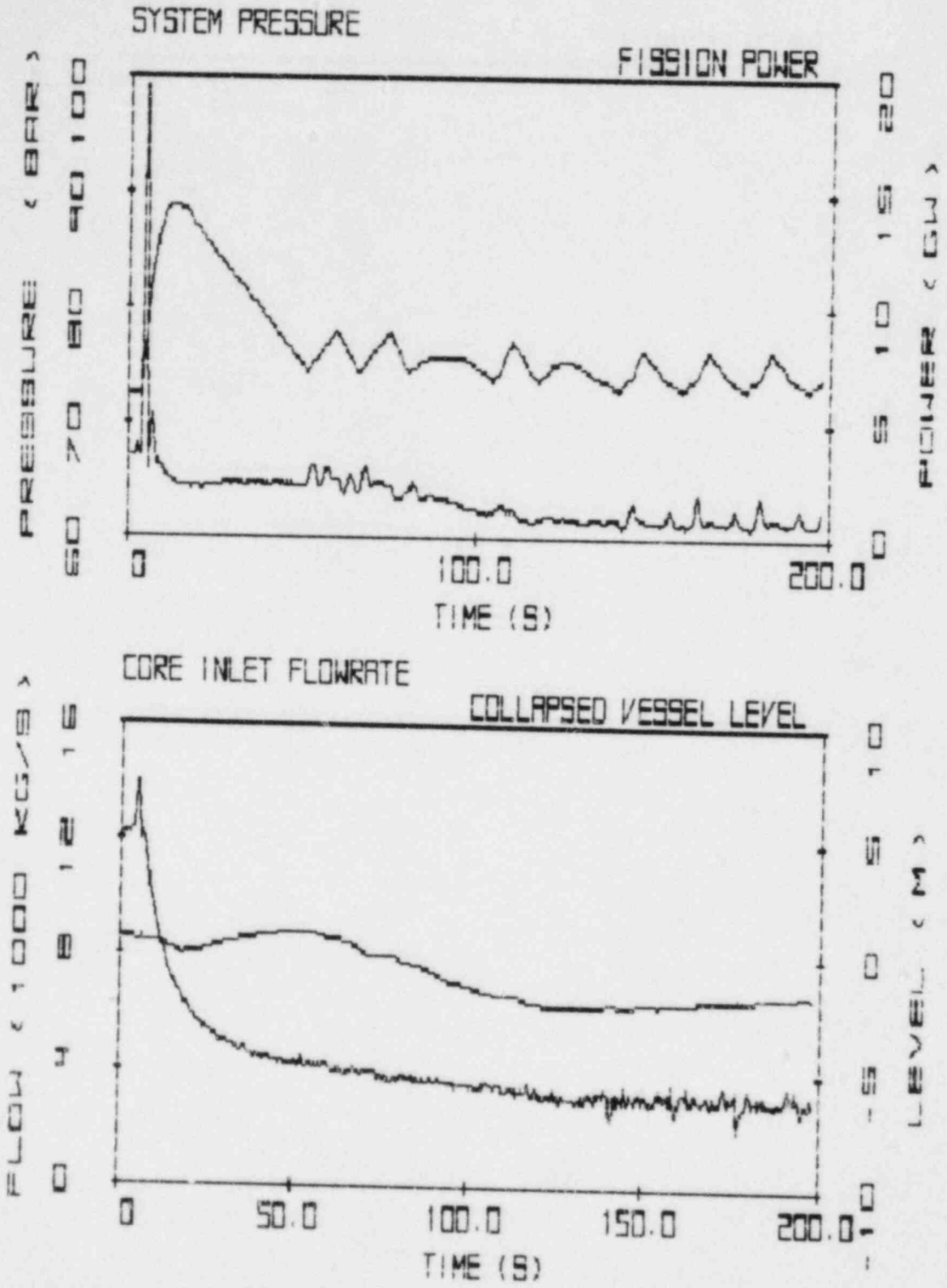

Figures 5.8 HIPA Simulation of Turbine Trip Without Bypass Flow and Without Scram (ATWS). No GE graphs available. Top graph shows fission power and vessel pressure, bottom graph mixture mass flow at core inlet and collapsed liquid level in downcomer.

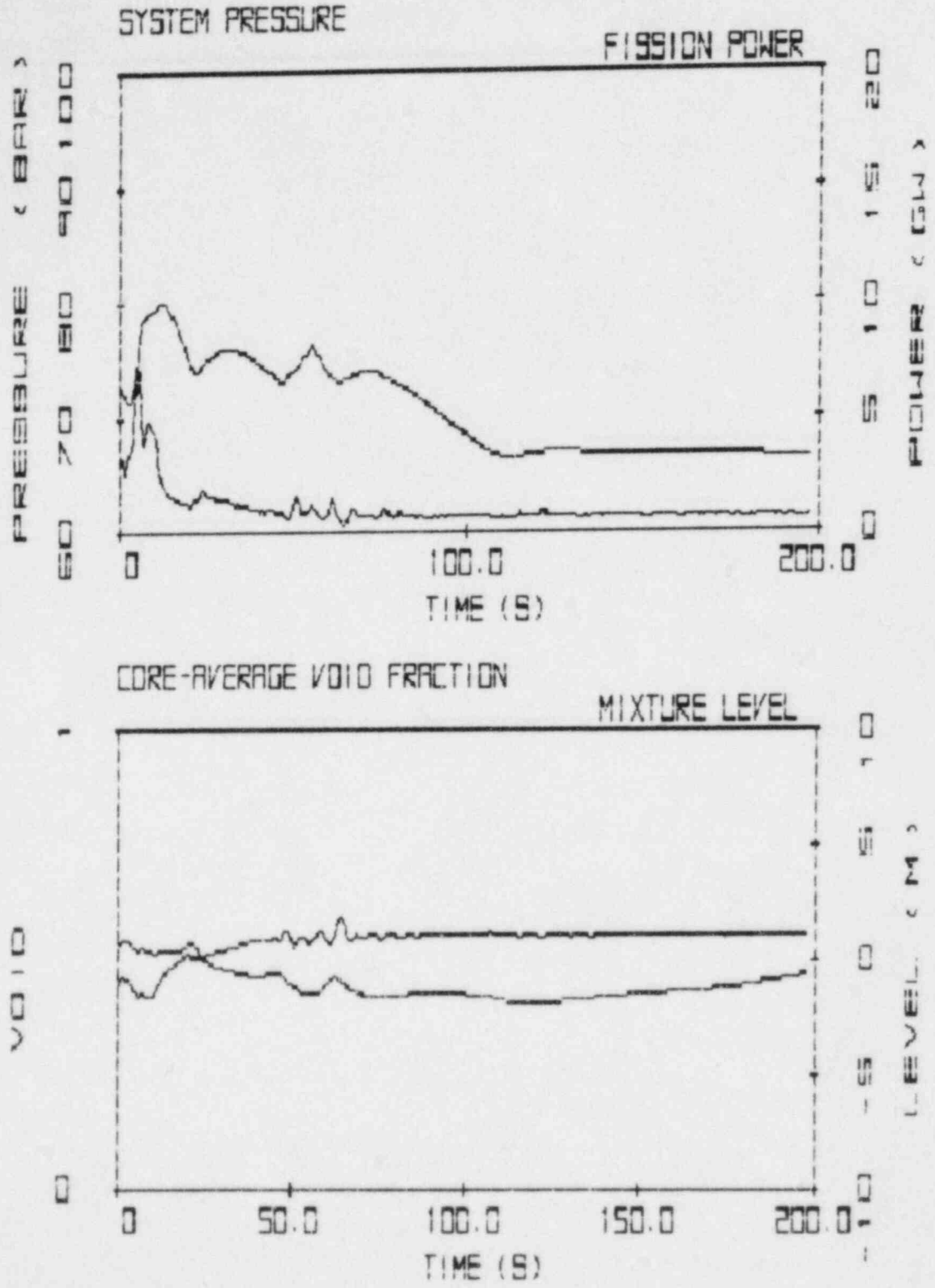

Figures 5.9 HIPA Simulation of an ATWS Caused by Pressure Regulator Failure at Zero Demand. No GE data available. Top graph shows fission power and vessel pressure, bottom graph mixture level in downcomer and avg. core void fraction.

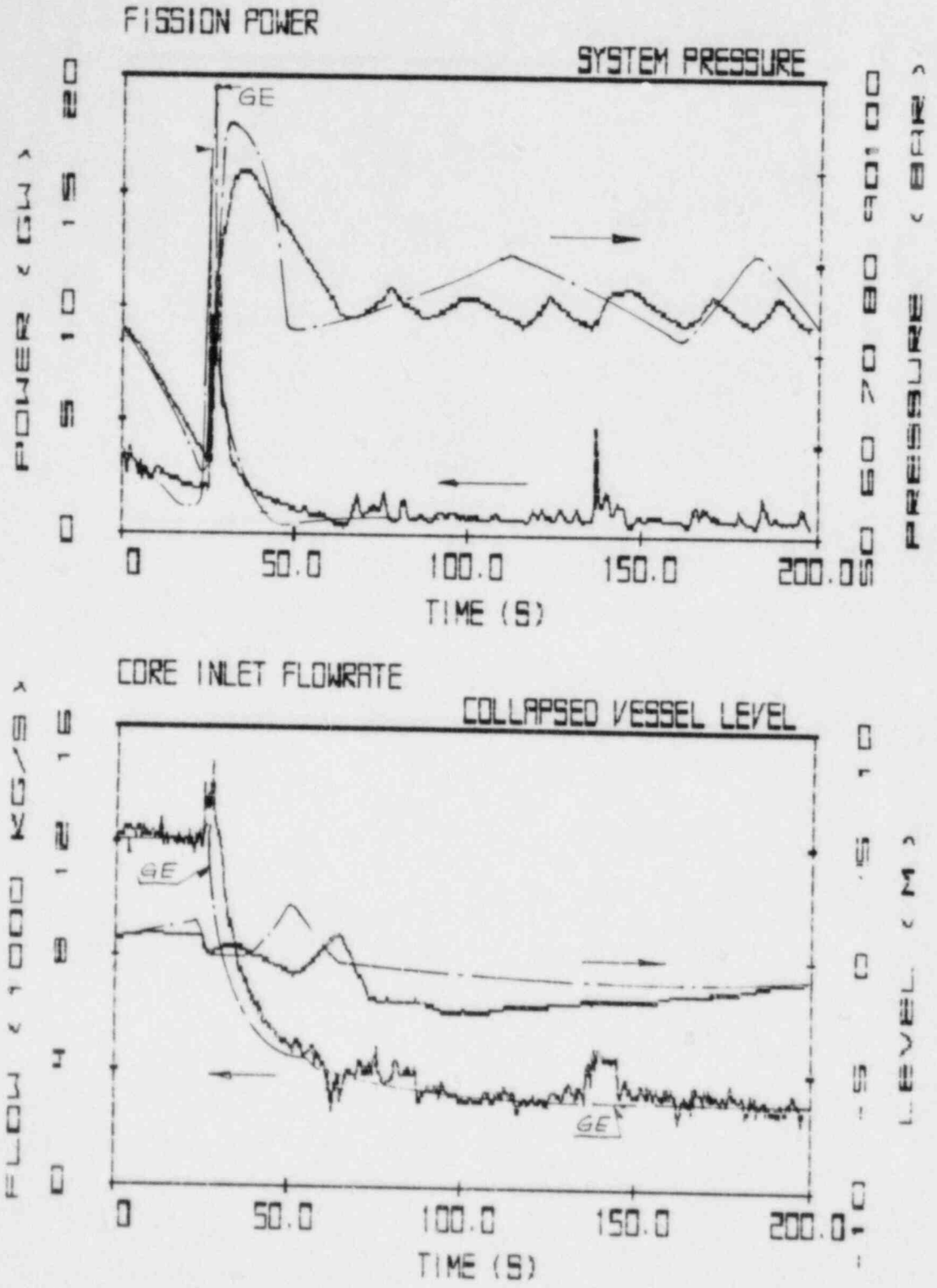

Figures 5.10 HIPA-GE Comparisons for ATWS after Pressure Regulator Failure at Maximum Demand. --- HIPA, - - GE. Top graph shows vessel pressure and fission power, bottom graph core inlet mass flow rate and collapsed liquid level.

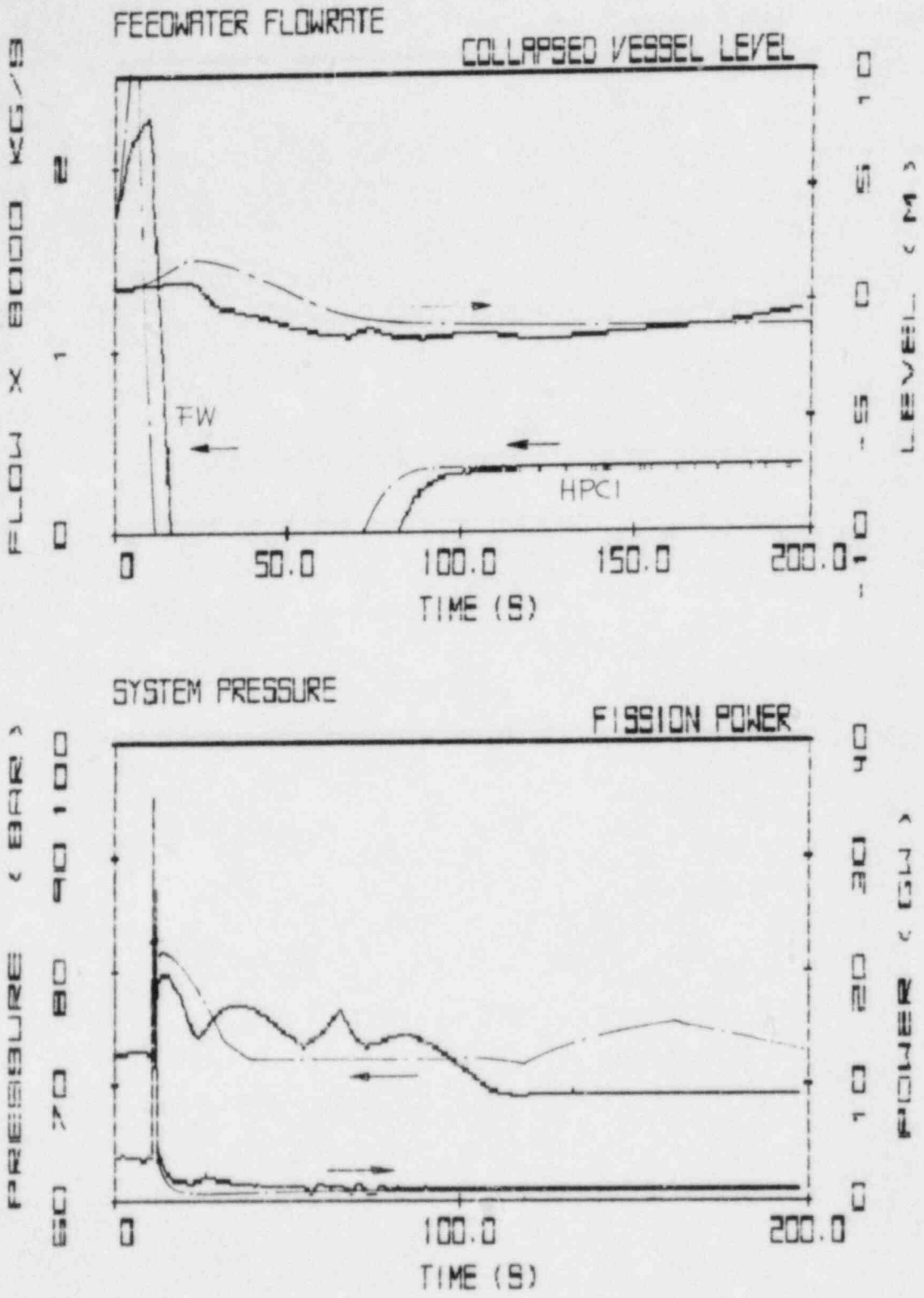

Figures 5.11 HIPA-GE Comparisons for ATWS after Feedwater Regulator Failure at Maximum Demand. —— HIPA, -·- GE. Top graph shows feedwater and HPCI flows and collapsed liquid level in vessel, bottom graph fission power and vessel pressure.

GE predicts the fission power to peak at 5.1 times normal power. The plant analyzer produces a ratio of 9.0. The higher fission power peak is reached in the plant analyzer because the turbine stop valve closes before the bypass valve opens. The early turbine stop valve closure produces a sharper pressure rise, a faster vapor void collapse and, via void feedback, a sharper rise in fission power.

The GE calculations produce a pressure rise up to 82.4 bar, the plant analyzer up to 80 bar. The maximum feedwater flow predicted by the plant analyzer is 133% of full flow, the GE predictions went off scale above 140% of full flow.

Conclusions

The assessment carried out so far shows that the plant analyzer can carry out realistic and accurate simulations of transients in BWR-4 power plants if the correct specifications for the plant control system and the engineered safety systems are used. The plant analyzer has not yet been shown to simulate conditions of flow reversal and departure from nucleate boiling (DNB). All comparisons presented here were produced without any change in system parameters.

5.5 Future Plans

Assessment work will continue. The BWR simulation capability will be expanded to accommodate flow reversal, phase separation via the drift flux model instead of the present slip flow model, and DNB conditions.

The plant analyzer will be presented and demonstrated to domestic industries and foreign institutions interested in nuclear power plant simulation for the purpose of developing cooperative programs directed toward PWR simulations.

REFERENCES

CHENG, H. S. and WULFF, W., (1981), "A PWR Training Simulator Comparison with RETRAN for a Reactor Trip from Full Power," Informal Report, BNL-NUREG-30602, Brookhaven National Laboratory, September 1981.

GE, NEDO-24222 (1981), Assessment of BWR Mitigation of ATWS, Vol. II, NUREG-0460, Alternate No. 3.

PHILADELPHIA ELECTRIC COMPANY (1981), "Final Safety Analysis Report, Peach Bottom Atomic Power Station Units 1 and 2."

MILTON, J. D. (1982) "TRAC-BWR Control System Model Developmental Assessment," Interim Technical Report, EG&G, Idaho, Inc., WR-CD-82-073.

WULFF, W., (1980), "PWR Training Simulator, An Evaluation of the Thermohydraulic Models for its Main Steam Supply System," Informal Report, BNL-NUREG-28955, September 1980.

WULFF, W., (1981a), "BWR Training Simulator, An Evaluation of the Thermohydraulic Models for its Main Steam Supply System," Informal Report, BNL-NUREG-29815, Brookhaven National Laboratory, July 1981.

WULFF, W., (1981b), "LWR Plant Analyzer Development Program," Ch. 6 in Safety Research Programs Sponsored by the Office of Nuclear Regulatory Research, Quarterly Progress Report, April 1-June 30, 1981; A. J. Romano, Editor, NUREG/CR-2231, BNL-NUREG-51454, Vol. 1, No. 1-2, 1980.

WULFF, W., (1982a), "LWR Plant Analyzer Development Program," Ch. 5 in Safety Research Programs Sponsored by the Office of Nuclear Regulatory Research, Quarterly Progress Report, January 1-March 31, 1982; A. J. Romano, Editor, NUREG/CR-2331, BNL-NUREG-51454, Vol. 2, No. 1, 1982.

WULFF, W., (1982b), "LWR Plant Analyzer Development Program," Ch. 5 in Safety Research Programs Sponsored by the Office of Nuclear Regulatory Research, Quarterly Progress Report, July 1-September 30, 1982; compiled by Allen J. Weiss, NUREG/CR-2331, BNL-NUREG-51454, Vol. 2, No. 3, 1982.

WULFF, W. (1982c), "LWR Plant Analyzer Development Program," Ch. 5 in Safety Research Programs Sponsored by the Office of Nuclear Regulatory Research, Quarterly Progress Report, October 1-December 31, 1982; compiled by Allen J. Weiss, NUREG/CR-2331, BNL-NUREG-51454, Vol. 2, No. 4, 1982.

WULFF, W., (1983a), "LWR Plant Analyzer Development Program," Ch. 5 in Safety Research Programs Sponsored by the Office of Nuclear Regulatory Research, Quarterly Progress Report, January 1-March 31, 1983; compiled by Allen J. Weiss, NUREG/CR-2331, BNL-NUREG-51454, Vol. 3, No. 1, 1983.

WULFF, W., (1983b),"LWR Plant Analyzer Development Program," Ch. 5 in Safety Research Programs Sponsored by the Office of Nuclear Regulatory Research, Quarterly Progress Report, July-September 30, 1983; compiled by Allen J. Weiss, NUREG/CR-2331, BNL-NUREG-51414, Vol. 3, No. 3, 1983.

WULFF, W. (1983c), "NRC Plant Analyzer Development," Proc. Eleventh Water Reactor Safety Research Information Meeting, held at National Bureau of Standards, Gaithersburg, MD, Oct. 24-28, 1983, U.S. Nuclear Regulatory Commission. To be published.

WULFF, W., CHENG, H. S., DIAMOND, D. J. and KHATIB-RAHBAR, M., (1981c), "A Description and Assessment of RAMONA-3B MOD.0 CYCLE4: A Computer Code with Three-Dimensional Neutron Kinetics for BWR Systems Transients," NUREG/CR-3664, BNL-NUREG-51746, Manuscript completed 1981, published 1984.

6. Code Assessment and Application (Transient and LOCA Analyses)

(P. Saha, U. S. Rohatgi, J. H. Jo, L. Neymotin,
H. R. Connell, and C. Yuelys-Miksis)

This project includes the independent assessment of the latest released versions of LWR safety codes such as TRAC, RELAP5, and RAMONA-3B, and the application of these codes to the simulation of plant accidents and/or transients. Two major code application tasks namely, the RESAR-3S large break LOCA study and the BWR/4 MSIV closure ATWS analysis, have been completed, and are being documented in two separate topical reports. The code assessment activity has also been resumed with the initiation of the preparation of an input deck for the FIST facility for the TRAC-BD1/MOD1 code. This code is currently being implemented on the BNL computer.

The details of the progress achieved during the reporting period of January to March 1984 are described below.

6.1 Code Assessment

6.1.1 Implementation of TRAC-BD1/MOD1 (H. R. Connell)

Work commenced on the implementation of Version 21 of the TRAC-BD1/MOD1 code on the BNL CDC-7600 computer. The implementation involves changes from the NOS/BE to SCOPE operating system and the reorganization of the code from Overlay to Segmentation to fit into the BNL computer with smaller central memory.

6.1.2 Simulation of FIST Facility with TRAC-BD1/MOD1 (J. H. Jo)

BNL has received a draft copy of the FIST facility description report from General Electric Co., and an input deck from INEL for this facility. An independent input deck is being prepared for the TRAC-BD1/MOD1 code, and it will be debugged after the code is available on the BNL computer.

6.2 Code Application

6.2.1 LOCA Analysis of Westinghouse RESAR-3S Plants (U. S. Rohatgi and C. Yuelys-Miksis)

The BNL study of conservatism in Appendix K guidelines for a 200% cold leg break in a Westinghouse 4-loop RESAR-3S plant using TRAC-PD2/MOD1 has been completed and a topical report documenting the calculations is being prepared.

In the previous quarter, the best-estimate calculation was completed (Rohatgi, 1984). The transient was computed for 64.6 seconds and all of the rods were quenched by that time. The peak clad temperature of 800.6K (981°F) occurred at 2.5 seconds. The reflood began at 39 seconds and core wide quenching was attained by 45 seconds. The average core liquid fraction at the time of complete quenching was between 0.35 and 0.4. This calculation provided the best-estimate values of the key parameters, i.e., PCT, refill time, quench time, etc. for a 200% cold leg LBLOCA.

The second calculation performed in this study was also for the 200% cold break LOCA, but with the evaluation or licensing type boundary and initial conditions. The nodalization and the code were the same as those used for the best-estimate calculation. Table 6.1 compares the initial and boundary conditions for the two calculations. There were some differences in the arrangement of the rods and their radial peaking factors. In the best-estimate calculation, there were two radial and four azimuthal sectors for average rods as shown in Figure 6.1. The inner four sectors each had a radial peaking factor of 1.111. However, the Appendix K requires that the licensing calculation must have one hot channel with high power density and a hot rod be placed there for calculating the peak clad temperature. This Appendix K requirement was incorporated in the BNL evaluation type calculation by designating one of the inner quadrants as the hot channel with a radial peaking of 1.38, as shown in Figure 6.1. The second calculation was continued until 275 seconds, and substantial core cooling was achieved by that time. The sequence of events for the best-estimate and the evaluation type calculations have been compared in Table 6.2. For the E-M type calculation, the peak clad temperature of 1072°K (1470°F) occurred at 65 seconds. The reflood began at 48.5 seconds and the clad started quenching at 244 seconds. The accumulator emptied at 86.5 seconds in the evaluation type calculation, but did not empty in the best-estimate calculation. This indicates that the PCT was not affected by the non-condensibles in the accumulators in either of the two calculations.

The clad temperatures for the second calculation, i.e., the E-M type calculation, have been shown in Figure 6.2. As was the case with the first (B-E) calculation, there were two peaks in the blowdown phase. The first peak appeared at approximately 2.5 seconds due to flow reversal at the core inlet and stagnation inside the core. This initial clad heat-up was quenched when the core inlet flow was restored as the break flow decreased and was less than the intact cold leg flows. The fuel clad again started to heat up and this time the quenching occurred due to the flow reversal at the core outlet resulting in a second peak. It should be noted that the peak clad temperature in the blowdown phase in the second calculation was about 100K higher than in the best-estimate calculation. This is due to a combination of 2% more initial core power, higher decay heat and hot channel configuration.

Figure 6.3 shows a comparison of the lower plenum liquid mass predictions in both the calculations. As expected, the lower plenum was filled about 9 seconds earlier in the B-E calculation due to larger ECC flow. Figure 6.4 shows the core average liquid fractions estimated in the two calculations. The first observation is that the core rapidly filled up in the B-E calculation, while there were considerable oscillations in the E-M type calculation. Furthermore, the core liquid fraction stayed close to 0.25 during most of the transient in the second calculation and was increasing at the time of the termination of the calculation. In this last calculation the break flows were comparable to the safety injection flows and the core power was higher. This resulted in continuous boiling and evaporation in the core and a slower refilling. Strong multidimensional effects in the void fraction distribution in the core were also observed.

Table 6.1 Differences in the BNL Best-Estimate (B-E) and Evaluation Model (E-M) Type Calculations

Item		Best-Estimate	Evaluation
Initial Conditions			
1.	Total Power	3411 MWt	3479 MWt
	Decay Power	100% of ANS 79	120% of ANS 71
2.	Fuel-to-Clad Gap	0.0000379 m	Westinghouse Proprietary
3.	Gap Conductance	6000 W/m^2K	"
4.	Axial Power Profile	Chopped Cosine (0.55 1.145 0.55)	Chopped Cosine (0.24 1.416 0.24)
5.	Radial Power Dist.	0.919 to 1.11	0.919 to 1.38
Boundary Conditions			
1.	Break or Containment Pressure	Supplied	Less than B-E
2.	Safety Injection Sys.		
	Delay	1.5 & 6.5 Sec.	25 Sec. Delay
	No. of ECCS Trains	Two	One
3.	Accumulators	All four loops	Three Intact Loops; Smaller Inventory than B-E
Scenario			
	Pump Trip	Did not Trip	Tripped

Table 6.2 Comparison of Sequence of Events for BNL B-E and E-M Type Calculations

	Events	Time (s) BE/BNL	EM/BNL
1.	Break	0.0	0.0
2.	Safety Injection Signal Generated.	1.1	5.1
3.	Broken Loop Accumulator Injection.	2.2	N/A
4.	Intact Loop Accumulator Injection.	10.5	11.3
5.	Pressurizer Empties (Water Level < 0.005 m).	16	17.5
6.	Safety Injection (Charging, Residual Heat Removal, High Head Safety Injection).	2.6 to 7.6	30.1
7.	Lower Plenum Refilled (Liquid Fraction 0.97) and Beginning of Reflood.	39	48.5
8.	Peak Clad Temperature.	2.5	65
9.	Accumulator Empty	Did Not	86.5
10.	Quenching of Hot Spots Begins	44	244

The conclusion from this study is that the licensing type boundary and initial conditions contribute about 500°F of the total conservatism of 1200°F (Rohatgi, 1984) in the PCT. In addition, when these calculations were compared with the Westinghouse Appendix K calculation, the conclusion was that the hot channel configuration and the conservative physical models contributed about 700°F of conservatism in PCT. Also, the PCT occurred in the reflood phase in the evaluation type and Westinghouse calculations, indicating that the decay power and ECCS are more important for determining the PCT. Finally, we believe that there is a need for continuing this study to determine the sensitivity of PCT, refill and quench time to various important phenomena occurring during a LBLOCA.

6.2.2 BWR/4 ATWS Calculations Using the RAMONA-3B Code (L. Neymotin and P. Saha)

It was stated in the previous quarterly report (Hsu, 1984) that a typical BWR/4 MSIV closure ATWS calculation was completed using the TRAC-BD1 (Version 12) code. Calculation of the same transient using the RAMONA-3B (MOD0/Cycle 6) code has been completed during this reporting period, and the long term results of this calculation will be discussed here. (The short term results of both TRAC-BD1 and RAMONA-3B were discussed in the last quarterly report (Hsu, 1984).)

As a part of the transient scenario, it was assumed that highly concentrated borated water would be injected into the reactor vessel at 165 seconds in the transient. The flow rate of the injected borated water was assumed to be 2.78 kg/s (or 43 gpm) with boron concentration of 23800 ppm. This is equivalent to activating one SLCS pump in most of the BWR/4's with 13% solution of Sodium Pentaborate. The HPCI and RCIC systems were assumed to be in the automatic mode during this transient.

As the boron concentration in the core started to increase, the reactor power dropped momentarily resulting in a drop in the void fraction which, in turn, increased the power again. These competing effects of negative boron reactivity and positive reactivity insertion due to void collapse kept the reactor critical for a long time. Meanwhile, the downcomer collapsed water level reached the high level shut-off point or Level 8 at approximately 1275 seconds due to continuous injection of HPCI and RCIC water. After this water injection was terminated, the boron concentration in the core started to increase at a higher rate and the reactor power eventually dropped to approximately three percent of the rated power at 1400 seconds. However, at that time, the downcomer collapsed water level reached the low level setting again, and the HPCI and RCIC water was turned on automatically. This caused the reactor to become critical again. The calculation was intentionally terminated at 1500 seconds.

Figures 6.5 through 6.9 show the long term RAMONA-3B results for the downcomer water level, boron concentration (per unit liquid mass) in the core, reactor power, core average void fraction and core flow rates, respectively. Close interactions among these variables are quite clear. It can be seen that if the HPCI and RCIC water was not turned on again at 1400

seconds, the reactor power would have stayed at the decay heat level. System pressure, in the long term, remained between 7.3 and 7.55 MPa (1070 and 1110 psia), and only the first bank of relief valves continued to cycle.

Since steam released through the S/R valves is dumped into the suppression pool, the pool water temperature starts to increase. To maintain the containment integrity, it is important to keep the suppression pool water temperature at a sufficiently low value. The pool water temperature is, therefore, an important variable from the plant safety viewpoint.

As mentioned earlier (Hsu, 1984), a stand-alone computer program was written to solve the mass and energy conservation equations for the suppression pool water. Steam flow rates and enthalpies calculated by RAMONA-3B were used as input to this program. Complete condensation of steam in the pool water was assumed, and no credit was taken for the pool cooling by the RHR system. The initial pool water volume and temperature were 3859 m^3 and 90°F (32.2°C), respectively. The calculated pool water temperature is shown in Figure 6.10 indicating the maximum temperature of 205°F (96.1°C) at 1500 seconds for RAMONA-3B. This temperature is high enough to cause concern for the containment integrity.

The results presented above clearly indicate that RAMONA-3B can be used to analyze long term ATWS events in a BWR. The results look physically reasonable, and the computer running time was quite acceptable (CPU to real time ratio of $\sim$4 in the BNL CDC-7600 computer). It has been found (Hsu, 1984) that the spatial power distribution does vary significantly during a BWR ATWS. Thus, RAMONA-3B with space-time neutron kinetics is a superior and preferable tool to a point-kinetics code for analyzing such events.

It should be noted that the present RAMONA-3B results, although not specific to any particular plant, do indicate that even an early boron injection (at a rate of 43 gpm with 23800 ppm of boron) may not be adequate for mitigating the adverse consequences of an MSIV closure ATWS in a typical BWR/4. This is based on the relatively high suppression pool water temperature as presented in Figure 6.10. In this connection, there are at least two items that need further discussion. These are: a) non-perfect mixing of boron, and b) suppression pool cooling.

Non-Perfect Boron Mixing

It is known that during a low flow or natural circulation cooling mode, all the boron injected into a BWR lower plenum may not carry into the core. This is because of higher specific gravity of the injected borated water, and the presence of hundreds of control rod guide tubes in the lower plenum. However, in the RAMONA-3B calculation, no such boron stratification effect was considered. Thus, the boron concentration shown in Figure 6.6 is probably higher-than-actual, which has probably resulted in a lower-than-actual hot shutdown time.

An attempt has been made to take into account the effect of possible boron stratification. Based on the boron mixing efficiency vs. recirculation flow as presented by Dente (1982), a value of 0.75 can be assumed for the boron mixing efficiency in the present estimate. Thus, the actual boron concentration in the core would be about 25% lower than the values shown in Figure 6.6. This would delay the drop in reactor power from ~1300 seconds (as shown in Figure 6.7) to ~ 1450 seconds. Even with the assumption of no HPCI and RCIC injection at 1400 seconds (so that the reactor does not become critical again), the additional reactor power would increase the suppression pool water temperature by another 12°F (6.7°C). Thus without RHR cooling, the pool would be boiling, increasing the probability of containment failure.

Suppression Pool Cooling

During a BWR ATWS, the operator would be expected to activate the RHR system to reduce the suppression pool heat-up rate. However, the RHR system is designed to remove only about 3% of the rated power. Therefore, even if the pool cooling is activated at the early stages of the transient, the maximum reduction of pool water temperature would be approximately 15°F (8.3°C).

A realistic boron mixing or stratification model coupled with maximum pool cooling by the RHR system can, therefore, result in a pool temperature of~202°F (94.4°C) at the time of reactor hot shutdown. This temperature is still high from the plant safety viewpoint. Thus, the effects or other mitigative features such as manual rod insertion, use of two SLCS pumps with total capacity of 86 gpm, lowering the downcomer water level to the top of active fuel (TAF), etc., should be investigated. The RAMONA-3B code is already being used for such investigations under the NRC Severe Accident Sequence Analysis (SASA) program.

REFERENCES

DENTE, T. J., (1982), "Schedule for BWR Owner's Group Compliance with NUREG-0737, Item II.K.3.18," Letter to D. G. Eisenhut, USNRC, BWROG-8204, February 5, 1982.

HSU, C. J., NEYMOTIN, L., and CONNELL, H. R., (1984), "BWR/4 ATWS Calculations Using TRAC-BD1 and RAMONA-3B," in Safety Research Program Sponsored by Office of Nuclear Regulatory Research, Quarterly Progress Report, October 1 - December 31, 1983, NUREG/CR-2331, BNL-NUREG-51454, Vol. 3, No. 4, Section 6.2.2.

ROHATGI, U.S., and YUELYS-MIKSIS, C., (1984), "LOCA Analysis of Westinghouse RESAR-3S Plants," Ibid, section 6.2.1.

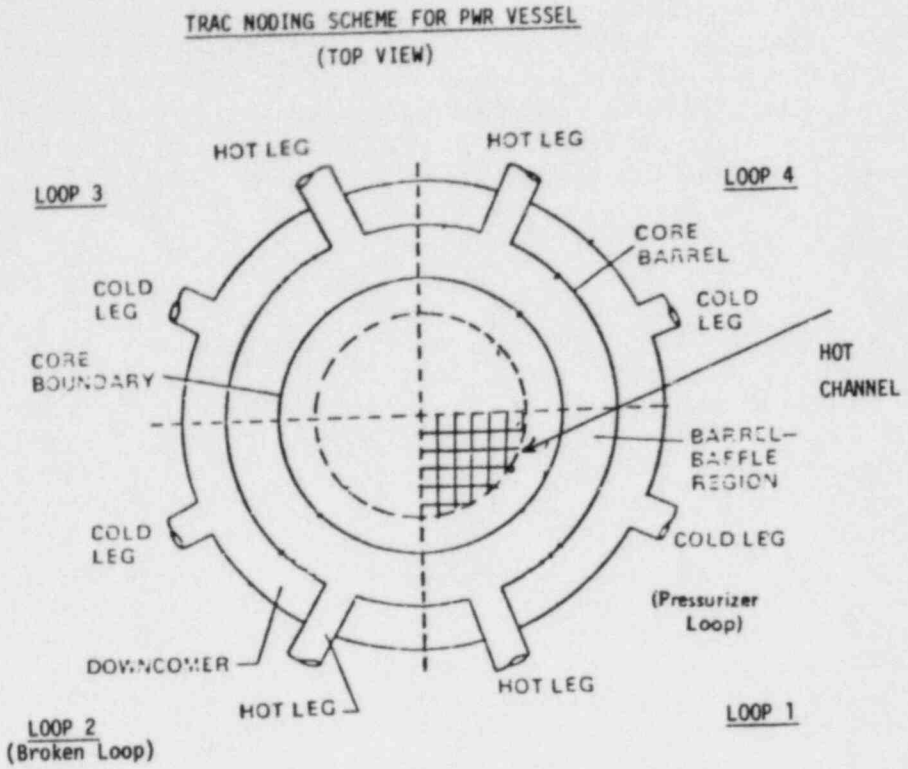

Figure 6.1 TRAC Radial and Azimuthal Noding Scheme for the Reactor Vessel (BNL Neg. No. 5-733-84)

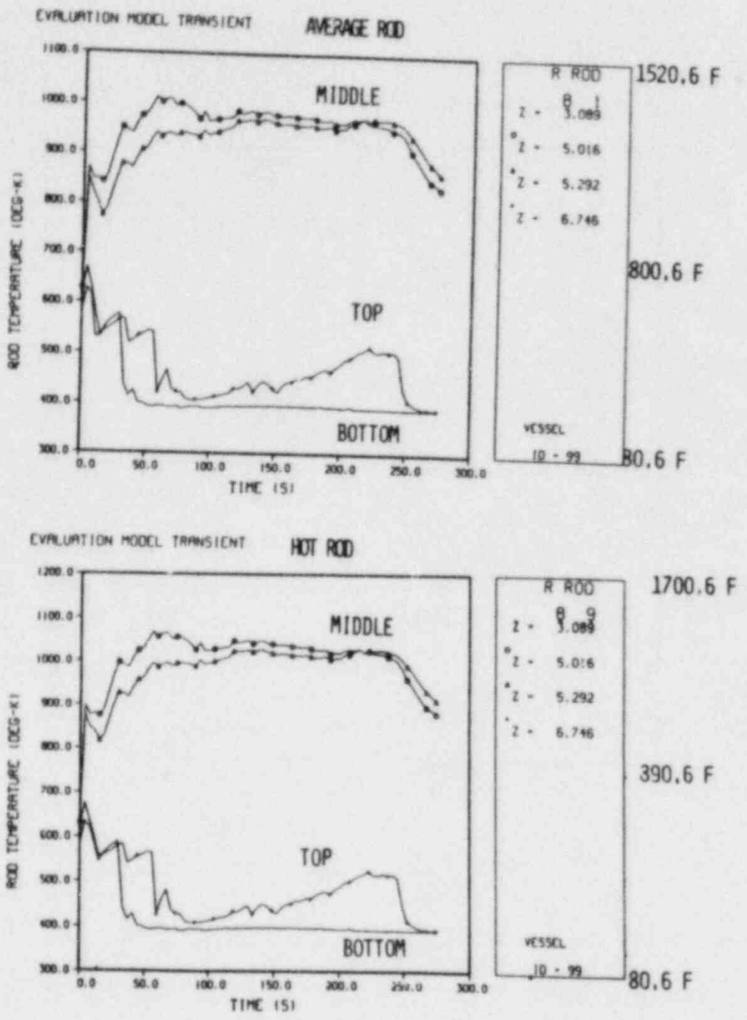

Figure 6.2 Clad Temperatures for the BNL E-M Type Calculation (BNL Neg. No. 5-730-84)

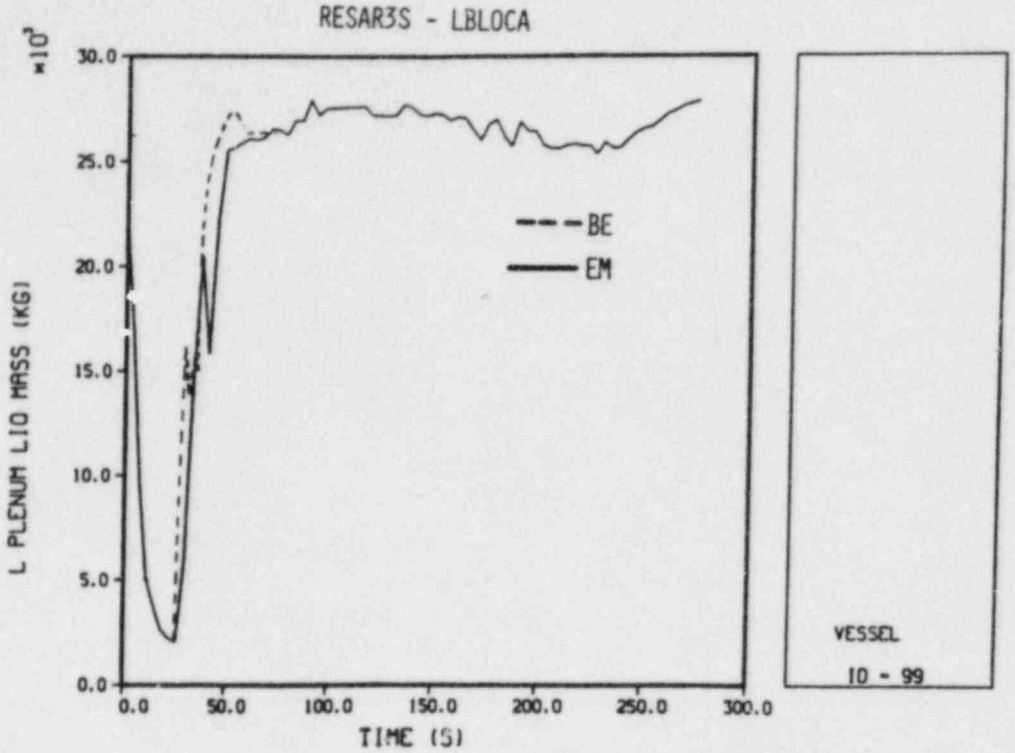

Figure 6.3 Comparison of Lower Plenum Liquid Mass for the B-E and E-M Type Calculations (BNL Neg. No. 5-731-84)

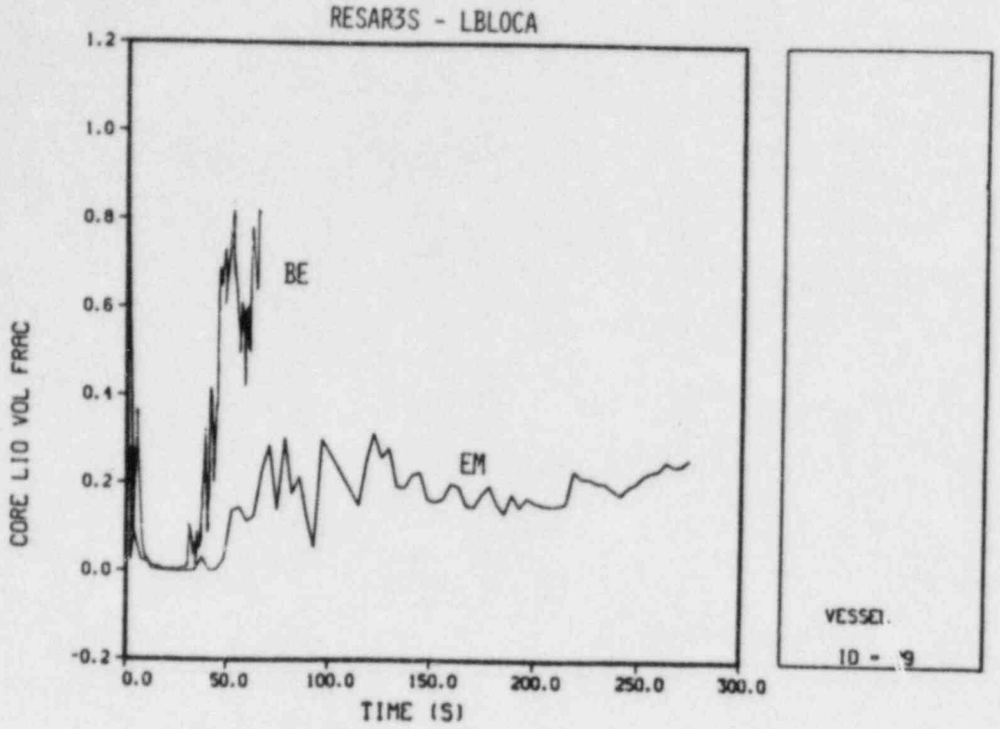

Figure 6.4 Comparison of Core Average Liquid Fraction for the B-E and E-M Type Calculations (BNL Neg. No. 5-732-84)

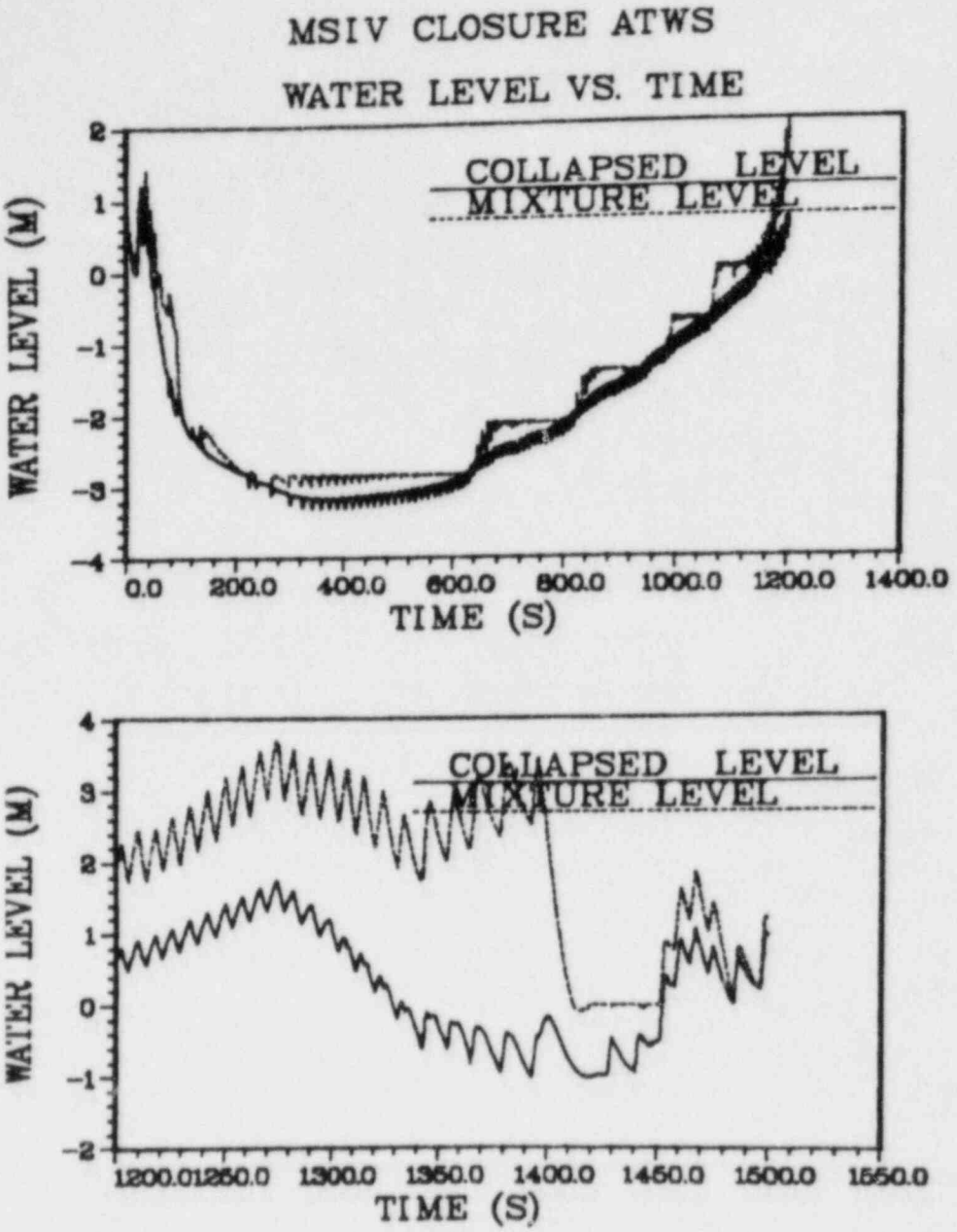

Figure 6.5 Long Term Downcomer Water Levels (Mixture and Collapsed) as Calculated by RAMONA-3B. (BNL Neg. No. 5-236-84)

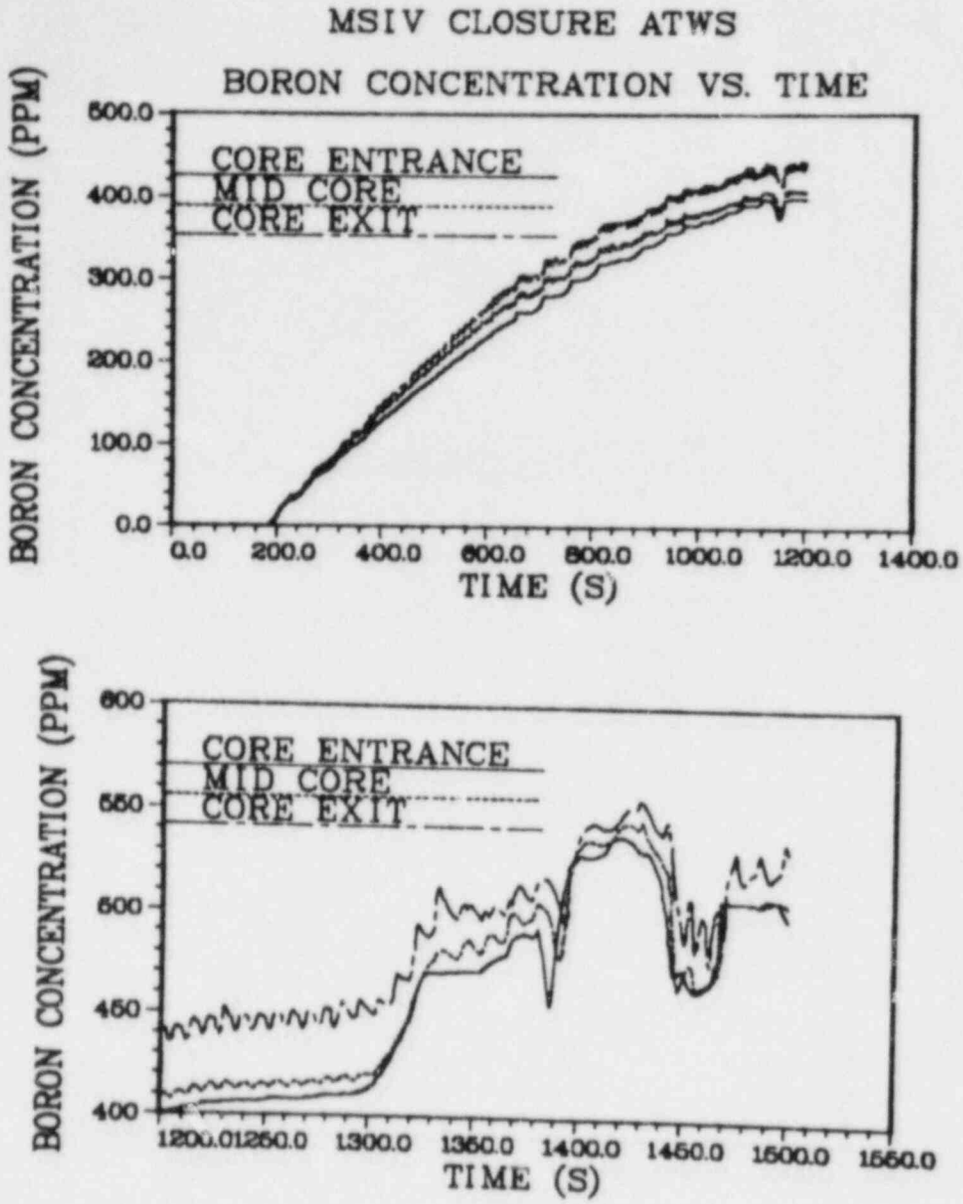

Figure 6.6 RAMONA-3B Boron Concentration per Unit Liquid Mass in Various Regions of Core. (BNL Neg. No. 5-328-84)

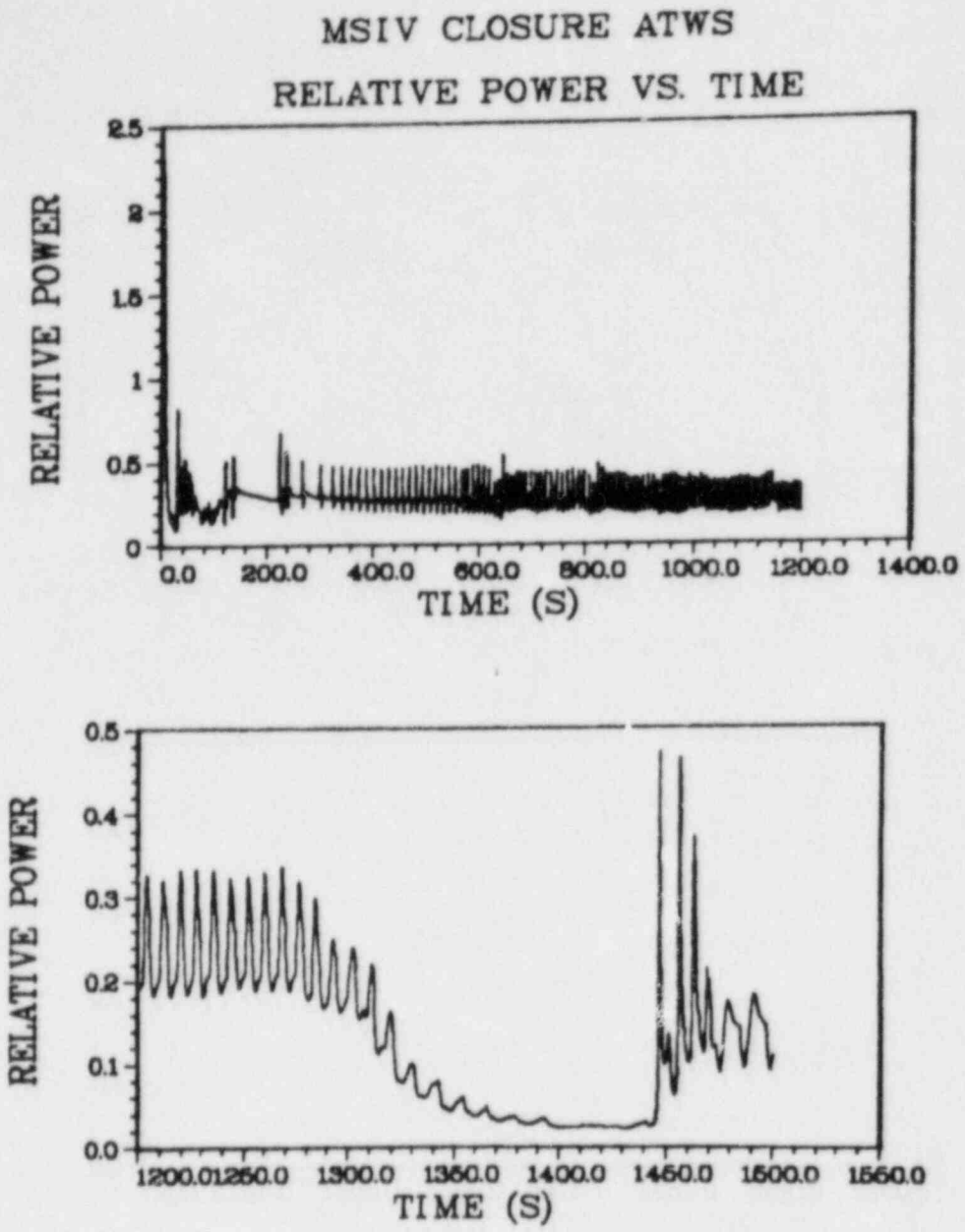

Figure 6.7 Long Term Reactor Power (Relative to Steady State) as Calculated by RAMONA-3B. (BNL Neg. No. 5-327-84)

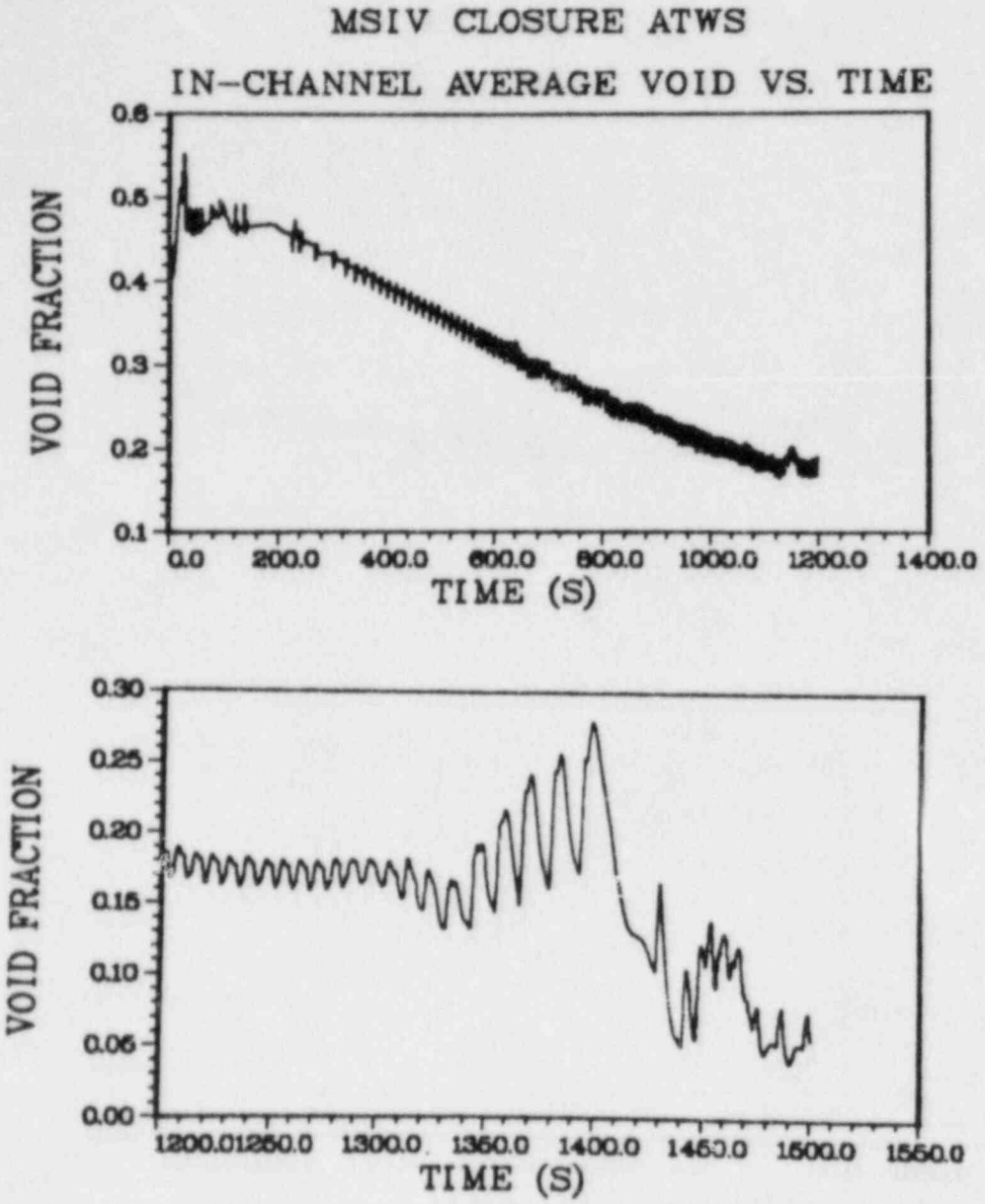

Figure 6.8 Long Term Core Average Void Fraction (Excluding Bypass) as Calculated by RAMONA-3B. (BNL Neg. No. 5-325-84)

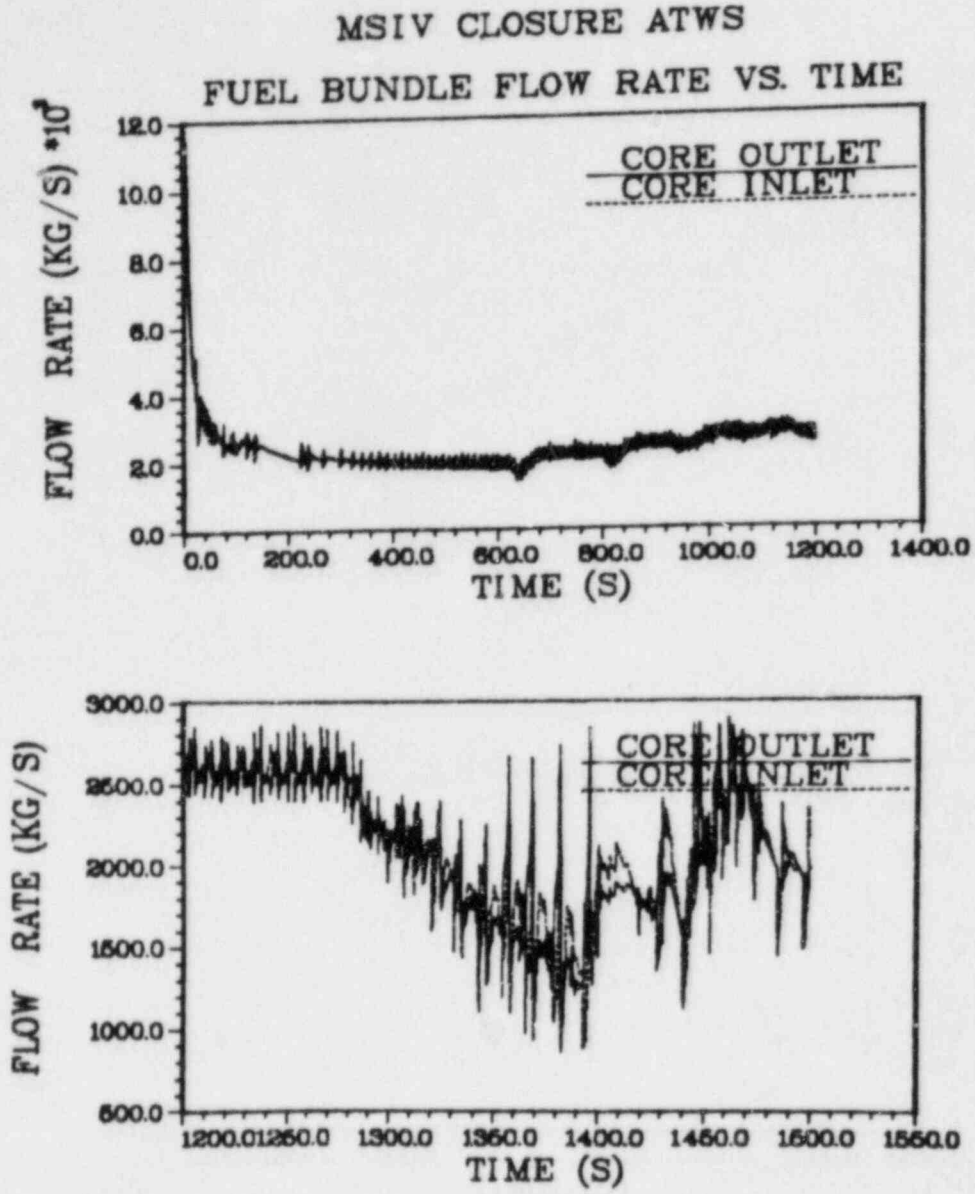

Figure 6.9 Long Term Flow Rates at Active Core Inlet and Outlet as Calculated by RAMONA-3B. (BNL Neg. No. 5-329-84)

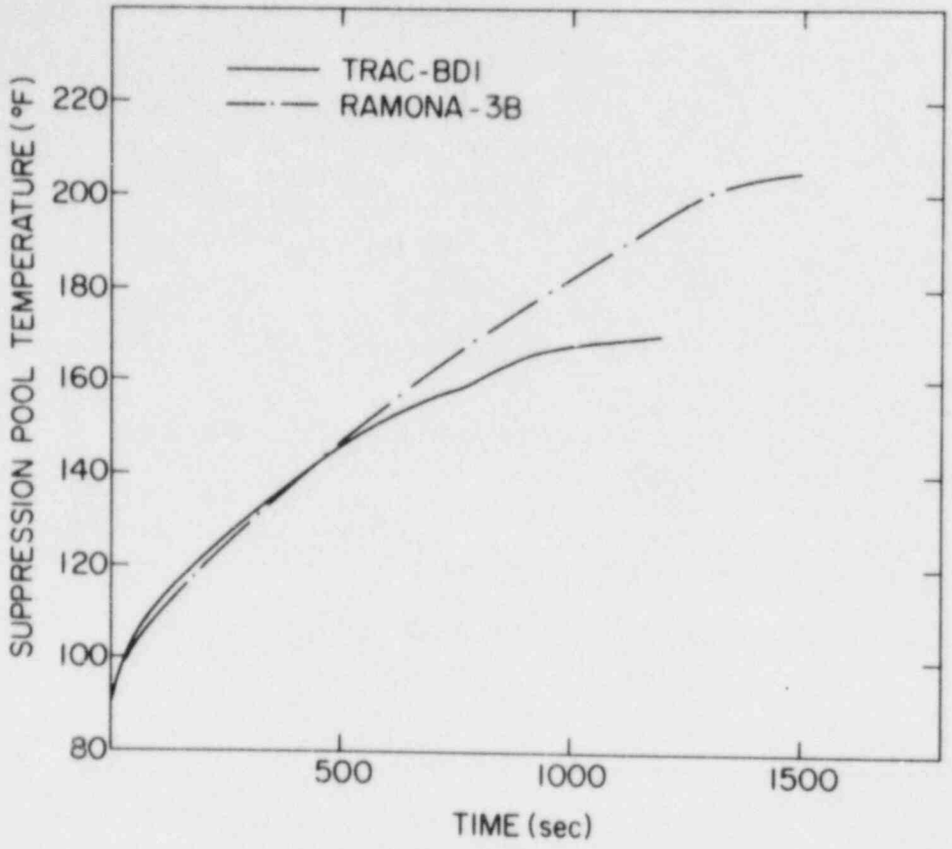

Figure 6.10 Suppression Pool Water Temperatures as Calculated by Using TRAC-BDI and RAMONA-3B Results. (BNL Neg. No. 3-1505-84)

7. Thermal Reactor Code Development (RAMONA-3B)

(P. Saha, L. Neymotin, G. C. Slovik, H. R. Connell, and E. Cazzoli)

This project includes the modifications, improvements and preliminary (or developmental) assessment of the BWR transient analysis code called RAMONA-3B. This is the only BWR systems transient code with three-dimensional neutron kinetics, and it is now available, at no cost, to U. S. organizations for the analysis of U. S. reactors.

During this reporting period of January to March 1984, support has been provided to several RAMONA-3B application projects. This has led to some corrections and improvements to the code. In addition, a draft User's Manual has been completed, and the code (RAMONA-3B/MOD0/Cycle 7) has been distributed to several U. S. organizations. The details of the progress achieved are described below.

7.1 Support for the BWR/4 MSIV Closure ATWS Calculation (L. Neymotin)

The previously reported (Neymotin, 1984) BWR/4 MSIV closure ATWS calculation was continued from 560 seconds and was normally terminated at 1500 seconds. A hot shutdown reactor condition was reached at about 1400 seconds. The reactor power remained at 3% of the steady-state value for 50 seconds, but then experienced an increase to approximately 15% when the HPCI and RCIC systems were reactivated on a low downcomer water level signal.

A detailed discussion of the RAMONA-3B long term results of this transient can be found in Section 6.2.2 of this quarterly report.

7.2 Support for the Eccentric Control Rod Drop Calculation (G. C. Slovik, H. R. Connell and L. Neymotin)

During this reporting quarter, an eccentric control rod drop accident in a typical BWR has been analyzed at BNL (by Dr. D. Cokinos) using RAMONA-3B under the NRC/NRR sponsorship. Support has been provided in the areas of input deck preparation and actual calculation. A more flexible control rod movement option has been added to the code so that a SCRAM signal would not necessarily insert all control rods. This was required so that the dropped rod would not be reinserted at the SCRAM signal.

7.3 Support for Browns Ferry ATWS Study (E. Cazzoli and L. Neymotin)

Support has been provided for the Browns Ferry MSIV closure ATWS calculations that are being performed at BNL using RAMONA-3B under the NRC Severe Accident Sequence Analysis (SASA) program. The first series of calculations included simulation of operator actions according to the new Emergency Procedure Guidelines (EPGs). These included lowering the downcomer water level to the Top of Active Fuel (TAF) and maintaining it there, and lowering the reactor vessel pressure in accordance with the heat capacity temperature limit curve for the pressure suppression pool. A transient calculation up to 600 seconds has been run.

During the above calculation, some code modifications in the area of hydraulics were made in order to simulate the EPG-imposed operator actions, i.e., level and pressure controls.

7.4 RAMONA-3B Improvements/Corrections (L. Neymotin)

7.4.1 Core Pressure Drop

A new feature has been developed for the code's thermal-hydraulic package. Until now, the user had to perform several trial and error steady-state calculations to adjust the form loss coefficients at the entrance of a number of parallel core channels in order to obtain the desired pressure drop across the core region (which is one of the few available plant characteristics). It is extremely difficult to obtain those coefficients from geometrical considerations alone. Also, knowledge of the total "lower plenum to core" form loss coefficient is not sufficient for determining form loss distribution at the core entrance.

The new feature allows for an imposed core pressure drop during the steady-state phase of the calculation. During iterations between the neutronics and the hydraulics, the entrance form loss coefficients for each hydraulic channel are adjusted such that at the end of iterations the core pressure drop is equal to the user supplied value, and the flow rate through each channel is proportional to the channel power predicted by the three-dimensional neutron kinetics.

7.4.2 General Corrections

A few corrections to the RAMONA-3B coding have been made during the reporting quarter:

a) Safety and Relief Valve (S/RV) lift characteristics calculation logic has been corrected. (Lift characteristic is a fraction of the valve relative opening or closing as a function of time since the valve is activated by the plant control or safety system.)

b) An upper limit on the condensation rate has been introduced in order to protect the calculation from error when the condensation rate multiplied by the current time step exceeds the amount of steam present in a particular hydraulic cell.

c) A number of built-in convergence criteria in the hydraulic and neutronic areas have been readjusted for a more efficient code operation.

7.5 Reactivity Edits (G. C. Slovik)

Two previously unresolved technical issues, i.e., the total reactivity from the perturbation theory not agreeing with the sum of the component reactivities, and exclusion of the second order term from the void feedback reactivity calculation, have been resolved during this reporting quarter. The appropriate updates have been received from Scandpower, and they will soon be incorporated into the BNL-version of RAMONA-3B.

7.6 User's Manual and Code Distribution

(P. Saha, L. Neymotin, G. C. Slovik, and H. R. Connell)

A draft of the RAMONA-3B user's manual including input instructions, code structure and user guidance has been completed. The document corresponds to the latest version of the code, i.e., RAMONA-3B/MOD0/Cycle 7, which has been distributed to the following U.S. organizations:

a) Westinghouse Electric Corporation, Pittsburgh, PA.
b) NUS Corporation, Gaithersburg, MD.
c) Energy Incorporated, Idaho Falls, ID.
d) New York Power Authority, New York, NY.
e) GPU Nuclear Corporation, Parsippany, NJ.

REFERENCES

NEYMOTIN, L., (1984), "Support for the BWR/4 MSIV Closure ATWS Calculation," in Safety Research Program Sponsored by Office of Nuclear Regulatory Research, Quarterly Progress Report, October 1 - December 31, 1984, NUREG/CR-2331, BNL-NUREG-51454, Vol. 3, No. 4, Section 7.1.

8. Calculational Quality Assurance in Support of PTS

(P. Saha, J. H. Jo, U. S. Rohatgi and C. Yuelys-Miksis)

The objective of this project is to provide a peer review of the thermal-hydraulic calculations that have been performed at LANL (using the TRAC-PWR code) and INEL (using the RELAP5 code) for the NRC Pressurized Thermal Shock (PTS) study. Specifically, this includes a review of the plant decks and the calculations, and an assessment of the reasonableness of the results. The major activities performed during January to March 1984 are described below.

8.1 Review of TRAC Calvert Cliffs Calculations (J. H. Jo)

The detailed, in-depth review of several selected Calvert Cliffs PTS transients calculated by LANL using the TRAC-PF1/MOD1 code has been completed and the results of the review are being documented. In general, the temperature and pressures of the primary system as calculated by TRAC have been found to be quite reasonable.

Six out of the thirteen transients have been selected for detailed review at BNL. They are: Transient numbers 1 and 11 for the Hot Zero Power (HZP) condition and Transient numbers 3, 6, 7A and 9 for the Hot Full Power (HFP) condition. These transients cover all the various categories of transients calculated by LANL using the TRAC-PF1/MOD1 code.

For a quantitative review of the TRAC results, a simple method has been developed at BNL to predict the primary system temperature based on the mass and energy balances. In this approach, the whole reactor system, including the secondary sides of the steam generators, is lumped into a single volume and the energy balance is applied to the volume. Separate mass balance equations are retained for the primary system and the secondary side of each Steam Generator (SG). This approach assumes that the temperature difference between the cold and hot legs of the primary loops and between the primary and secondary sides of SGs is relatively small. The primary temperatures calculated by TRAC have been found to be quite close to those obtained by this simple hand calculation for most of the transients.

The primary and secondary pressures have been more difficult to calculate with this simple approach due to significant nonequilibrium effects associated with condensation and evaporation. Therefore, in some transient calculations, the pressurizer water levels obtained by the TRAC and BNL calculations were compared instead of the primary side pressures. It has been observed that the trend of the pressurizer pressure calculated by TRAC is very closely approximated by the trend of the water level in the pressurizer in many transients. Whenever possible and applicable, we have also calculated the pressurizer pressure based on the adiabatic frozen and/or equilibrium assumptions, which provide the upper or lower bound depending on whether the pressurizer is being filled or emptied. The actual pressure is expected to be somewhere in between these two extreme pressures. We have found that the pressure calculated by TRAC is usually closer to the adiabatic than to the equilibrium pressure.

Similar nonequilibrium effect has also been observed in the secondary side pressure of SG calculated by TRAC, especially when the SG is being filled with cold Auxiliary Feedwater (AFW). In several transients, the secondary pressure remains high while the temperature declines. It appears that further code assessment work is needed to verify the code calculation of the U-tube steam generator pressure when the cold auxiliary feedwater is introduced into the SG. However, it is expected that this uncertainty would not significantly change the overcooling transient calculations.

Only the first transient (Transient No. 1) will be discussed in detail in this report. For the remaining five transients, only the comparison between the primary temperatures obtained by the LANL and BNL calculations will be shown. Details of the review of these transients can be found in a separate topical report (Jo, 1984).

Transient 1 is a steam line break accident initiated by a 1-ft^2 break at the main steam line during the HZP operation. This transient was also calculated by NSEA for BG&E (Baltimore Gas and Electric) using the RETRAN code.

Figure 8.1 shows the downcomer temperature calculated by TRAC with the system average temperature obtained by the BNL hand calculation. Two BNL calculated temperatures are shown in the figure. One is calculated with the assumption that heat transfer between the wall of the reactor vessel (and other structure) and liquid is instantaneous, and thus, the metal temperature changes with the liquid temperature. The other assumes that the heat transfer is so slow that the metal temperature does not change at all. The actual temperature should be between these two extremes. The TRAC downcomer temperature initially agrees well with the temperature calculated without the metal mass accounted for, and then it eventually approaches that calculated with the metal mass accounted for, as expected. This indicates that the metal takes a considerably longer time to cool. The liquid temperatures calculated by TRAC at various locations are shown in Figure 8.2 along with the RETRAN and BNL temperatures without the metal in the initial 1500 seconds. The figure shows that the downcomer temperature may be representative of the system average temperature, and the TRAC, RETRAN and BNL calculations agree very well.

Figure 8.3 shows the system pressure calculated by TRAC, RETRAN and BNL. It shows that the RETRAN pressure is virtually identical to the TRAC pressure, while the BNL pressure which is calculated based on the adiabatic assumption, is higher than these, as expected. The figure also shows, for comparison, the water level in the pressurizer calculated by BNL. As expected, the pressure and the water level behave similarly.

Figure 8.4 shows the pressure in the steam generators from both the RETRAN and TRAC calculations. The saturation pressure corresponding to the system average temperature calculated by BNL is also shown in this figure. The BNL saturation pressure matches the broken SG pressures for both TRAC and RETRAN calculations very closely. However, the intact SG pressure for

TRAC increases while the RETRAN pressure continues to decrease for the initial 1020 seconds and also shows several sharp drops. A similar steam generator pressure response is observed in several other transients for the TRAC calculations when the steam generator is being filled with cold AFW. This is apparently related to the severe nonequilibrium effect caused by the TRAC condensation model. As discussed earlier, further work is needed to clarify this uncertainty. However, it is not expected to alter the course of the rest of the transient significantly.

The calculation was terminated at 7200 seconds. Beyond this time, the system temperature is expected to continue to decrease until it eventually reaches 357°K, where the decay heat balances with the cooling by the charging water and the AFW.

As mentioned earlier, only the comparison between the primary temperatures obtained by the LANL and BNL calculations are shown for the remaining five transients (Figures 8.5 - 8.10). For Transient 11, the RETRAN temperature calculated by ENSA is also shown during the first 600 seconds.

In general, the temperatures and pressures of the primary system calculated by TRAC are very reasonable.

8.2 Review of RELAP5 H. B. Robinson-2 Calculations
(C. Yuelys-Miksis and U. S. Rohatgi)

An informal report documenting the RELAP5/MOD1.6 results of the H. B. Robinson PTS transients simulated at INEL has been received, and is being reviewed. Review of the RELAP5 input decks for the full power and hot zero power transients for the H. B. Robinson plant has been completed. Results of the review have been documented in a BNL memorandum (Rohatgi, 1984) which has been transmitted to NRC and INEL. In general, the plant input was consistently represented in both decks with minor variations from the Robinson FSAR values. These differences are described in the aforementioned memorandum.

Work is in progress in reviewing the RELAP5 calculations. In particular, hand calculations based on the simple BNL model as applied to the Calvert Cliffs PTS calculations, will also be employed to the Robinson PTS activity.

REFERENCES

JO, J.H., and ROHATGI, U.S., (1984), "Review of TRAC Calculations for Calvert Cliffs PTS Study," BNL Report, to be published.

ROHATGI, U.S. and YUELYS-MIKSIS, C., (1984), "BNL Review of RELAP5 Input Decks for H. B. Robinson from INEL," BNL Memorandum to P. Saha, March 22, 1984.

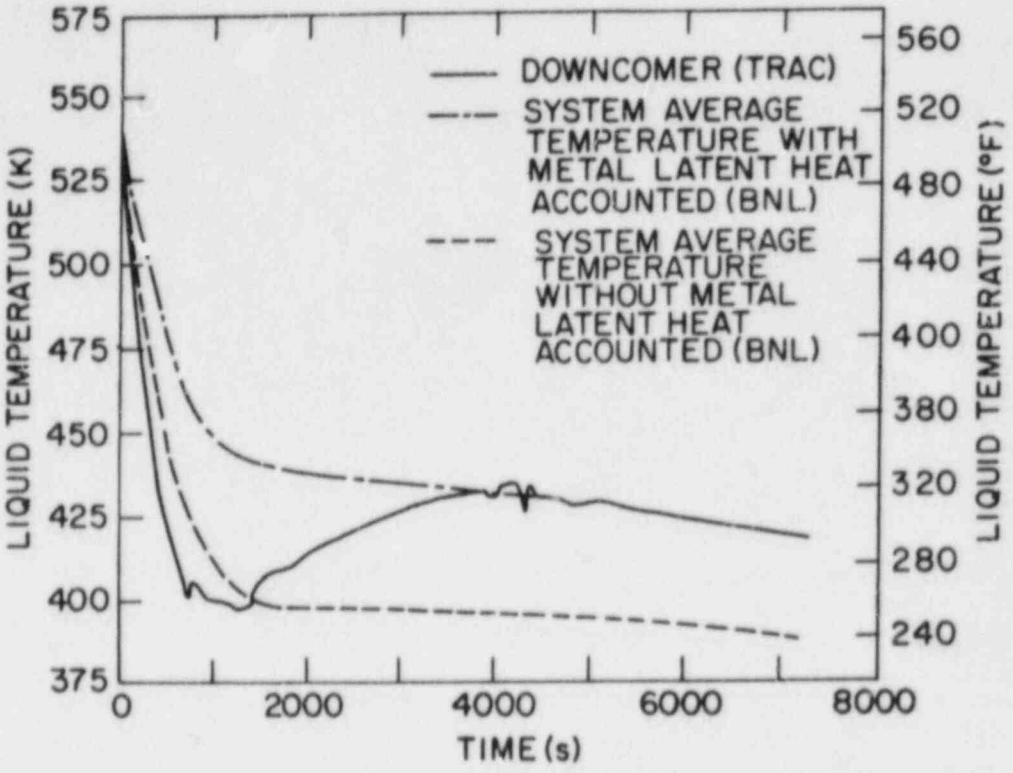

Figure 8.1 Transient HZP Small Steam Line Break
(BNL Neg. No. 5-407-84)

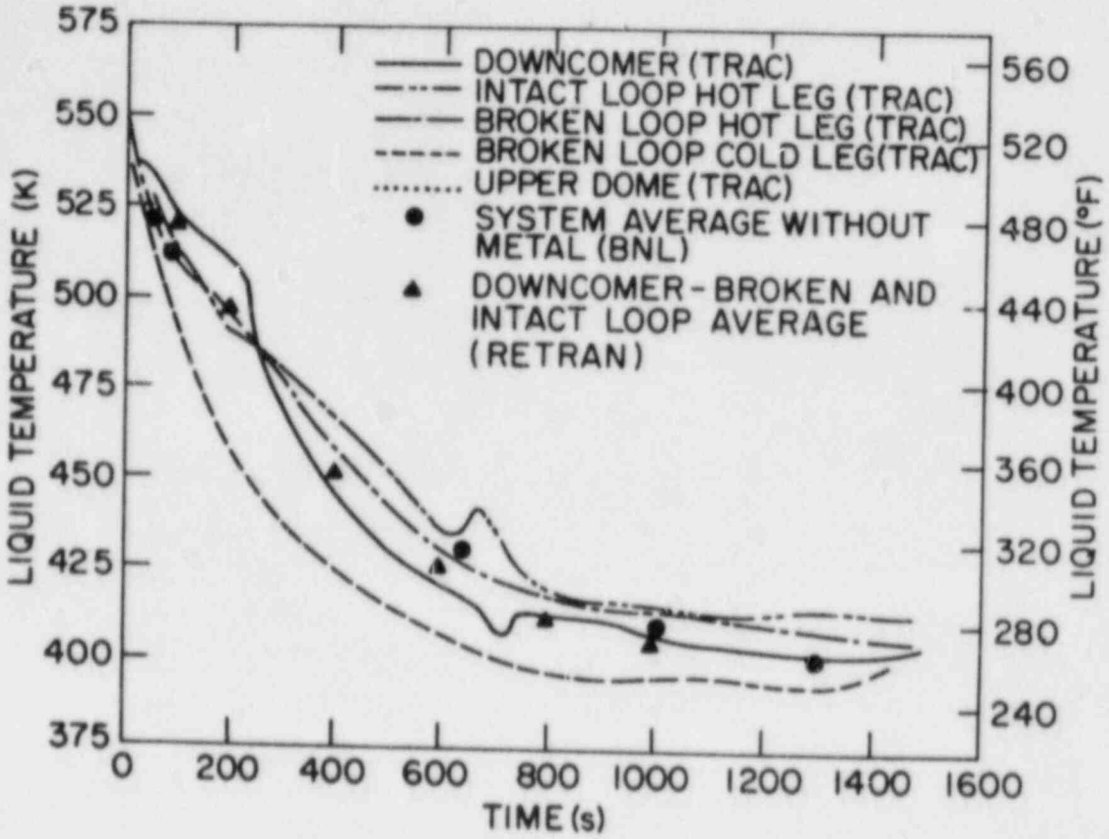

Figure 8.2 Transient 2 HZP Small Steam Line Break
(BNL Neg. No. 5-1086-84)

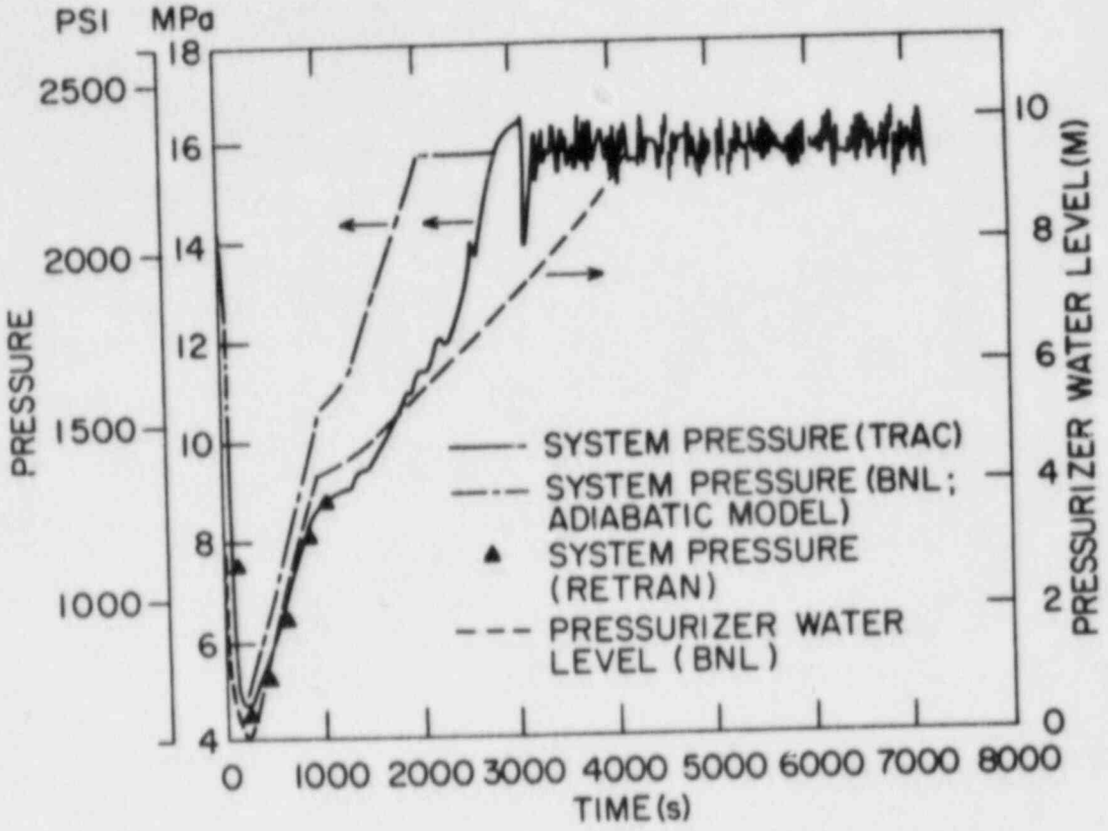

Figure 8.3 Transient 1 HZP Small Steam Line Break
(BNL Neg. No. 5-1087-84)

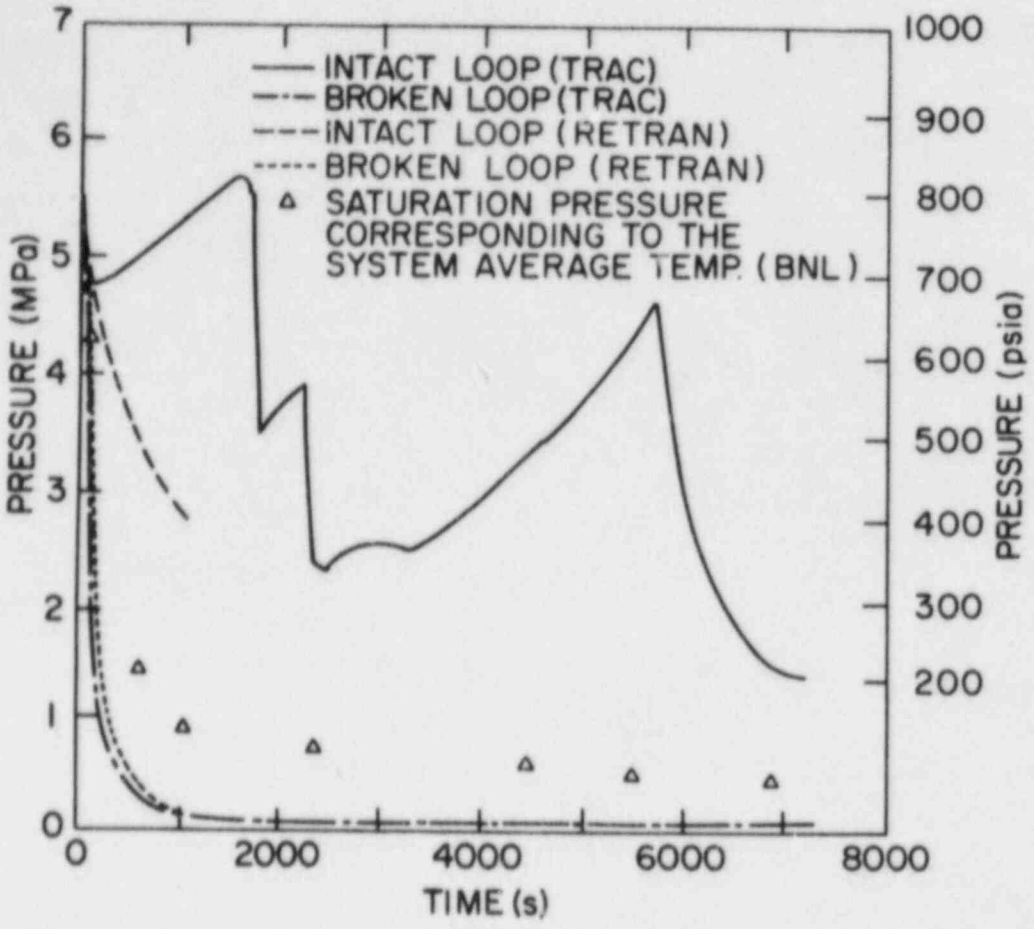

Figure 8.4 Transient 1 HZP Small Steam Line Break
(BNL Neg. No. 5-1088-84)

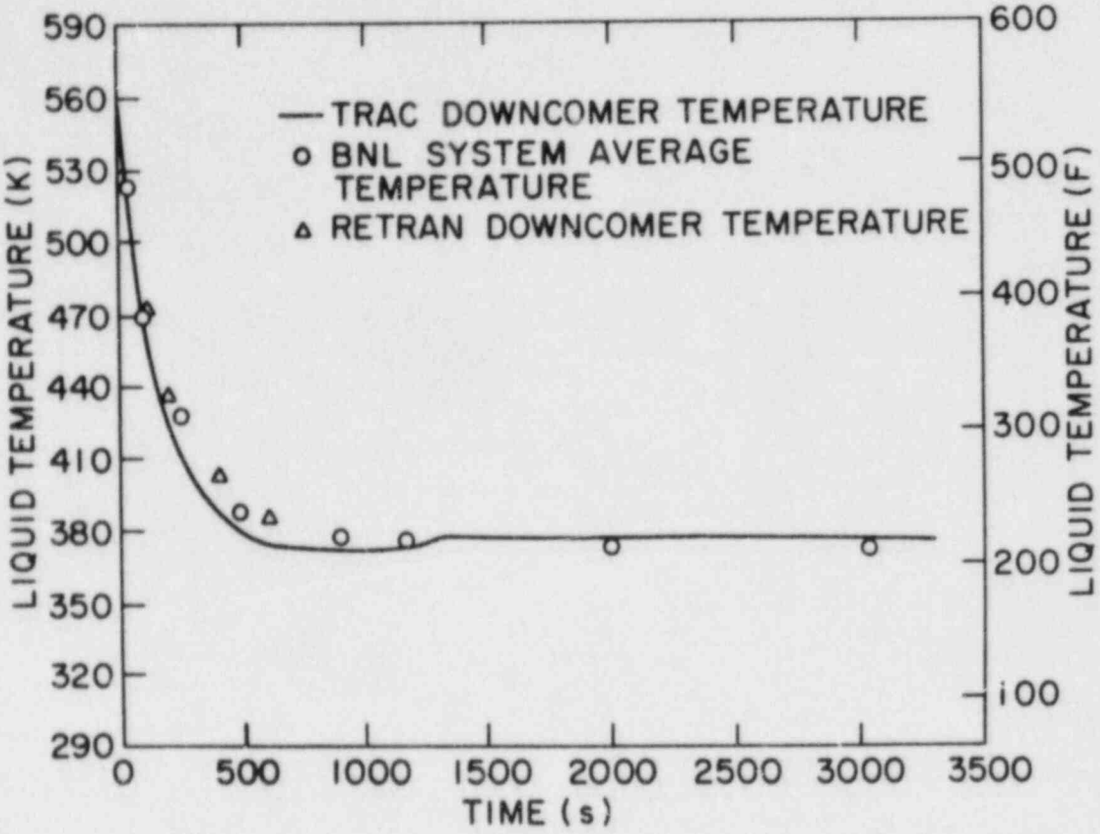

Figure 8.5 Transient 11 Full Steam Line Break with Stuck Open MSIVs
(BNL Neg. No. 5-1085-84)

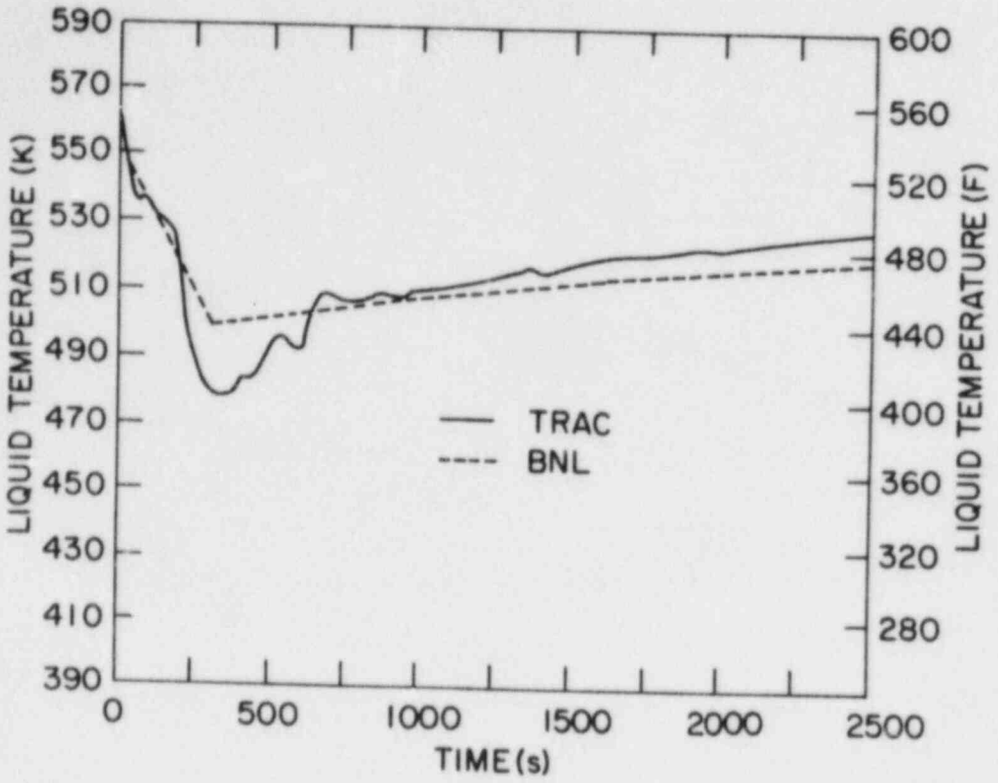

Figure 8.6 Transient 3 Small Steam Line Break at HZP Downcomer Liquid Temperature (BNL Neg. No. 5-419-84)

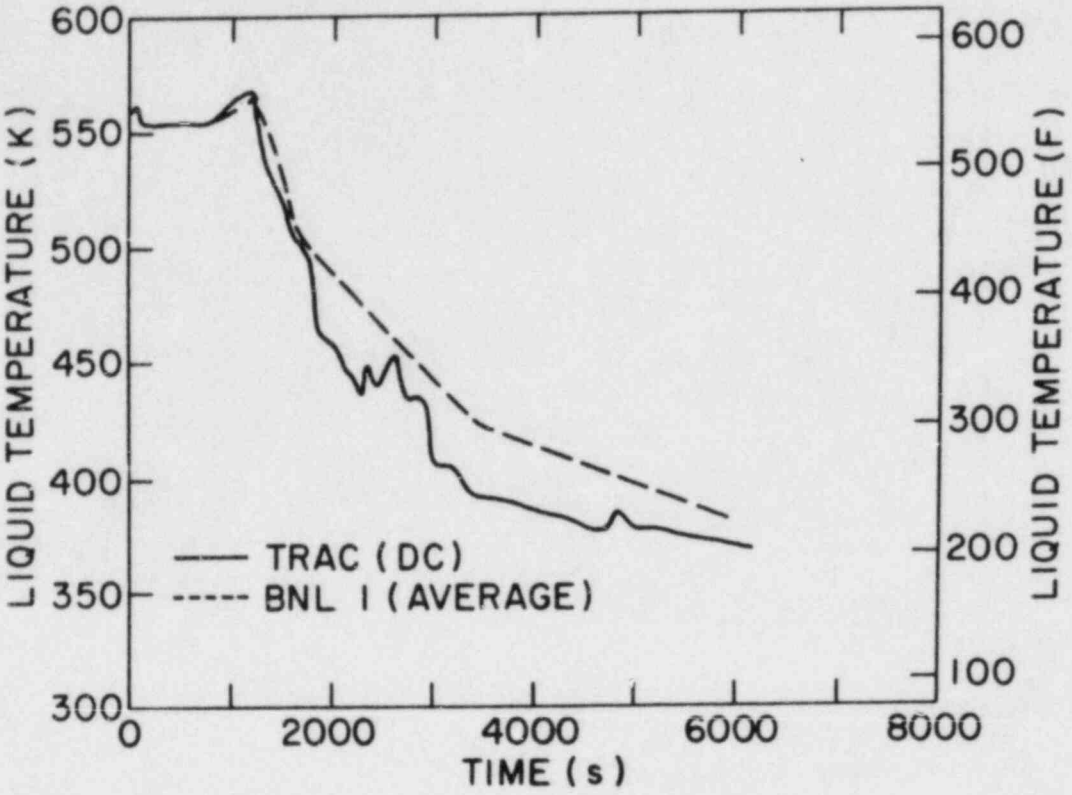

Figure 8.7 T-ansient 6 HFP AFW Overfeed
(BNL Neg. No. 5-435-84)

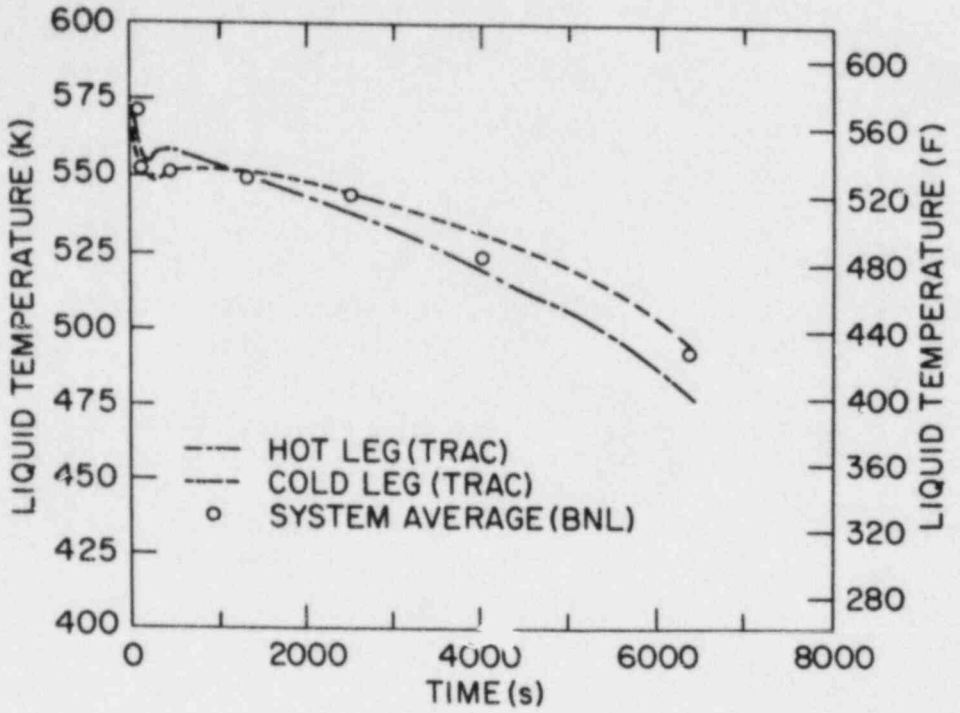

Figure 8.8 Transient 7A Small Break LOCA
(BNL Neg. No. 5-429-84)

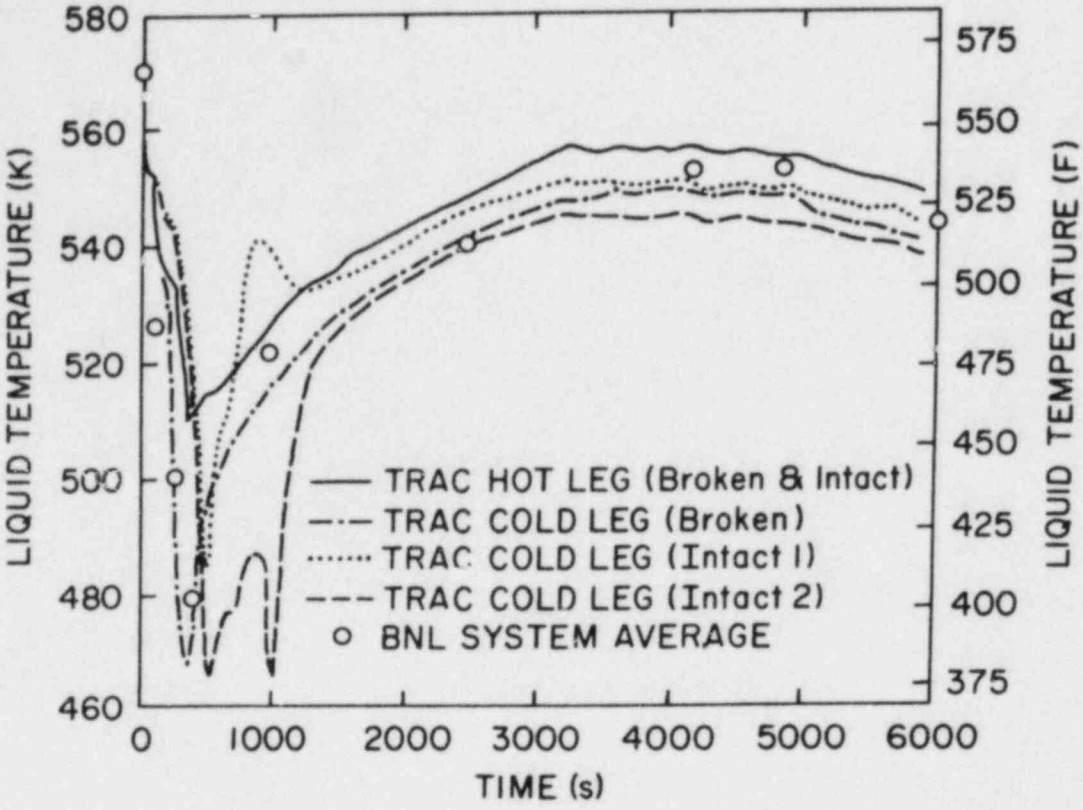

Figure 8.9 Transient 9 MFW Overfeed to One SG
(BNL Neg. No. 5-436-84)

II. DIVISION OF ENGINEERING TECHNOLOGY

SUMMARY

Stress Corrosion Cracking of PWR Steam Generator Tubing

The experimental program on stress corrosion cracking (SCC) at Brookhaven National Laboratory (BNL) is aimed at the development of a quantitative model for predicting the behavior of Inconel 600 tubing in high temperature aqueous media. Much of this has been done in an ongoing experimental program in which empirical relationships are being established between stress corrosion cracking failure time or crack velocity and factors influencing cracking. These include stress, strain and environmental and metallurgical variables. Environments are related to the ingredients of primary or secondary water. Cold work of Alloy 600 is included, and activation energies are determined. A major item that is preventing a final analysis of the slow strain rate factor is the development of a method to detect crack initiation.

SSC was found earlier in four U-bends of production tubing exposed in deaerated, pure water at 315°C, and provided a continuous Arrhenius plot from 365°C to 315°C. More cracks occurred during this quarter. CERT with 0.01% carbon material was continued in secondary water ingredients. Tests at constant load were not active during this period. Computer programs are available for handling the proposed model used for predictive purposes for Inconel steam generator tubing, but the CERT data have to be improved before this can become reliable; no funding is available for this purpose now. Also,verification of the model with tubes from service is due.

A proposed standard test procedure for ASTM balloting is in final modified form, dealing with Electrochemical Potentiokinetic Reactivation (EPR) tests used in detecting sensitization of stainless steels. The first ballot produced two negative votes, which were resolved. It may be beneficial to use a slight modification in the present procedure for best results.

Model verification with tubing from the Surry Steam generator at PNL is still stongly advocated, together with some tests in constant extension.

Bolting Failure Analysis

All work on the Bolting Failure Analysis Program was completed during this quarter, and a final report was transmitted to Technical Information for publication.

Probability Based Load Combinations for Design of Category I Structures

For developing probability-based load combination criteria for design of Category I structures, a procedure has been established. This procedure is utilized in developing load factors for concrete containments. The proposed load combination is in load and resistance factor design (LRFD) format and follows the Turkstra combination rule. Four sample containments are constructed using the Latin hypercube sampling technique. Furthermore, an objective function is defined and a minimization scheme is also developed to find the optimum load factors. Work on derivation of load factors for dead load, accidental pressure due to a large LOCA and safe shutdown earthquake has been carried out. A report on this topic is currently being prepared.

Mechanical Piping Benchmarking Problems

A report of the key results from the Multiple Supported Piping study was presented to the PVRC Committee for Piping. As a result of this presentation, additional tasks pertinent to the study were undertaken. Further, responding to the interest in the results, a best effort is being made to complete the entire study and prepare a report in time for the May meeting of the PVRC Committee for Piping.

Identification of Age Related Failure Modes

The objective of this program is to determine what aging and service wear effects are likely to impair plant safety, and what methods of inspection and surveillance will be effective in detecting significant aging effects.

The first groups of components to be addressed are small motors in mild environments, battery chargers/inverters, and circuit breakers and relays.

The program for each component will proceed through three phases: a reseach phase, an experimental phase, and an evaluation and conclusion phase. At the end of this quarter, the motor research phase is 50% completed, and the experimental phase will be conducted in the next quarter.

9. Stress Corrosion Cracking of PWR Steam Generator Tubing

(D. van Rooyen)

The objective of this program is to develop quantitative data to serve as a predictive basis for determining the useful life of Alloy 600 tubing in service. For this purpose, tests are being run on production tubing of Inconel 600 at different carbon levels to examine the various factors that influence the cracking of tubing. Verification was planned with tubing to be obtained from a decommissioned steam generator, but this will not be possible due to a reduction in funding level for 1984, but is still strongly recommended.

The present experimental program addresses two specific conditions, i.e., 1) residual stress conditions where deformation occurs but is no longer active, such as when denting is stopped and 2) where plastic deformation of the metal continues, as would occur during denting. Laboratory media consist of pure water as well as solutions to simulate environments that would apply in service; tubing from actual production is used in carrying out these tests. The environments include both normal and "off" chemistries for primary and secondary water. Material condition also includes various degree of cold work.

9.1 Constant Load

No work was done in this area during this quarter.

9.2 CERT

It is repeated that CERT data on SCC require a better distinction between the initiation and propagation stages than can be achieved by our present extrapolation technique. Corrections are needed to improve the quantitative determination of SCC induction times. New data confirm an activation energy of 33 Kcal/mole for crack growth, pending the introduction of a better correction in the calculation.

No complete sets of data are yet available for CERT in AVT, although this work is continuing.

We have discontinued plans for the new test that would permit simulation of an active dent. Static dents continue in test.

9.3 U-Bends

Split tube type U-bends cracked in earlier tests at 325°C-365°C and suggested a possibility that the carbon level of the Inconel influences the crack initiation/temperature relationship, i.e., activation energy seemed to increase with increasing carbon content. A larger number of replicate samples have been exposed in water at 290°C and 315°C since 1981. These U-bends have now shown cracking for 0.02, but not yet at higher carbon. The 0.01% material continued to give cracks in the previous quarter.

9.4 Future Work

Future work will be the continuation of long-term tests, and exposures in AVT. However, it is strongly recommended that work on the model, especially in crack propagation rates, be re-started to complete the quantitative relationships. These may be simplified by limited further work, and without the effort the work to data may lose much of its potential application.

10. Bolting Failure Analysis

(J. R. Weeks and C. J. Czajkowski)

All work on the Bolting Failure Program was completed during this quarter, and a final report was transmitted to Technical Information for publication. It will appear as BNL-NUREG-51767.

The conclusions from the work were given in the previous quarterly report.

11. Probability Based Load Combinations for Design of Category I Structures

(H. Hwang, M. Reich, J. Pires, P.C. Wang,
M. Shinozuka, B. Ellingwood and S. Kao)

11.1 Load Combination Criteria for Design of Concrete Containments

In the previous quarterly progress report, the procedure for developing probability-based load combination criteria for design of concrete containments was summarized. In addition, four sample containments as shown in Table 11.1 were constructed in order to test the objective of the proposed load combination design criteria.

On the basis of flexual limit state of the concrete containments, the load factors for three loads, i.e., dead load, accidental pressure due to a large LOCA and safe shutdown earthquake have been determined. The results will be included in a technical report which is currently being prepared.

Under the condition that the containments are only subjected to dead load and accidental pressure during its service life of 40 years, the results are summarized as follows.

The proposed load combination for design of concrete containment is

$$0.9D + \gamma_p P_a \leq \phi R \qquad (11.1)$$

where

D = load effect due to design dead load
P_a = load effect due to design pressure
γ_p = load factor for accidental pressure
R = nominal structural resistance
ϕ = resistance factor

Some load factors may be preset in order to simplify the task. For example, in Eq. 11.1 the dead load factor is preset to be 0.9 because the dead load has a stabilizing effect. With regard to resistance factor ϕ, the values recommended by MacGregor will be adopted for this study.

The accidental pressure is caused by an event of Loss of Coolant Accident (LOCA). The design value of such a pressure is determined by a Design Basis Accident (DBA). For each representative containment, a design pressure is specified as shown in Table 11.1. The accidental pressure is assumed to be static and uniformly distributed on the containment wall.

The dead load mainly arises from the weight of the containment wall. The design value of the dead load is computed based on the unit weight of reinforced concrete as 150 lb/ft^3.

A three-dimensional finite element model is used for the structural analysis of the containment. The finite element utilized in the analysis is the shell element as described in the SAPV computer code. A detailed cross-sectional view of the containment model is shown in Fig. 11.1. As can be seen from this figure, the containment is divided into 20 layers. Except at the top of the dome, each layer has 24 elements such that the nodal points are taken every 15° in the circumferential direction. This discretization requires a total of 481 nodes and 468 elements.

Using the finite element model, the analysis of the containments under dead load and accidental pressure are carried separately. The individual load effects are then combined according to Eq. 11.1 with assigned load factors. The limit state considered in the study is the flexural limit state. Finally, on the basis of the ultimate strength design of reinforced concrete, the amount of the required rebar area is determined as shown in Table 11.2.

Since the loads intrinsically involve random and other uncertainties, an appropriate probabilistic model for each load must be established in order to perform reliability analysis.

Dead Load

The dead load primarily arises from the weights of the containment wall. It is noted that there are some uncertainties as to the actual magnitude of the dead load. For the purpose of this analysis, however, dead load is assumed to be deterministic and is equal to the design value, which is computed on the basis of the weight density of reinforced concrete as 150 lb/ft^3.

Accidental Pressure

The accidental pressure is considered as a quasi-static load and it is uniformly distributed on the containment wall. The accidental pressure is idealized as a rectangular pulse and it will occur in accordance with the Poisson law during the containment life. Under these assumptions, three parameters are required to model the accidental pressure: the mean occurrence rate λ_p (per year), the mean duration μ_{dP} (in seconds) and the intensity P. The intensity P is considered as a random variable. Two sets of parameter values shown in Table 11.3 are considered in this study.

Based on the limit state and probabilistic models for loads and material strength, the reliability analysis of containments was carried out. The unconditional limit state probability is shown in Table 11.4 in which the lifetime of the structures is taken to be 40 years.

The objective function for this case may be written:

$$\Omega(\phi, \gamma_D, \gamma_p) = \sum_{i=1}^{N} \omega_i \, (\log P_{f,i} - \log P_{f,T})^2$$

in which ω_i is set to be 1 while ϕ and γ_D are fixed. Hence, only γ_p is an unknown variable to be determined. $P_{f,T}$ is the specified target limit state probability. It is assumed to be one of the following three values: 1.0×10^{-5}, 1.0×10^{-6} and 1.0×10^{-7}. Using the limit state probability of the samples, $P_{f,i}$ as shown in Table 11.4, the objective function Ω is computed at several values of γ_p and a parabolic curve passing through these values is plotted as shown in Fig. 11.2. From this figure, the load factor γ_p, which minimizes the objective function, is determined and tabulated in Table 11.6.

PUBLICATIONS

KAWAKAMI, J., HWANG, H., CHANG, M. T., AND REICH, M. "Reliability Assessment of Indian Point Unit 3 Containment Structure", BNL-NUREG-51740, NUREG/CR-3641, January 1984.

Table 11.1 PWR Reinforced Concrete Containment Samples

Design parameters	Sample 1	Sample 2	Sample 3	Sample 4
inside radius	70'-0"	60'-0"	60'-0"	70'-0"
dome rise ratio	1.0	1.0	1.0	1.0
cylindrical height	150'-0"	150'-0"	150'-0"	150'-0"
cylindrical wall thickness	4'-6"	3'-6"	4'-6"	3'-6"
dome wall thickness	3'-6"	2'-6"	3'-6"	2'-6"
concrete compressive strength (psi)	4000	4000	5000	5000
steel yield strength (psi)	60,000	60,000	60,000	60,000
dead load (lb/ft^3)	150	150	150	150
accidental pressure (psi)	47	42	52	57
safe shutdown earthquake (g)	0.17	0.32	0.50	0.25

Table 11.2 Required Rebar Area ($D+P_a$)

Sample	Design Pressure (psi)	Load Combination	A_s (in^2/in)			
			Cylinder		Dome	
			X	Y	X	Y
1	47	0.9D+1.0P	0.411	0.265	0.290	0.183
		0.9D+1.1P	0.452	0.303	0.318	0.203
		0.9D+1.2P	0.493	0.341	0.346	0.223
		0.9D+1.3P	0.534	0.380	0.373	0.243
2	42	0.9D+1.0P	0.314	0.189	0.221	0.143
		0.9D+1.1P	0.345	0.218	0.242	0.159
		0.9D+1.2P	0.376	0.247	0.263	0.174
		0.9D+1.3P	0.408	0.276	0.285	0.189
3	52	0.9D+1.0P	0.394	0.239	0.276	0.175
		0.9D+1.1P	0.433	0.274	0.303	0.194
		0.9D+1.2P	0.472	0.310	0.329	0.213
		0.9D+1.3P	0.511	0.346	0.356	0.232
4	57	0.9D+1.0P	0.495	0.353	0.344	0.231
		0.9D+1.1P	0.544	0.400	0.377	0.255
		0.9D+1.2P	0.594	0.448	0.410	0.279
		0.9D+1.3P	0.643	0.495	0.444	0.304

NOTE: X = Hoop Direction

Y = Meridional Direction

Table 11.3 Probabilistic Characteristics of Accidental Pressure

Item		Case A	Case B
Mean Occurrence Rate		1.68×10^{-3}/YR	1.0×10^{-4}/YR
Mean Duration		1200 SEC	1200 SEC
Intensity	Mean/Design Value	0.9	0.83
	CoV	0.12	0.20
	Distribution	Gaussian	Gaussian

Table 11.4 Limit State Probability ($D+P_a$)

Case A

Load Combination	Sample 1	Sample 2	Sample 3	Sample 4
0.9D+1.0P	5.59 -5	1.21 -4	9.95 -5	3.64 -5
0.9D+1.1P	4.50 -7	9.66 -7	8.79 -7	2.10 -7
0.9D+1.2P	7.89 -10	1.72 -9	1.84 -9	2.46 -10

Case B

Load Combination	Sample 1	Sample 2	Sample 3	Sample 4
0.9D + 1.0P	2.69 -5	4.15 -5	3.73 -5	2.15 -5
0.9D + 1.1P	2.06 -6	3.37 -6	3.21 -6	1.53 -6
0.9D + 1.2P	8.65 -8	1.48 -7	1.52 -7	5.61 -8
0.9D + 1.3P	2.15 -9	3.52 -9	3.67 -9	3.98 -10

NOTE: 2.69 -5 = 2.69×10^{-5}

Table 11.5 Pressure Load Factor ($D+P_a$)

Target Limit State Probability	Pressure Load Factor, λp	
	Case A	Case B
1.0×10^{-5}	1.04	1.05
1.0×10^{-6}	1.08	1.12
1.0×10^{-7}	1.12	1.19

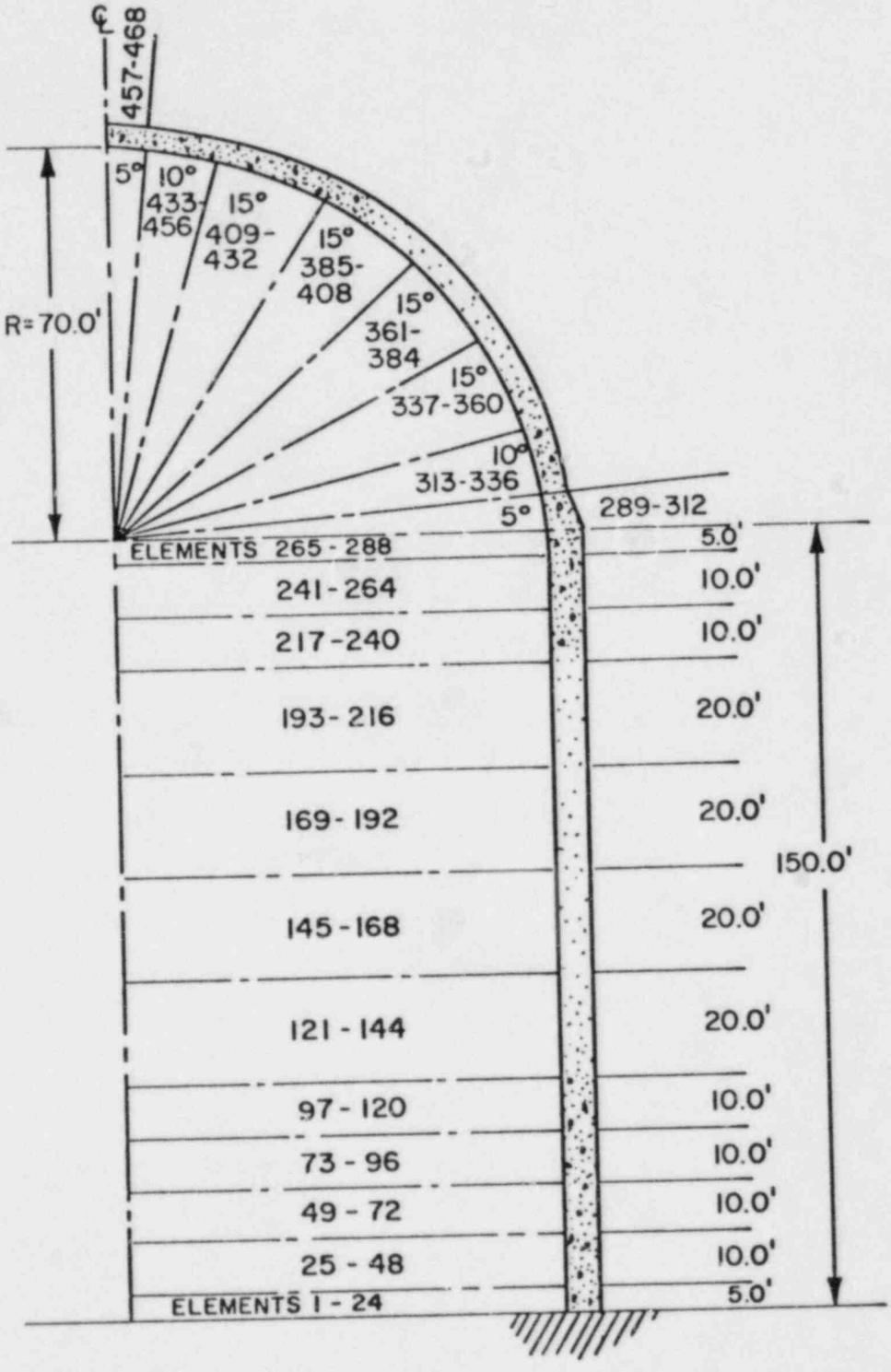

Fig. 11.1 Cross Section of Containment Model.

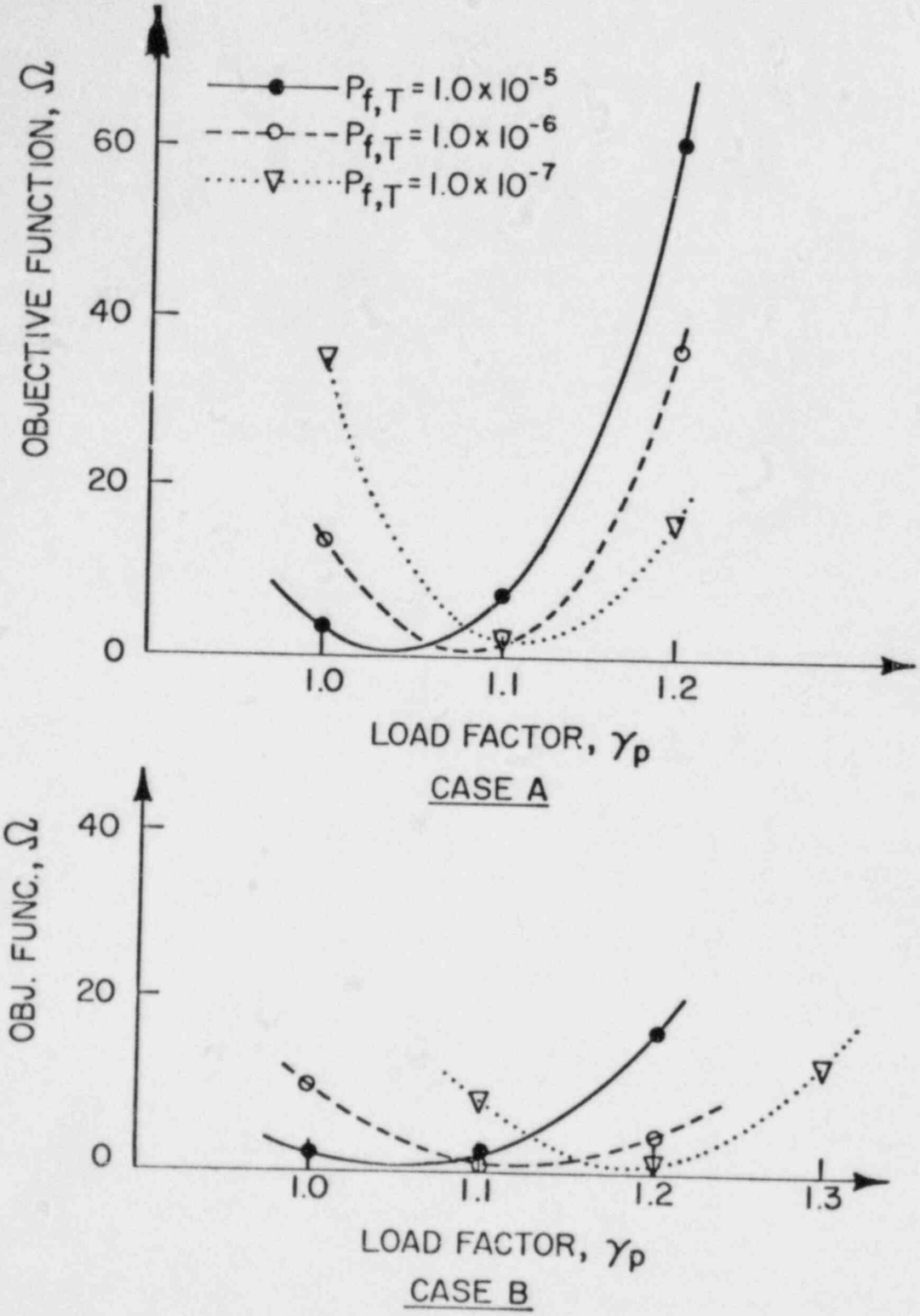

Fig. 11.2 Load Factor γ_p $(D+P_a)$

12. Mechanical Piping Benchmark Problems

(P. Bezler, M. Subudhi, Y.K. Wang and S. Shteyngart)

12.1 Physical Benchmark Development

The report entitled "Physical Benchmark Evaluation, Extended Z Bend", dated February 1984, describing the blind predictions for the extended Z bend test was issued.

The physical benchmark evaluation of the NRC/EPRI Main Pipe Line 1 has not been carried further during this period. Owing to the need for an expeditious completion of the Multiple Supporting Piping study tasks and the addition of new tasks to that area, the physical benchmarking efforts have been delayed. As indicated in the last period the piping model is ready for use. Also, in this period the data tape of the input forcing functions for the benchmark evaluation were transmitted by ANCO to BNL. The tape was successfully processed on the BNL system. Some further modeling data has been requested from ANCO.

12.2 Multiple Supported Piping System

As noted above, during this period, the entire effort was devoted to the Multiple Supported Piping study. All the scheduled calculations were completed and processed by mid-January. Following a preliminary review of the data a presentation of key results was made to the PVRC Committee for Piping at their January 24th meeting in Ft. Lauderdale, FL. Definite interest in the study results were expressed and, in fact, the committee chairman suggested several additional areas for study. Further, the BNL representatives were requested to prepare a complete description of the study results for presentation at the May meeting of the PVRC Committee for Piping in New York.

Following the Ft. Lauderdale meeting the NRC project monitor requested that the following additional tasks, which are in accord with the PVRC chairmans requests, be undertaken:

(i) Consider the "Center of Mass Approach" as another candidate method for computing the dynamic component of response and assess its adequacy.

(ii) Assess the study results for all critical pipe locations to assure that observed trends apply equally as well to those locations.

(iii) Apply the independent support motion methodology to the modified AFW model, reference LLNL report NUREG/CR-3526.

These tasks were undertaken with the PVRC committee meeting date being selected as the desired completion date. To comply with the third task area interaction with LLNL representatives was initiated. A summary of the LLNL results as well as the input spectra data for the modified AFW model were requested. At the end of this period tasks (i) and (ii) were well underway.

As a further result of the PVRC meeting, the NRC project manager requested that every effort be made to prepare and complete a report describing the Multiple Supported Piping study before the May meeting date. To accommodate this request and to address the additional task areas above, the physical benchmarking effort was delayed. Throughout the remainder of the period a major effort was directed towards preparing the desired draft report.

The basic results of the study are summarized in table form. Examples of these tables have been presented in earlier quarterlies. For the LLNL models, involving thirty-three earthquakes, figures depicting the pertinent results of the study have been developed. Figures 12.1 - 12.3 show a sample of these for the resultant pipe moments for the RHR model. The abscissae of each figure represents the different cases for the dynamic or the total response and the different methods of evaluation for the static response. The ordinate represents the degree of exceedance (TH-PREDICTED/TH) associated with each of the candidate procedures. The dashed horizontal line corresponds to the time history (TH) solution and is assumed to represent the true response. Only two to four response estimates for different ponits on the model are plotted. These data exhibit the least degree of exceedance for all points on the model.All other data for the respective response parameter would fall above the plotted values. The data plotted then define the lower bound of the response parameter. Each plot entry shows a vertical line. The center of the line is the mean value, and the line extends one standard deviation above and below this value. Data of this type as well as all the tabular results will be included in the report being prepared.

It is anticipated that the preliminary report will be completed by the desired date. Further, a best effort will be made to also complete the additional tasks by that date.

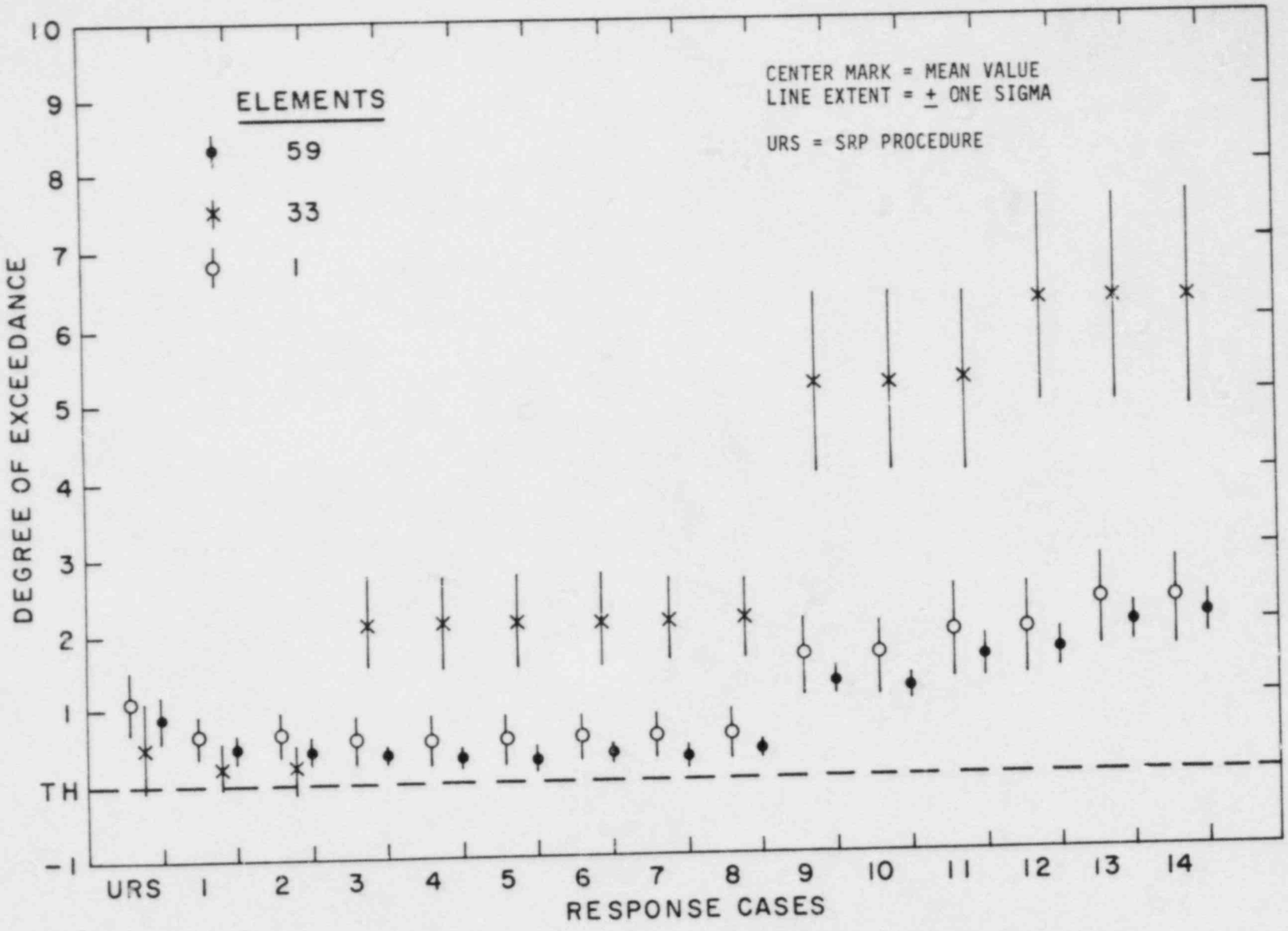

Figure 12.1 - Dynamic Pipe Resultant Moment Responses for RHR Model

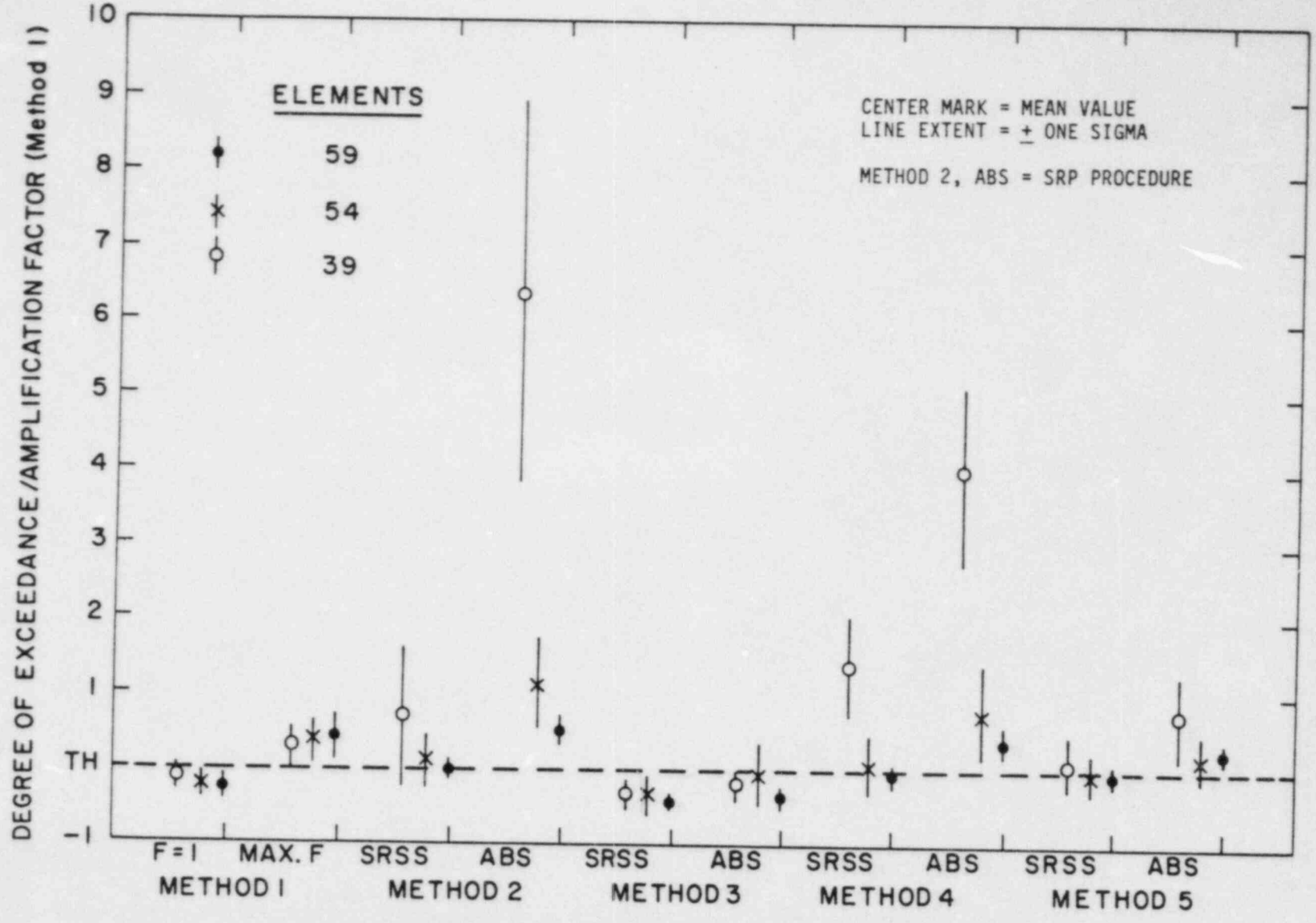

Figure 12.2 - Static Pipe Resultant Moment Responses for RHR Model

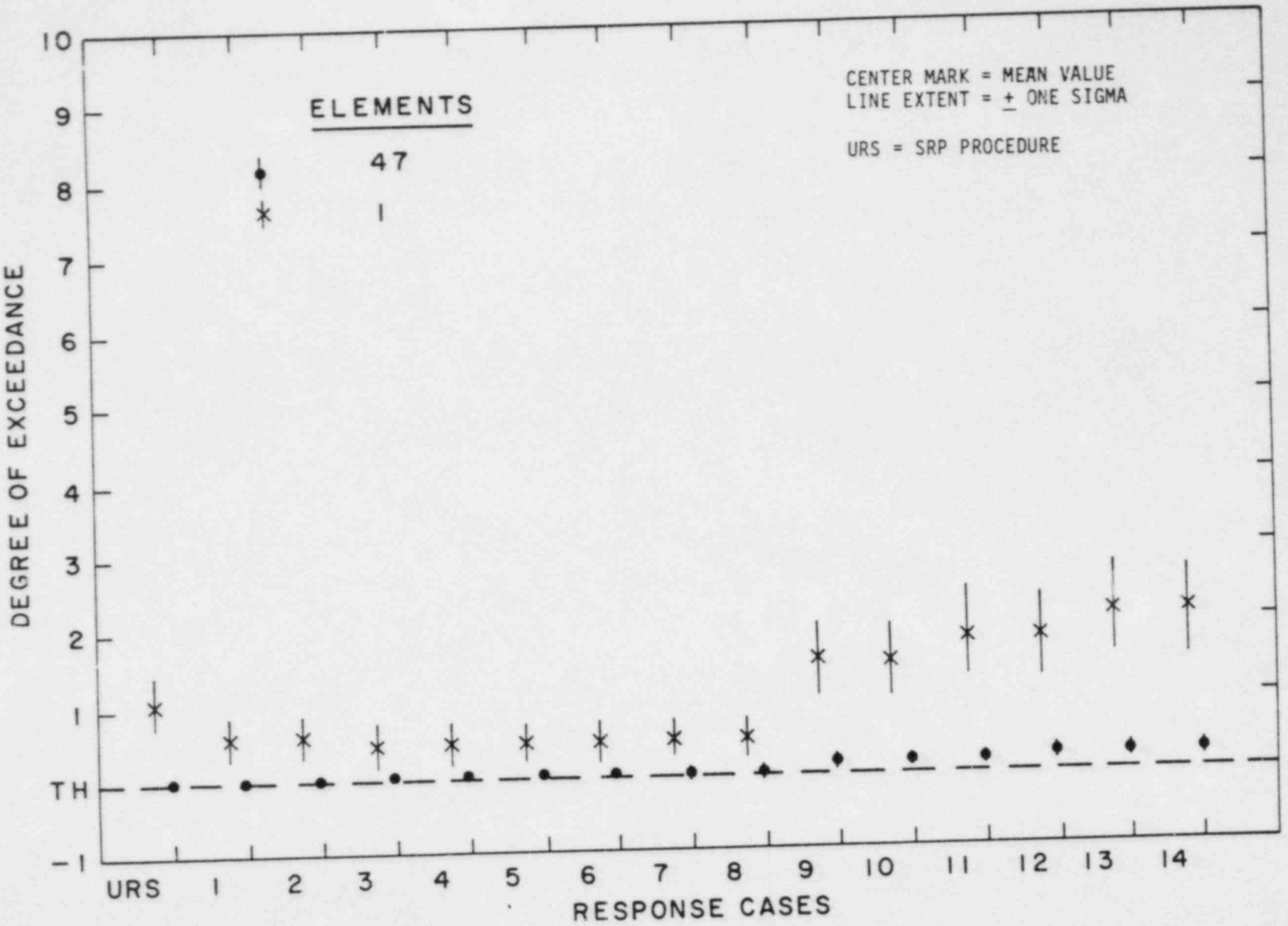

Figure 12.3 - Total Pipe Resultant Moment Responses for RHR Model Using SRSS Combination

13. Identification of Age Related Failure Modes (J.H. Taylor)

The objectives of this program are twofold: 1) to determine what aging and service wear effects are likely to impair plant safety, and 2) to determine what methods of inspection and surveillance will be effective in detecting significant aging effects prior to the loss of safety function so that proper maintenance and timely repair or replacement can be implemented.

The objectives mentioned above will be obtained by addressing components used in nuclear power plants on an individual basis. The selection of components to be studied will be made by using risk analysis, failure histories, special NRC interests, and expert judgement. The components to be addresed are small motors in mild environments, battery chargers/inverters, circuit breakers and relays.

The program will proceed through three phases for each component: review of operating data, aging assessment, and recommendation for surveillance and monitoring. As of the end of the second quarter of FY 1984, significant progress has been made on the motors, which is detailed below. Work on the other components is scheduled for the next quarter.

13.1 Review of Operating Data - Motors (M. Subudhi, L. Burns)

The acquisition of motors (and other components for future use) is being pursued at operating and decommissioned reactors. Some motors have been identified at a decommissioned plant. They are of an older design and their relevancy to contemporary equipment is under evaluation.

Available sources of information are being researched to provide input to the scope and type of examinations to be conducted and towards defining the functional parameters important for defect characterization, and determination of the aging and service wear effects that are likely to impair plant safety. Typical examples of the sources of information are failure analyses and reports by other national laboratories, licensees, architect engineers, and equipment manufacturers. Preliminary results indicate that aging is not a problem that affects the performance of motors. That is, motor failures are caused not by aging but by improper maintenance or by external stresses, such as failures of the driven equipment.

13.2 Aging Assessment - Motors (F. Cifuentes and J. Curreri)

A test plan has been prepared, which includes visual examinations, operational tests, and seismic testing according to a generic floor response spectra. This testing will be conducted at BNL. The testing will be conducted in the third quarter of FY 1984.

III. DIVISION OF FACILITY OPERATIONS

SUMMARY

Analysis of Human Error Data for Nuclear Power Plant Safety-Related Events

Brookhaven National Laboratory has been tasked in this program to develop and apply realistic human performance data and models to help evaluate the human's role in nuclear power plant (NPP) safety. To meet this objective, the major current efforts are being placed in the following areas of investigation, namely:

- The prediction of Human Error Probabilities (HEPs) using Licensee Event Report (LER) data and nuclear systems expertise--a utility analysis.
- The use of Performance Shaping Factors (PSFs) and quantified expert judgment in the evaluation of human reliability - the Success Likelihood Index Method (SLIM).
- The development and testing of the Multiple Sequential Failure (MSF) Model.
- The usefulness of Probabilistic Risk Assessment (PRA) related human reliability data in resolving human factors regulatory issues.

As a result of these efforts, BNL has developed several documents which report on the findings in the above areas, namely:

- Human Error Probability Estimation Using Licensee Event Reports (NUREG/CR-3519).
- SLIM-MAUD: An Approach to Assessing Human Error Probabilities Using Structured Expert Judgment (NUREG/CR-3518).

Human Factors Aspects of Safety/Safeguards Interactions During Routine Reactor Operations and Off-Normal Conditions

Brookhaven National Laboratory has been tasked in this program to describe potential staff interaction problems during safety-related events to prevent or mitigate those problems. Eight scenarios have been developed which have identified human factors which may cause conflicts or inefficiencies as the plant staff and off-site response personnel work to deal with each scenario. Interviews are being conducted with knowledgeable NRC staff to determine what licensees would generally do during each scenario. Then NRC guidance will be closely examined and changes and additions recommended.

Emergency Action Levels

Brookhaven National Laboratory has been tasked in this program to develop guidance for Emergency Action Levels (EALs) that can be integrated into Emergency Operating Procedure (EOP) guidelines. From this guidance, a method will be developed that can be applied by licensees to verify that the EALs incorporated into their EOPs are usable in the control room under accident conditions. This should result in a reliable and timely basis for declaring emergencies without being too complex or burdensome to those who are trying to safely mitigate an accident. Thus far, a preliminary assessment has been made to integrate EALs and EOPs based on the degradation of the fission product barrier criteria.

Protective Action Decisionmaking

In this program, BNL staff are developing a technical basis for NRC guidance on protective action decisionmaking based on an evaluation of the consequences of nuclear power plant accidents. Potential actions under consideration include sheltering, evacuation, and relocation. In the past, specific recommendations have proven to be difficult to justify because of uncertainties in potential accident sequences. Consequently, BNL will establish strategies appropriate to those sequences for which emergency planning is necessary, emphasizing credible failure modes, links to emergency action levels based on in-plant observables and containment status, and other factors such as weather. A final NUREG report will be written in a manner understandable to laypeople.

14. Analysis of Human Error Data for Nuclear Power Plant Safety Related Events

(W. J. Luckas, Jr.)

Brookhaven National Laboratory (BNL) has been tasked in this program to develop and apply realistic human performance data and models to help quantify and qualify the human's role in nuclear power plant (NPP) safety. To meet this objective, the major current efforts are being placed in the following areas of investigation, namely:

- The prediction of Human Error Probabilities (HEPs) using Licensee Event Report (LER) data and nuclear systems expertise - a utility analysis.
- The use of Performance Shaping Factors (PSFs) and quantified expert judgement in the evaluation of human reliability - the Success Likelihood Index Method (SLIM).
- The development of the Multiple Sequential Failure (MSF) Model.
- The usefulness of Probabilistic Risk Assessment (PRA) related human reliability data in resolving human factors regulatory issues.

14.1 Utility Analysis of Using LER Data for HEPs Prediction
(J. N. O'Brien, K. J. Voska)

The objective of this research has been the development of a methodology which can be used to obtain human error rate (HER) data from an analysis of Licensee Event Reports (LERs). A further objective has been to assess the practicality, acceptability, and usefulness of using the HERs obtained to predict HEPs for use in PRAs.

In order to calculate HER, the total number of observed errors must be divided by the total opportunity for error as follows:

$$\text{HER} = \frac{\text{total number of a particular type of human errors}}{\text{total number of opportunities for those errors}}$$

A method for the calculation of HERs was originally presented in NUREG/CR-1880 and -2417. This method has undergone several revisions to provide a more structured set of procedures for the identification, classification, and quantification of human errors reported in LERs. It is intended that the procedures be "stand-alone" in the sense that consistent and reproducible results can be obtained by different users with minimal support.

During the second quarter of FY 1984, work continued on the drafting of a finnl report (see NUREG/CR-2744). The final report NUREG/CR-3519 has been

given a new title: "Human Error Probability Estimation Using Licensee Event Reports" and will be issued during the next quarter.

14.2 Success Likelihood Index Method (SLIM) Development
(E. A. Rosa)

The use of Performance Shaping Factors (PSFs) and quantified expert judgment using SLIM is important in the evaluation of human reliability. It should be noted that the amount of authentic quantitative human reliability data that exists is small (and is likely to remain small for the foreseeable future). It is therefore likely that subjective judgment and extrapolation will continue to play an important part. Nevertheless, present extrapolation techniques are covert, unsystematic, and rely on the knowledge of a limited number of judges. They do not systematically take into account the ways in which PSFs combine together to affect the probability of success in particular situations. Moreover, certain tasks cannot effectively be quantified using reductionist approaches. For these tasks, involving diagnosis, decision making and other cognitive activities, a holistic technique will probably be necessary.

Quantified subjective judgment has emerged from the previous analysis as being of critical importance for human reliability evaluation. SLIM is a quantified subjective judgment approach which uses PSFs as comprising any or all of the factors which combine to produce the observed likelihood of success. The basic premise of the approach is that when an expert judge (or judges) evaluate(s) the likelihood that a particular task will succeed, he or she is essentially considering the utility of the combination of PSFs in the situation of interest in either enhancing or degrading reliability. SLIM has the means of positioning a task on a subjective scale of likelihood of success, which is subsequently transformed to a probability scale. This positioning is derived by considering the judges' perceptions of the effects of the PSF in determining task reliability. NUREG/CR-2986 documents the initial appraisal of SLIM.

During the second quarter of FY 1984, efforts were devoted to finalizing the draft of NUREG/CR-3518 entitled "SLIM-MAUD: An Approach to Assessing Human Error Probabilities Using Structured Judgment." The addition of Multi-Attribute Utility Decomposition (MAUD) to the basic SLIM procedure represents the incorporation of an interactive microcomputer based program into the elicitation procedures so that assessors may generate their own PSFs. The assessor generated PSFs are evaluated for theoretical consistency by the program and then converted to failure probabilities. An assessment of progress on the development of the MAUD addition to SLIM is an essential precursor to the actual field testing of the technique.

The principal objective of current work devoted to SLIM development is a comprehensive test of the MAUD-based implementation of SLIM. To accomplish this objective required: (1) the acquisition of the MAUD program software and (2)

a microcomputer capable of running the program. Both of these tasks were completed during this second quarter of FY 1984. In addition, training and demonstration sessions were held at both BNL and NRC. Progress continues on scheduling and operationalizing the test of SLIM-MAUD.

14.3 Multiple Sequential Failure Model Development and Testing
(P. K. Samanta, J. N. O'Brien)

The dependence of human failure on multiple sequential action is important in the evaluation of human reliability. NUREG/CR-2211 has analyzed the nature of this dependence and has distinguished it from other types of multiple failures. Human error causes selective failure of components depending on when the failure started. Two models have been initially developed for quantifying the failure probability in a multiple sequential action. The first is very general in nature and does not require any dependent failure data. The failure probability obtained from this model is a conservative one with associated uncertainty. The uncertainty is calculated considering many possible sources such as data, coupling, and modeling. In the second model, details of the process in multiple sequential failures (MSF) are taken into account. The model increments the conditional failure probabilities by a certain amount from their lower bounds (independent failure probability). This approach provides important insights into the influence of dependence of failures on system reliability. The model can be used effectively to choose an optimum system considering the individual failure probability, dependence factor, and the amount of redundancy in a system.

During the second quarter of FY 1984, the small-scale psychological experiment being used to test the model was further developed. Programming of test sequences was initiated and experimental tasks were further refined. Subject training approaches were further developed along with other experimental design considerations. Subjects were being selected and expected to be performing in the experiment during the next two quarters.

14.4 PRA Human Reliability Data
(J. N. O'Brien)

An assessment of the usefulness of PRA human reliability data in resolving human factors regulatory issues facing NRC has been undertaken. In order to accomplish this, two efforts are being undertaken. First, a list of all human factors issues is being assembled and the technical research questions which must be addressed to resolve them developed. Second, all PRAs are being reviewed to illicit exactly what type of data is presented. After both of these efforts are completed, PRA data will be compared to the human factors technical questions to determine their usefulness.

During the second quarter of FY 1984, the above two efforts have been commenced.

References

COMER, M. K., KOZINSKY, E. J., SECKEL, J. S., AND MILLER, D. P. (1983). "Human Reliability Data Bank for Nuclear Power Plant Operations," NUREG/CR-2744.

EMBREY, D. E. (1983). "The Use of Performance Shaping Factors and Quantified Expert Judgement in the Evaluation of Human Reliability: An Initial Appraisal," NUREG/CR-2986.

EMBREY, D. E., HUMPHREYS, P., AND ROSA, E. A. (1984). "SLIM-MAUD: An Approach to Assessing Human Error Probabilities Using Structured Judgment," NUREG/CR-3518.

HALL, R. E., FRAGOLA, J., AND LUCKAS, W. J., JR., Tech. Eds. (1981). Conference Record for NRC/BNL/IEEE Standards Workshop on Human Factors and Nuclear Safety, NUREG/CP-0035.

HALL, R. E., FRAGOLA, J., AND WREATHALL, J. (1982). "Post Event Human Decision Errors; Operator Action Tree/Time Reliability Correlation," NUREG/CR-3010.

LUCKAS, W. J., JR. AND HALL, R. E. (1981). "Initial Quantification of Human Errors Associated with Reactor Safety System Components in Licensed Nuclear Power Plants," NUREG/CR-1880.

LUCKAS, W. J., JR., LETTIERI, V., AND HALL, R. E. (1982). "Initial Quantification of Human Error Associated with Specific Instrumentation and Control system Components in Licensed Nuclear Power Plants," NUREG/CR-2416.

SAMANTA, P. K. AND MITRA, S. P. (1981). "Modeling of Multiple Sequential Failures During Testing, Maintenance, and Calibration," NUREG/CR-2211.

SAMANTA, P. K., HALL, R. E., AND SWOBODA, A. L. (1981). "Sensitivity of Risk Parameters to Human Errors in Reactor Safety Study for a PWR," NUREG/CR-1879.

SCHMALL, T. M., Ed. (1979). Conference Record for NRC/BNL/IEEE Standards Sponsored December 1979 Workshop on Human Factors and Nuclear Safety.

SPEAKER, D. M., THOMPSON, S. R., AND LUCKAS, W. J., JR. (1982). "Identification and Analysis of Human Errors Underlying Pump and Valve Related Events Reported by Nuclear Power Plant Licensees," NUREG/CR-2417.

SPEAKER, D. M., VOSKA, K. J., AND LUCKAS, W. J., JR. (1983). "Identification and Analysis of Human Error Underlying Electrical/Electronic Component Related Events Reported by Nuclear Power Plant Licensees," NUREG/CR-2987.

VOSKA, K. J. AND O'BRIEN, J. N. (1984). "Human Error Probability Estimation Using Licensing Event Reports," NUREG/CR-3519.

15. Human Factors Aspects of Safety/Safeguards Interactions During Routine Operations and Off-Normal Conditions

(J. N. O'Brien)

Brookhaven National Laboratory has been tasked in this program to describe potential staff interaction problems during safety-related events and recommended actions to prevent or mitigate those problems.

The first step of this effort is to examine and address human factors issues which arise from consideration of impacts on the ability of personnel at nuclear power plants to effectively perform their duties as documented in NUREG-0992. Of particular interest are situations at plants which may involve conflicts in roles and missions between security measures and the other organizational units which operate the plant. An example of this is the conflict between security measures aimed at restricting access to critical plant system components to thwart sabotage and vandalism and the needs of operational personnel to have ready access to those same components to safety operate the plant. While this type of conflict has not occurred at any plant in such a way as to produce a significant threat to safety, the potential for such a conflict must be examined to assure adequate performance of plant personnel. This program sets out to examine the human factors aspects of these potential problems and, further, to recommend measures to prevent or mitigate any potential adverse impacts on safety.

In order to effectively address potential problems involving conflicts between security requirements and operational practices, potentially trouble some situations and human factors issues relevant to them must be identified. This involves the consideration of a wide range of situations and human factors issues. Once situations have been identified and relevant human factors issues defined, a systematic examination will reveal how potential conflicts can be prevented or mitigated.

After potentially troublesome situations and relevant human factors issues are identified, a matrix will be constructed with situations on one axis and human factors on the other. The cells in the matrix represent the basis of the analysis from which proposals will be developed to prevent or mitigate adverse effects.

The scope of the resultant report will include input from a number of individuals in the fields of operational safety, security, and human factors. However, no site visits will be conducted. Instead, the data contained in the NUREG-0992 is considered to be representative of that which would come from site visits since that is how the committee's data were generated. NUREG-0992 has been extensively analyzed and conclusions are drawn on the basis of that information and subject to review by a panel of experts in the relevant fields. No formal attempt has been made to corroborate or verify the data presented in NUREG-0992.

16. Emergency Action Levels

(W. J. Luckas, Jr.)

Brookhaven National Laboratory (BNL) has been tasked in this program to develop guidance for Emergency Action Levels (EALs) that can be integrated into Emergency Operating Procedure (EOP) guidelines. From this guidance, a method will be developed that can be applied by licensees to verify that the EALs incorporated into their EOPs are usable in the control room under accident conditions. This should result in a reliable and timely basis for declaring emergencies without being too complex or burdensome to those who are trying to safely mitigate the accident.

EALs are a plant specific, predetermined observable and/or measurable set of indications (such as a particular set of control room instrument readings having reached specific off-normal values) which are used to declare one of the Emergency Classes (Alert, Site Area Emergency, or General Emergency).

After appropriate examination, an attempt will be made to utilize currently available EALs developed by utilities, such as Kansas Gas and Electric Company on their Wolf Creek Generating Station, that use the breach of fission-product barrier approach as a starting point. The EAL guidance will be verified by testing sample EALs against the example initiating conditions listed in Appendix 1 of NUREG-0654.

During the second quarter of FY 1984, the existing classification system for the emergency classes based on the degradation of fission products barrier was improved by applying the example in severe accident seqences examples.

17. Protective Action Decisionmaking

(W. T. Pratt, A. G. Tingle, H. Ludewig,
W. R. Casey*, and A. P. Hull*)

17.1 Background

NRC regulations require that, in the case of a major nuclear power plant accident, licensees recommend protective actions to reduce radiation dose to the public. When certain emergency action levels are exceeded, the licensee recommends protective actions to State and local officials. The nature of the protective actions recommended is determined by which emergency action levels are exceeded.

In practice drills, decisions on protective action recommendations have proven to be difficult. NUREG-0654 states that if containment failure is imminent, sheltering is recommended for areas that cannot be evacuated before the plume arrives, but evacuation is recommended for other areas. The assumption in NUREG-0654 is that there would be a greater dose savings if the population were sheltered during plume passage rather than evacuated, but this assumption has not been proven. Furthermore, the recommended protective actions must be based on estimated containment failure times, which are difficult to determine.

Alternatively, other NRC publications suggest that the appropriate response would be early evacuation of everyone within a distance of about 2 or 3 miles for all events that could lead to a major release even if containment failure is imminent or a release is underway. Those at greater distances should take shelter. Further, if a release occurs, the appropriate action would be for monitoring teams to find "hot spots" (radiation dose rate exceeding about 1 R/hr) and for people to evacuate these "hot spots."

17.2 Project Objectives

The objectives of the activities to be performed in this project are to:

(1) characterize the family of potential accident sequence for which emergency planning is necessary,

(2) establish strategies appropriate to these sequences, emphasizing credible failure modes,

(3) identify those factors which would influence the implementation of these strategies,

(4) determine how these factors should be incorporated into the decisionmaking process, and

(5) develop a guidance report on the protective actions to be recommended for combinations of these factors.

---

*BNL Safety and Environmental Protection Division

The final NUREG report for the project will be written in a simplified manner that can be readily grasped by people not intimately familiar with accident consequence modeling. In addition, the report will also have a clear and concise summary understandable to laypeople.

17.3 Technical Approach

The technical approach is based on an evaluation of the consequences of nuclear power plant accidents as they relate to protective action decision-making. The evaluation includes a careful review of previous work (e.g. NUREG/CR-2339, NUREG-0654, NUREG/CR-2025, NUREG-0396, and reports and memoranda by the NRC staff) and its applicability to protective action decision-making. The approach is also based on a consideration of a wide range of potential accident sequences and on up-to-date assessments of containment performance. Thus the technical basis will reflect the new fission product source term information under development by the NRC/RES Accident Source Term Program Office (ASTPO). BNL staff are closely following the activities of ASTPO and, in addition, are participating in the SARP Containment Loads Working Group and in the Containment Performance Group. The work of these groups will be integrated into our development of protective action strategies.

The evaluation will be based in large part on results obtained from the CRAC2 computer code (Consequence of Reactor Accident Code, version 2). The output is being analyzed in terms of dose vs. distance for a variety of release characterizations, weather sequences, and protective action strategies.

In accordance with the above, we have selected the following six facilities to represent the range of potential reactor and containment designs:

Zion: PWR with a large dry containment
Surry: PWR with a subatmospheric containment
Sequoyah: PWR with an ice condenser containment
Brown's Ferry: BWR with a Mark I containment
Limerick: BWR with a Mark II containment
Grand Gulf: BWR with a Mark III containment

17.4 Project Status

17.4.1 Summary of Activities

BNL attended the Second Annual Workshop on Emergency Preparedness Plans and Programs hosted by Battelle, Pacific Northwest Laboratories, in Park City, Utah, January 16-20. The workshop covered most aspects of Emergency Preparedness from the perspectives of the NRC, utilities, scientific assessments, and public response. The information presented indicated that the content of the report being prepared by BNL is current and comprehensive. In addition, the information will assist us in writing our report in a manner that will clearly address these perspectives.

We are assessing appropriate links between proposed protective actions and emergency action levels based on in-plant observables and containment status (see Section 16 of this report). The assessment is being used to determine the format for CRAC2 calculations for various accident sequences and the related credible warning times and release characterizations. Emphasis is being given to the compatibility of protective actions designed for very rapidly developing accidents with those designed for more slowly developing scenarios.

We have made several CRAC2 runs for two accident sequences appropriate to the Zion facility. We discovered a minor error in the CRAC2 codes for the particular weather sampling procedure we were using. A correction update for the code was supplied by Sandia Laboratory, and this has been incorporated into our copy of the code.

Since the manner of population response is important to a recommended protective action strategy, BNL staff are also reviewing previous studies and current testimony at licensing board hearings.

17.4.2 Preliminary Conclusions

The results of these analyses to date have permitted certain preliminary conclusions to be developed.

(1) In-plant conditions - BNL staff have been evaluating specific accident sequences to determine if readily identifiable plant conditions exist which permit selection of appropriate protection action strategies. Preliminary results indicate that such links do exist and that protective action strategies can be based on in-plant observables for those accident sequences examined to this point.

(2) Warning time: BNL staff analysis of severe accidents indicates that warning times of several hours or more can be expected for the more probable accident sequences, e.g. small break LOCA or transients. Short warning times of 1 hour or less are associated only with less probable accident sequences such as ATWS, which should be readily identified.

(3) Weather: The importance of weather in defining the consequences of a radioactive release has been convincingly reconfirmed in our analyses of different accident scenarios. The type of weather occurring at the time of a release can dramatically affect the type of protective action recommended and the size of the area for which protective action is warranted. Since weather is an observable condition, it is apparent that the recommended protective action strategies should be highly weather dependent.

(4) Plume rise: In the accident scenarios that BNL staff have evaluated, the energy of release is an important parameter affecting downwind doses. It appears that this information will also be important in selecting the appropriate strategy.

NRC FORM 335 (11-81)

U.S. NUCLEAR REGULATORY COMMISSION

BIBLIOGRAPHIC DATA SHEET

1. REPORT NUMBER (Assigned by DDC)
NUREG/CR-2331
BNL-NUREG-51454, Vol. 4, No. 1

4. TITLE AND SUBTITLE (Add Volume No., if appropriate)
Safety Research Programs Sponsored by Office of Nuclear Regulatory Research; Quarterly Progress Report January 1 - March 31, 1984.

2. (Leave blank)

3. RECIPIENT'S ACCESSION NO.

7. AUTHOR(S)
Compiled by Allen J. Weiss

5. DATE REPORT COMPLETED
MONTH: June YEAR: 1984

9. PERFORMING ORGANIZATION NAME AND MAILING ADDRESS (Include Zip Code)
Brookhaven National Laboratory
Department of Nuclear Energy
Upton, New York 11973

DATE REPORT ISSUED
MONTH: August YEAR: 1984

6. (Leave blank)

8. (Leave blank)

12. SPONSORING ORGANIZATION NAME AND MAILING ADDRESS (Include Zip Code)
U. S. Nuclear Regulatory Commission
Office of Nuclear Regulatory Research
Washington, D. C. 20555

10. PROJECT/TASK/WORK UNIT NO.

11. FIN NO.
A-3011,14,15,16,24,41 A-3208,15, 19,25,26,27,57,61,66,68,70,71

13. TYPE OF REPORT
Quarterly

PERIOD COVERED (Inclusive dates)
January 1 - March 31, 1984

15. SUPPLEMENTARY NOTES

14. (Leave blank)

16. ABSTRACT (200 words or less)

This progress report will describe current activities and technical progress in the programs at Brookhaven National Laboratory sponsored by the Division of Accident Evaluation, Division of Engineering Technology, and Division of Facility Operations of the U.S. Nuclear Regulatory Commission, Office of Nuclear Regulatory Research.

The projects reported are the following: High Temperature Reactor Research, SSC Development, Validation and Application, CRBR Balance of Plant Modeling, Thermal-Hydraulic Reactor Safety Experiments, Development of Plant Analyzer, Code Assessment and Application (Transient and LOCA Analyses), Thermal Reactor Code Development (RAMONA-3B), Calculational Quality Assurance in Support of PTS; Stress Corrosion Cracking of PWR Steam Generator Tubing, Bolting Failure Analysis, Probability Based Load Combinations for Design of Category I Structures, Mechanical Piping Benchmark Problems, Identification of Age-Related Failure Modes; Analysis of Human Error Data for Nuclear Power Plant Safety-Related Events, Human Factors Aspects of Safety/Safeguards Interactions During Routine Reactor Operations and Off-Normal Conditions, Emergency Action Levels, and Protective Action Decision Making.

17. KEY WORDS AND DOCUMENT ANALYSIS

17a. DESCRIPTORS

High Temperature Graphite Reactor
Super System Code
MINET Code
Thermal-Hydraulic Reactor Safety
Emergency Action
Plant Analyzer
RAMONA-3B
Pressurized Thermal Shock
Stress Corrosion Cracking
Protective Action
Bolting Failure
Load Combinations
Nuclear Plant Aging
Human Error
Human Factors

17b. IDENTIFIERS/OPEN ENDED TERMS

18. AVAILABILITY STATEMENT

19. SECURITY CLASS (This report)

21. NO. OF PAGES

20. SECURITY CLASS (This page)

22. PRICE
$

NRC FORM 335 (11-81)